Graphene in Epoxy System:

Dispersion, Preparation and Reinforcement Effect

SUBMITTED IN PARTIAL FULFILLMENT OF THE

REQUIREMENTS FOR THE DEGREE OF DOCTOR OF

PHILOSOPHY

Sep 2017

By

Jiacheng Wei

Department of Mechanical and Construction Engineering

Northumbria University

Newcastle upon Tyne NE1 8ST, UK

Declaration

I declare that the work presented in this thesis is performed entirely by myself during the course of my PhD studies at Northumbria University at Newcastle and has not been submitted for a degree at this or any other universities.

I declare that the word count of this thesis is 42275words.

Jiacheng Wei

Acknowledgements

I would like to express my sincere gratitude to the following people who helped me during my PhD.

FIRST OF ALL, I want to express my sincere and special appreciation for my principle supervisor Dr Fawad Inam, who is a great mentor in study and an excellent companion in life. I would like to thank him for providing me with continuous support and guidance both in research for PhD, and in life. Without his encouraging supervision, it would be impossible for me to finish this project.

I am also deeply grateful to my co-supervisor Dr Thuc Vo for his positive support, proofreading, and valuable feedback of the research articles, which played a key role in the completion of my research work.

The experimental part would not be completed without the assistance of the academics and lab technicians in Northumbria University. I would like to thank Dr Pietro Maiello, who trained me on SEM and XRD. I would also like to thank Dr Guillaume Zoppi for training me on UV-Vis spectroscopy. I am also deeply thankful to Mr Phil Donelley, Mr Simon Neville, and Mr Sam Hutchinson, for training me on the versatile mechanical testing machine and hardness tester.

During my time in Newcastle, many people supported and helped me in various stage. I would like to thank Dr Atif Resheed, Dr Mohd Shaneel Saharudin in the research group and Dr Mohamed Abduelmula in the office. I would like to thank them for their company and support.

Thank Northumbria University for providing me the scholarship, the research facilities, and the chance of studying here.

Lastly, I would like to thank my parents for always giving me their selfless and the greatest love.

Abstract

Epoxy is one of the most adaptable and widely sold high performance material in the world because of its excellent mechanical properties, thermal stability, chemical and corrosion resistance, low shrinkage, low cost, and ease of processing, etc.

Graphene shows good potential for the fabrication of high performance polymer nanocomposites because of its unique planar structure and its superlative mechanical properties, thermal conductivity and excellent electrical conductivity. The layered structure allows a large surface contact area with the matrix and thus leads to improvements in the properties.

This work aims at exploiting the potential use of graphene as a filler to reinforce epoxy matrix and the preparation of homogeneously dispersed epoxy/graphene nanocomposites. To explore the maximum property enhancement of graphene in epoxy, dispersion is the key factor. However, in the preparation of epoxy/graphene nanocomposites, there still exist some challenges. One of the largest obstacles it that graphene tends to reagglomerate in liquid epoxy, which is due to the strong van der Waals force on the graphene surface. If not properly dispersed, the agglomerated graphene will act as a defect within the matrix and consequently lower the properties of the nanocomposites. Therefore, the dispersion of graphene and the processing techniques should be studied.

In this work, epoxy/graphene nanocomposites had been made by different processing techniques. Different characterization methods had been applied to evaluate the reinforcement effect. By end of this work, graphene dispersion techniques and sample preparation methods have been optimized. Epoxy/graphene nanocomposites have been prepared with enhanced properties.

Key words: Epoxy; Graphene; Processing; Dispersion; Homogenization.

Contents

List of Figures

List of Tables

List of Abbreviations

0-D: 0 Dimensional

1-D: 1 Dimensional

2-D: 2 Dimensional

3-D: 3 Dimensional

CB: Carbon Black

CNT: Carbon Nanotube

SWCNT: Single Wall Carbon Nanotube

MWCNT: Multi Wall Carbon Nanotube

G: Graphene

GNP: Graphene Nanoplatelet

GO: Graphene Oxide

r-GO: Reduced Graphene Oxide

m-G: Modified Graphene

m-GO: Modified Graphene Oxide

CVD: Chemical Vapour Deposition

DMA: Dynamic Mechanical Analysis

TGA: Thermal Gravimetric Analysis

SEM: Scanning Electron Microscopy

XRD: X-Ray Diffraction

FTIR: Fourier Transform Infrared Spectroscopy

UV-Vis: Ultraviolet-Visible Spectroscopy

AFM: Atomic Force Microscopy

TEM: Transmission Electron Microscopy

FRP: Fiber Reinforced Polymer

CFRP: Carbon Fiber Reinforced Polymer

DMF: N,N-Dimethylformamide

DCB: Dichlorobenzene

DCM: Dichloromethane

MEK: Methyl Ethyl Ketone (MEK)

THF: Tetrahydrofuran

IPA: Iso-Propyl Alcohol

SDS: Sodium Dodecyl Sulphate

GA: Gum Arabic

K_{1C}: Mode-I Fracture Toughness

G_{1C}: Critical Strain Energy Release Rate

HV: Vickers Hardness

T_g: Glass Transition Temperature

T_d: Thermal Decomposition Temperature

σ: Tensile strength

E: Tensile Modulus

κ: Electrical conductivity

λ: Thermal conductivity

1. Introduction

1.1Research Background

The combination of nanofillers and polymeric materials has led to a new class of multi-functional materials denoted as polymer nanocomposites. The category of the nanofillers can be generalized on the basis of their dimensions such as one-dimensional ones (nanotubes and nanowires), two-dimensional ones (graphene) and three-dimensional ones (spherical and cubic nanoparticles). For instance, graphite, three-dimensional (3-D) carbon allotrope, is made of graphene stacked on top of each other with a spacing of 0.33-0.34 nm [1]. Also, the zero-dimensional (0-D) fullerenes can be considered to be made by wrapping a piece of graphene. The one-dimensional (1-D) carbon nanotubes (CNTs) can be made by rolling graphene into single- or multi-walled tubular nanostructures. As for these structures, graphene has been viewed as a building block of all the other graphitic carbon allotropes with different dimensionality, as shown in Figure 1.1.

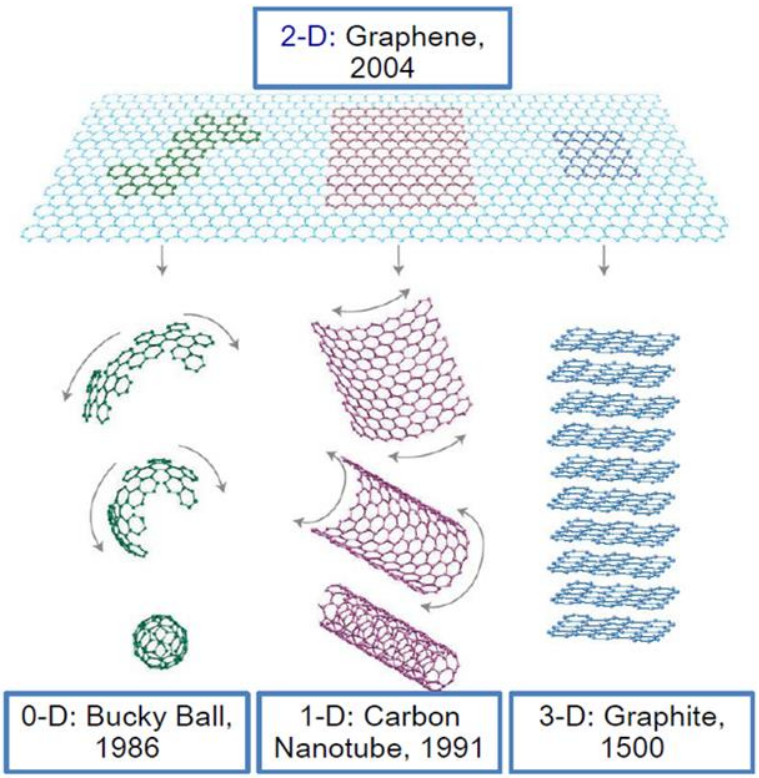

Figure 1. 1. Graphene, the building block of all graphitic forms.

With the discovery of graphene, the properties, production, and use of graphene have become an avid area of research during the past decade. Due to their planar structure, high thermal conductivity and low electrical resistivity, as well as high strength, graphene has gained lots of favour for many technological applications such as batteries, sensors, transparent conducting films, hydrogen storage and super capacitors; whilst the most attractive application of which is employed as an effective reinforcement filler for polymer matrix [2].

As the most widely sold highperformance thermosetting polymers in the world, epoxy resins are used in a wide variety of applications due to their excellent mechanical properties, thermal stability, solvent resistance, and ease of processing [3]. They are particularly useful as matrix resins for the advanced composites that are essential structural materials in both commercial and military fields. Exploration of property enhancement of graphene in epoxy is rapidly advancing and Figure 1.2.shows the dramatic increase in epoxy/graphene nanocomposites research in recent years.

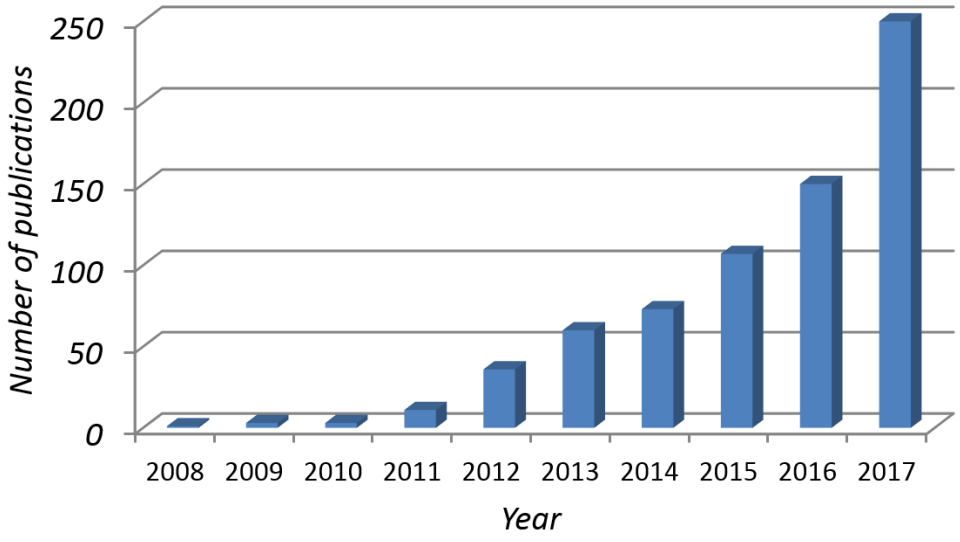

Figure 1. 2. Numbers of publications returned using “graphene epoxy” as keywords in Web of Science. (By 1st Sep. 2017)

According to the number of publications, graphene has attracted a significant increase of attention in the last three years and shows promise as a novel filler to improve properties of epoxy matrices.

1.2 Methodology

Pristine graphene materials are unsuitable for intercalation by large species, such as polymer chains. This is due to graphene's pronounced tendency to reagglomerate in the matrix due to the strong van der Waals force between separately dispersed graphene sheets. As occurred with other nanofillers, the maximum improvements in final properties can only be achieved when graphene is homogeneously dispersed in the matrix and external stresses are efficiently transferred through the strong graphene-epoxy interface. Thus, dispersion and strong interaction between graphene and matrix plays a challenging role in the performance of graphene/matrix composites and requires research in order to understand the reagglomeration behaviour of graphene in an epoxy system.

Reagglomeration of graphene starts with investigation into different processing parameters that affect the dispersion and reagglomeration behaviour of graphene in an epoxy system. Varying sonication times, storage times, graphene concentrations, and sonication temperatures will be studied, and the light transmittance of the graphene-epoxy suspension will be analysed using Ultra-Violet Visible (UV-Vis) spectroscopy.

Different processing techniques affect the final properties of nanocomposites. This part will be carried out by prepare nanocomposites using different processing techniques such as bath sonication, tip sonication, and hand mixing. After the nanocomposites have been prepared, the properties of nanocomposites will be tested to find out the best processing technique.

Graphene concentration affects the properties of nanocomposites significantly. In general, with the incorporation of graphene, the properties of nanocomposites increase. However, the problem of agglomeration also occurs with the incorporation of graphene, thus graphene will agglomerate in matrices at high concentrations. Therefore, epoxy/graphene nanocomposites with different graphene concentrations will be made to evaluate the optimum graphene loading for the best property enhancements.

Research in solvents for graphene dispersion will be carried out in two parts. First is to research how solvent dosage affects the processing and how it's associated with the final properties of nanocomposites. Different dosage of solvents will be used to prepare nanocomposites, namely: 100ml, 300ml, 500ml, and 1500ml.

And then how different solvents affect the dispersability of graphene will be investigated, common solvents such as N, N-Dimethylformamide (DMF), ethanol and dichlorobenzene (DCB) will be used to prepare nanocomposites. Properties of the nanocomposites will be studied in order to compare the dispersion efficiencies of those commonly used solvents.

Surface modification of graphene is particularly attractive because it can improve both solubility and processability, concurrently increasing the interactions of graphene and epoxy. The functional groups attached on graphene can be small molecules or long polymer chains. Various functionalization methods had been used such as covalent functionalization and non-covalent functionalization, however, covalent functionalization often induces defects on the graphene surface and involves more complicated processing steps. Therefore, non-covalent functionalization by Sodium Dodecyl Sulphate (SDS) and Gum Arabic (GA) will be used in this work to modify graphene. Final properties of nanocomposites will be tested to evaluate their dispersing effectiveness.

Obtaining a good distribution of the graphene reinforcement is one of the greatest challenges in the preparation of epoxy/graphene nanocomposites. A well-dispersed state ensures a maximised contact surface area of graphene and the matrix, which will affect the neighbouring polymer chains and, consequently, the macro properties of the nanocomposites. When dispersed in an epoxy matrix, dispersion highly depends on the processing techniques. Therefore, research to enhance the dispersion should be carried out by optimising the processing parameters, such as the dispersing methods, processing time, solvents used, etc.

1.3 Aims and Objectives

The existing literature suggests that more research should be carried out on graphene dispersion and the optimization of processing techniques for better understanding of the relationships between graphene dispersion and final properties. The main research areas include:

1. Processing techniques and parameters carried out to process the nanocomposites.
2. Dispersion stability of graphene in solvents and liquid epoxy systems.
3. Surface modification of graphene.
4. Characterising the mechanical and thermal properties of the nanocomposites.
5. Understanding the relationship between dispersion and the properties of nanocomposites.

The overall aim of this project is to understand how different processing variables affect the dispersion of graphene along with the final properties of the nanocomposites. It is expected that at the end of this project epoxy/graphene nanocomposites could be prepared with: (1) improved properties and (2) a wider range of application fields.

1.4 Achievements in This Work

The literature review on processing and properties of epoxy/graphene nanocomposites has been performed and a comprehensive understanding in this field has been gained. The key technical barriers in the processing of epoxy/graphene nanocomposites are:

(1). Uniform dispersion of graphene in epoxy matrix and;

(2). Strong interaction of graphene-epoxy interface.

Most of the literature focuses on the surface modification of graphene, as well as the analysis of the properties of nanocomposite materials and have achieved some interesting progress. However, the processing of nanocomposite materials have been the object for only a few scientific publications, thus, the processing methods and parameters are suggested to be studied to further optimize the processing. By doing this research, the following parts should be highlighted in this work:

(1). Effects of processing parameters such as sonication time, storage time, graphene concentration, and sonication temperature had been studied. The dispersion and reagglomeration of graphene in two-component epoxy systems had been quantificationally measured by UV-Vis spectroscopy. The results show that sonication time and sonication temperature significantly contribute to the dispersion of graphene, lower concentrations produce a lower reagglomeration profile (size and trend) and vice versa. In this part, UV-Vis spectroscopy had been used for the first time to measure the dispersion and reagglomeration behaviour of graphene in epoxy system.

(2). The efficiencies of different processing techniques had been investigated. Bath sonication, tip sonication, and hand mixing had all been applied to prepare nanocomposites. After comparing the properties of nanocomposite materials prepared using each technique, it is concluded that bath sonication has the best dispersing efficiency, followed by tip sonication, and then finally, hand mixing.

(3). Graphene content on the properties of the epoxy matrix had been studied. Epoxy/graphene nanocomposites with different graphene contents had been made. The results show that nanocomposites with 0.1 wt% and 0.3 wt% graphene show good dispersion and property enhancement in epoxy matrices. Higher concentration of graphene reaggregates and causes a decrease in the properties of nanocomposites. In general, 0.3 wt% epoxy/graphene nanocomposites show the best property enhancements.

(4). One set of experimental work concentrated on the effects of solvent dosage on the properties of epoxy/graphene nanocomposites. Different dosages of solvent were used to prepare nanocomposites. To evaluate their effects, mechanical properties such as tensile, flexural strength, modulus, hardness and thermal properties such as glass transition temperature were tested. The results show that large dosage of solvents would cause reagglomeration of graphene during the process, which was due to the long solvents removal time. In this part, the relationship among solvent dosage, graphene dispersion state, and the properties of the nanocomposites had been reported for the first time.

(5). Work on the effectiveness of different solvents on the properties of epoxy/graphene nanocomposites were conducted by comparing DCB, ethanol and DMF. These three solvents had been chosen to prepare nanocomposites. Visual stability, mechanical properties, dynamic mechanical analysis (DMA), thermal gravimetric analysis (TGA) and scanning electron microscopy (SEM) tests of nanocomposites had been conducted. The results show that DCB prepared nanocomposites showed the highest mechanical properties, glass transition temperature and thermal decomposition temperature, the visual stability also shows that DCB produces the most stable dispersion of graphene. DCB had been reported for the first time as an effective solvent for preparing epoxy/graphene nanocomposites.

(6). Non-covalent functionalization of graphene had been conducted by using SDS and GA as a surface modifier. Fourier transform infrared spectroscopy (FTIR) results show that both SDS and GA had been grafted to graphene surface successfully. Both SDS and GA are able to de-bundle graphene from their agglomerates and enhance the properties of nanocomposites. The SDS prepared nanocomposites shows better performance than the GA prepared nanocomposites, which means SDS has better dispersing efficiency than GA. In this part, SDS and GA have been selected to compare their dispersion effect for graphene in epoxy matrix for the first time.

In general, this project focuses on the processing of epoxy/graphene nanocomposites, investigates how different processing variables affect the dispersibility of graphene and its association with the final properties of the nanocomposites. Furthermore, this project seeks to apply the understanding of the processing to enhance the properties of the material as well as exploring advanced engineering applications of epoxy/graphene nanocomposites.

Techniques were developed to in-situ observe the dispersibility of graphene and enhance its dispersion. This multidisciplinary project covers knowledge across mechanical, chemistry and polymer science. In the last, homogeneously dispersed graphene along with enhanced properties of epoxy/graphene nanocomposites had been developed. Graphene dispersion method, sample preparation process had been optimized, and a better graphene surface modification method had been suggested.

2 Literature Review: Epoxy/Graphene Nanocomposites

2.1 Introduction

Materials play a key role in every field of technology such as aeronautics, electronics, energy, health, sensors, etc [4]. It is critical to develop novel materials with improved properties so that superior performance for future applications can be materialized [5]. Compared to traditional composite materials, nanocomposites exhibit extraordinary properties because of the exceptionally high surface to volume ratio of the nanofiller and/or its exceptionally high aspect ratio [6]. Polymer nanocomposites combine the functionalities of polymer matrices, such as low cost, and easy processability [7], with the unique features of the nanofillers such as high aspect ratio, excellent mechanical properties etc [8]. In the past few years, polymer nanocomposites with enhanced optical, mechanical, electrical, thermal, and fire retardant properties have been developed [9, 10]. However, nanofillers used in these applications have a strong tendency to agglomerate which would result in non-uniformed dispersion in the polymer matrix [11], and degradation of the mechanical and thermal properties of the nanocomposites. The optimum enhancement in the properties of a resin could only be attained when the nanoparticles are uniformly dispersed in the matrix [12]. Achieving the optimum dispersion is one of the main challenges for processing of nanocomposites and therefore it is essential to review the current processing techniques used for preparing nanocomposites.

In this part, mechanical properties, electrical conductivity, thermal stability, and fire retardant properties of epoxy/graphene nanocomposites have been reviewed. Additionally, processing methods and properties have been correlated. Furthermore, some of the listed points that have been highlighted in this part are:

1. Summarised a new method of epoxy/graphene nanocomposite preparation - resin impregnation, which involves impregnating epoxy into a graphene filter cake without pre-mixing.

2. Summarised the synergic effects of graphene and other fillers in epoxy matrices.

3. Summarised the reason thermal stability decreased with the incorporation of graphene.

To the best of our knowledge, this literature review covers most of the important publications relating to the processing and properties of epoxy/graphene nanocomposites.

2.2 Epoxy

2.2.1 Introduction to Epoxy

Discovered in 1936 by Dr Castan of Switzerland and Dr Greenlee of USA, epoxy based materials are used widely because of their superlative mechanical properties, thermal stability, solvent resistance, and ease of processing [13].

Epoxies are one of the most adaptable and widely sold high-performance materials in the world [14], and some of the applications of epoxy and its nanocomposites include aerospace, automotive, marine, sports materials, construction, structures, electronic systems, biomedical devices, thermal management systems, adhesives, paints and coatings, industrial tooling, and other general consumer products [15]. Because of its versatile nature, epoxy is replacing many conventional materials, for example, epoxy-based materials have already replaced wood in most boats and various sporting goods. Epoxy resins are thermosetting polymers and are defined as a molecule containing more than one epoxide group, as shown in Figure 2.1.

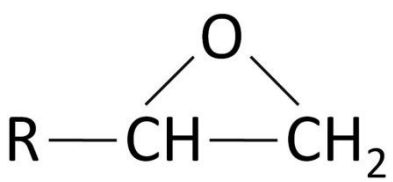

Figure 2. 1. Molecular structure of epoxide group.

Epoxy resins are very important matrix for advanced composite materials which are essentially used in both civil and military fields, however, epoxy resins are inherently brittle due to the high cross-linking density [16]. The epoxy materials for engineering applications are often limited by their brittle nature and the poor electrical and thermal properties. This lack of toughness is a major reason to prevent the widespread use of epoxy in various applications. Therefore, the work to toughen epoxy has become an area of intense research and has attracted a lot of research interest. In general, the most commonly used method to enhance the mechanical properties is to add a filler into the epoxy resin. While the epoxy act as the matrix, the filler act as a toughening phase to toughen the epoxy [17]. Many different fillers have been investigated as second phases in recent years, and those second phases include graphene, CNTs, fibers, clays, rubbers, or thermoplastic polymers in many studies. Most of those fillers are able to toughen epoxy effectively, however, their incorporation sometimes causes a decrease in the properties, if not appropriately processed [18]. It is reported that there are three parameters of particular importance for hardening in multiphase systems, which are: (1) the distribution of the particles within the matrix, (2) the strength of the fillers, and (3) the interfacial interaction between the filler and the matrix [19].

2.2.2 Curing of Epoxy

The curing process is a chemical reaction in which the epoxide group in epoxy resin reacts with a hardener (curing agent) to form a highly crosslinked, three dimensional network [20]. Epoxy resins cure at temperatures ranging from 5-150 ℃ depending on the choice of hardener, with a wide variety of hardeners available [21].

The commonly used curing agents for epoxies include amines, polyamides, phenolic resins, anhydrides, and isocyanates [22-24]. The cure kinetics and the T_g of cured systems depend on the molecular structure of the epoxy and hardener. The choice of resin and

hardeners depends on the application, the process selected, and the properties desired [25]. The stoichiometry of the epoxy - hardener system also affects the properties of the cured material [26]. Employing different types and amounts of hardener tends to control the cross-linking density of epoxy and vary the structure. Specifically, the amine and phenolic resin based curing agents, described below, are widely used for curing of epoxy resins. Amines are the most commonly used curing agents for epoxy cure. Primary and secondary amines are highly reactive with epoxy. Tertiary amines are generally used as catalysts, commonly known as accelerators for cure reactions [27]. Use of excessive amounts of catalyst achieves faster curing, but often at the expense of working life and thermal stability [28]. The catalytic activity of the catalysts affects the physical properties of the final cured polymer. When cured with phenolic hardener, epoxy resins show excellent adhesion, strength, and flame resistance [29]. Furthermore, phenolic cured epoxy systems are mainly used for encapsulation because of their low water absorption, as well as their excellent heat and electrical resistance.

There are also different types of curing, such as room temperature curing, heat curing, and photo curing [30, 31]. Epoxy resins cure at room temperature, and use room temperature curing agents, such as aliphatic polyamines, alicyclic polyamines, and low molecular weight polyamide [32]. Room temperature curing provides a lower T_g, higher flexibility, greater impact resistance, and greater electrical and thermal shock resistance [33]. For heat curing, epoxy resins generally cure at elevated temperatures and uses aromatic polyamines, acid anhydrides, amino resins, dicyandiamide, or hydrazides as curing agents. Heat curing is generally divided into a pre-curing stage at low temperature and then a post-curing stage at higher temperatures [34]. Heat cured epoxy resins usually have a higher T_g, greater tensile strength, higher heat resistance, and greater chemical resistance. Epoxy resins can also be cured using infrared, ultraviolet light, or electron beam irradiation in the presence of a photoinitiator [35]. Photocuring dramatically reduces the curing time from hours to minutes.

2.2.3 Epoxy Based Nanocomposites

For epoxies, there are some drawbacks and unsatisfactory properties. For example, the high cross-linking density of epoxy leads to low fracture toughness, which restricts its applications [36]. Toughness is a measure of a material's resistance to fracture. It is usually measured as either the critical stress intensity factor or the energy required to fail a specimen under a specific loading condition [37]. A number of researchers have concluded that high cross-linking density will decrease the fracture toughness of epoxy resins [38-40]. Within a highly cross-linked epoxy resin, resistance to crack initiation is very poor and the crack growth due to plastic deformation is very fast [41]. The applications of epoxy resins in many engineering areas are often limited by their brittle nature [42]. Therefore, the development of novel epoxy based materials with higher mechanical properties has become very important in recent years.

Epoxy based nanocomposites have attracted great interest both in industry and in academia, because they exhibit remarkable improvements in material properties when compared with neat epoxy or conventional micro and macro composites. Epoxy based nanocomposites have added a fresh number of advantages due to their superior properties such as higher modulus, strength, toughness, durability, flame retardancy and other excellent properties, along with the ease of processability [43]. Over past decades epoxy based nanocomposites have attracted great interest among researchers, and the studies show that the improvement of mechanical properties and thermal properties of the material can be achieved by using highly prospective fillers [44].

Conventional composites usually require high contents (usually >10 wt%) of fillers to achieve desired properties [45]. Such high filler contents increase the density of the product and can sometimes cause a decrease in some properties through interfacial incompatibility between the filler and the organic matrix [46]. More than that, the processability worsens as

filler content increases [47]. In contrast, nanocomposites show enhanced thermal, mechanical properties even with a small amount of filler loading [48]. These materials have a very high strength to weight ratio, low density, and enhanced modulus. Those prominent properties even permit the nanocomposites to compete with selected metals.

Much work has been conducted to enhance the mechanical properties and to improve the thermal properties of epoxy and various methods have been applied. Based on the structure - property relationship, some traditional methods have been: chemical modification of a given rigid epoxy backbone to a more flexible backbone structure [49]; lowering the cross-linking density by increasing the molecular weight of the epoxy monomers and/or decreasing the functionality of the curing agents [50]. The most popular method is the incorporation of dispersed toughener phase(s) in the cured epoxy matrix. The toughener phase includes rubbers, thermoplastics and rigid fillers such as clays, CNTs, graphene, etc [51, 52]. Fillers improve mechanical properties such as strength, stiffness, and modulus, etc. However, the fillers have a negative impact on the viscosity of the resin, which restricts their usage in some applications. Furthermore, sometimes the fillers would be filtered out by the fabric when the formulation is subjected to injection manufacturing methods for fiber reinforced composites [53].

The blending of epoxy resins with nanofillers is a step towards increasing the properties of epoxy. The nanofillers can be one-dimensional (like carbon nanotubes, nanowires, nanofibers, inorganic whiskers, etc.) [54], two-dimensional (layered minerals such as graphene) [55], and three-dimensional (graphite, etc.).

With the existing benefits provided by the resin such as good stiffness, specific strength, and low cure shrinkage, the performance of the epoxy can be further improved by the use of fillers and engineered according to a unique application [56]. Several different particles have been added to epoxy resins to improve their properties. Incorporation of

inorganic particles leads to a decrease in deformation and increase in crack propagation resistance. This is due to the very large surface area of interaction between the polymer matrix and the nanofiller [57]. Some of the representative epoxy-based nanocomposites will be introduced briefly here.

Epoxy/Graphene Nanocomposites

Graphene, known for its single-layered, one atom thick, flatbed structure, has brought a new dimension to the nanotechnology world [58]. Considered as a planar sheet of sp^2 bonded carbon atoms in a honeycomb crystal lattice, graphene is also considered as the prime element of carbon allotropes, including graphite, fullerenes, and carbon nanotubes [59]. It exhibits very good mechanical and electrical properties as well as fracture toughness performance. Graphene has very high thermal conductivity (5000 W/m K), high Young's modulus (1 TPa), high value of white light transmittance up to 97.7%, and exceptionally high room temperature electron mobility of 2.5×10^5 cm^2/V s. The graphene surface to volume ratio is higher than CNTs as the inner nanotube surface is inaccessible to polymer molecules [60].

Current research shows that the incorporation of graphene into epoxy is crucial to broaden the function and enhance the performance of the epoxy matrix. Graphene has an exciting future for utilization as reinforcement in epoxy with regards to specific applications such as paintings, structural materials, etc. The outstanding properties of graphene comprising of a large specific surface area and high mechanical strength make it ideal reinforcement to enhance the properties of epoxy.

Epoxy/CNT Nanocomposites

In recent years, the use of CNTs to improve the mechanical and thermal properties of epoxy has attracted a lot of research interest due to the unique properties of CNTs [61-63].To increase the strength and modulus of the matrix, CNTs are considered stronger than steel, lighter than aluminium, and more conductive than copper [64]. Made of cylindrical rolled up graphene sheets and fullerene structure, CNT consists of two different types: (1) single-walled CNTs (SWCNTs) and (2) multi-walled CNTs (MWCNTs) [65, 66]. Most SWCNTs have a diameter of close to 1 nanometer and can be millions of times longer [67]. MWCNTs consist of multiple rolled layers (concentric tubes) of graphene. Made up of numerous layers with a bigger diameter, MWCNTs demonstrate an enhancement of dispersion but offers a less significant interface for stress transfer. The high surface area of SWCNTs might lead to higher impact of the CNTs on the composite performance [68].

Since the last decade, epoxy/CNT nanocomposites have been widely investigated. Certain aspects of mechanical enhancement of different polymer systems using CNT have been reported in literature. Some encouraging results in fabricating strong epoxy/CNT composites have been reported [69-71].However, the low dispersibility and the weak interfacial interaction between CNTs and the epoxy matrices have limited their application in this area, and transferring stress from the matrix to the CNTs is still a research challenge [72]. Two main issues have to be solved for the improvement of the mechanical properties of the nanocomposites: (1) the proper dispersion of CNTs in the matrix and (2) a good interfacial bonding between the matrix and the CNTs [73]. The CNT dispersion in epoxy matrix is very important for achieving desired properties. The tendency of CNTs to form bundles reduces the ability to transfer the load and reinforce the matrix. This is an important factor that determines the composite performance and requires optimization [74]. Therefore, to disperse CNTs in epoxy, various processing methods had been used, such as ultrasonic dispersing,

shear mixing, and mechanical stirring [75-77]. Surface modification of CNTs, either by chemical or physical treatments, also helps to improve the CNT dispersion and aid the stress transfer [78]. Physical modification methods involve the adsorption and/or wrapping of polymers or surfactants on the CNT surfaces, and chemical methods consist of covalent bonding of chemicals to the CNT surfaces [79]. For example, nitrogen-doped CNTs are reported to be sufficiently chemically reactive to improve the interactions with epoxy [80].

In general, epoxy/CNT nanocomposites have high strength, lightweight, and multifunctional properties [81, 82]. A homogenous dispersion of CNTs with favourable interfacial interactions with the epoxy matrix should be achieved to ensure the maximum property enhancement of CNTs in epoxy matrix [83].

Epoxy/Clay Nanocomposites

Clays are hydrous silicates or aluminosilicates and fundamentally contain silicon, aluminum, magnesium, oxygen or hydroxyl with various associated cations [84, 85]. The structural framework of clay is basically composed of 1nm thick silicate layers, silica and alumina sheets joining together in various proportions in the layers and stack on top of each other [86, 87].There are four main groups of clays: kaolinite, montmorillonite, illite, and chlorite [88]. Among the different types of clay minerals, montmorillonite is the most commonly used for the preparation of polymer clay nanocomposites [89]. Montmorillonite owes special attention among the smectite group due to its ability to show extensive interlayer expansion or swelling [90].

Clays are highly potential nanofillers due to their exfoliated arrangements in the soft matrix [91]. They provide a good range of mechanical and fracture properties such as high stiffness and high modulus. Clays have been widely used as fillers to enhance the properties of epoxy nanocomposites [92]. Recently, there has been a growing interest in the

development of epoxy/clay nanocomposites due to the higher property enhancement when compared to conventional filled polymers.

Compared to conventional filled polymers, epoxy/clay nanocomposites show enhanced properties with only small amount of clay loadings (⩽5%) [93, 94]. Improvements comprise higher modulus, increased strength, heat resistance, decreased gas permeability, reduced coefficient of thermal expansion and decreased flammability when compared to neat epoxy and traditional micro/macro composites [95]. The improved properties are due to the good mechanical properties of clay and the large interfacial interaction between clay and epoxy [96]. However, when the loading of clay surpasses an optimal level, the properties of the nanocomposite decrease.

This decrease in the properties is caused by the agglomeration of clay. A large amount of clay is difficult to disperse in epoxy due to its hydrophilic nature. In order to make them dispersed homogeneously in an epoxy matrix, clays are normally treated by hydrophobic chemicals, such as alkylammonium ions [97]. The surface treated clays offer better interfacial bonding with the epoxy matrix, and the alkylammonium ions, creating surface functionalities on the clays, thereby improving their chemical compatibility/interactions with the matrix, leading to enhanced dispersion [98].

Rubber Modified Epoxy

The toughening of epoxy resins has been the subject of intense investigation throughout the world. The epoxy resins have been successfully toughened by incorporating a rubbery filler as a distinct phase [99, 100].

A number of rubbers have been considered and applied to toughen epoxy resins [101, 102]. The rubber system which attracts the most attention is the carboxyl-terminated copolymer of butadiene and acrylonitrile (CTBN) [103, 104], which is commercially

available with different acrylonitrile contents ranging from 10 wt% - 26 wt%. The low molecular weight (3400 - 4000 g/mol) butadiene-acrylonitrile rubbers are soluble in liquid epoxy resins [105]. When a solution of rubber in epoxy is cured, rubber particles precipitate out as a second phase. With just 10 percent rubber loading, the fracture toughness of modified epoxy resins increases dramatically with only a slight decrease in the glass transition temperature and the modulus [106, 107].

Thermoplastic Modified Epoxy

Rubber modified epoxy resins have proved to be successful with adhesives [108, 109], however, for high-performance epoxy resins, the toughening effect of rubber modification is usually only incremental. This is because of the low glass transition temperature of the rubber which lowers the maximum use temperature and the modulus of the epoxy resins [110, 111]. Therefore, tough, high-performance engineering thermoplastics such as poly(ether sulfone)s, poly(ether ketone)s and poly(ether imide)s have been used as toughеners for epoxy resins [112, 113]. They are used either as granulated particles or as polymers dissolved in the liquid epoxy and later precipitated out as second phase [114]. The major advantage of these thermoplastic modifiers is that their incorporation does not lead to are duction in the modulus and glass transition temperature of the epoxy matrix [115].

In comparison with rubber modified systems, the use of tough thermoplastic polymers offers better improvement in fracture toughness for higher crosslinking density epoxy systems [116]. The advantage of thermoplastic modified epoxy systems lies in the fact that the modulus and the T_g of the modified epoxy can be maintained, and the fracture toughness can be improved in direct proportion to the amount of thermoplastic added [117]. The use of reactive thermoplastic modifiers provides good adhesion between the epoxy and the thermoplastic phases via chemical connections, which allows predictable morphology and

chemical resistance of the material [118]. Commercial products of epoxy/thermoplastic systems are available and used in some applications, however, in some cases, the processing costs need to be considered.

Fiber Reinforced Epoxy

Fiber reinforced polymers (FRPs) are commonly used in aerospace, automotive, marine, and construction industries [119]. Fibers are thin rod-like structures that provide stiffness and strength to the composites [120]. Fiber reinforced epoxy is a composite material made by epoxy and reinforced with fibers. Glass fibers and carbon fibers are two of the most widely used fibers to reinforce epoxy [121, 122]. These composite materials are widely used due to their high specific strengths.

Carbon fibers have several advantages including high stiffness, high tensile strength, low weight, high chemical resistance, high-temperature tolerance and low thermal expansion [123]. These properties have made carbon fiber very popular in aerospace, civil engineering, military, and motorsports, along with other competition areas [124]. When a load is applied to the composite, the stress could be transferred from the matrix to the fiber. If a fiber - resin bond is weak, this load transfer will be weak or even break the bonds between the resin matrix and the fiber filaments [125]. Carbon fibers are usually coated with sizing, a polymeric solution applied to improve their adhesion with the resin matrix [126]. Carbon fiber reinforced polymers (CFRPs) are used more extensively for structural applications than other high-performance composites due to their overall high specific stiffness and strength properties.

Glass fiber is a material consisting of numerous extremely fine fibers of glass [127, 128]. Glass fiber has roughly comparable mechanical properties to other fibers such as polymer fibers or carbon fibers [129]. Although not as strong or as rigid as carbon fiber, glass

fiber is much cheaper when used in composites [130]. Glass fibers are therefore used as a reinforcing material for many polymer products to form a very strong and relatively light-weight fiber reinforced polymer composite material [131]. As with epoxy, the two materials act together, each overcoming the deficiencies of the other. For example, epoxy resins are strong in compressive loading but relatively weak in fracture toughness, whereas the glass fibers are very strong in tension but tend not to resist compression [132]. By combining the two materials, glass fiber reinforced epoxy becomes a material that resists both compressive and fracture forces [133, 134].

To sum up, fiber reinforced epoxies have emerged as a new range of materials, due to their ability to offer substantial advantages over traditional composite materials in terms of density and fatigue properties [135, 136]. In particular, the aerospace industry has increased the use of FRPs in aeroplanes, especially in airliners, because of the reduced weight compared to equivalent metal structures [137]. Currently, FRPs have taken up a major part of the structural mass of some civil and military aircraft. However, one of the main aspects currently limiting the large scale application of FRPs is their relatively high cost in relation to the raw materials, manufacturing and assembly [138].

Graphene based Carbon Fiber Reinforced Polymers

The combination of 2D graphene and 1D carbon fiber, with multi levels from the nanometer to the macroscopic scale, led to the formation of 3D hierarchical nanocomposites with excellent performance [139].

For CFRPs, the 1D carbon fiber act as scaffold, and thus enhance the mechanical stiffness and strength of the nanocomposites. Recently, it was found that the incorporation of graphene into CFRPs could further improve the mechanical properties of the composites due to consuming energy by pulling out graphene from the matrix or breakage of graphene, and

the graphene network in the matrix could also improve the stress transfer and distribution [140]. In addition, the carbon fibers in the matrix are also reported to separate the graphene sheets from reagglomeration [141].

The incorporation of graphene could also introduce some functional properties into the CFRPs. For example, due to the superior thermal conductivity of graphene, graphene could enhance the thermal conductivity of the CFRPs significantly. Individually dispersed graphene nanosheets are reported orderly interlinked in the 3D framework of carbon fibers, provide a convenient pathway for the heat transfer, and thus enhance the thermal conductivity of the composites [142]. For flame retardant applications, graphene can be used due to its planar structure, graphene wall shows excellent barrier resistance against gas permeation, and thus improve the flame retardant performance of the CFRPs [143].

In all, by introducing graphene into CFRPs, the composite material exhibits ultrahigh thermal conductivity, mechanical properties and other new performance.

2.2.4. Applications of Epoxy and Its Nanocomposites

The chemistry of epoxies and the range of commercially available variations allow this material to be produced with a broad range of properties [144]. Since large improvements have been observed in mechanical, thermal and barrier properties, epoxy based nanocomposites can be used for many specific applications in aerospace, military defence, automobile industries, and so forth [145]. Because epoxybased nanocomposites provide improved anticorrosion protection, it is possible to find new applications in modern aircraft anticorrosion coatings [146]. Epoxy based nanocomposites have been extensively used for structural adhesive applications, due to its potential improvement in adhesive properties with practicality and low cost [147]. These composites are also used in high-performance structural and functional applications such as laminates and composites, sealants, tooling,

moulding, casting, electronics and construction, etc. Some of the applications of epoxy and its nanocomposites will be introduced briefly here. Figure 2.2 shows the application fields of epoxy resins [148].

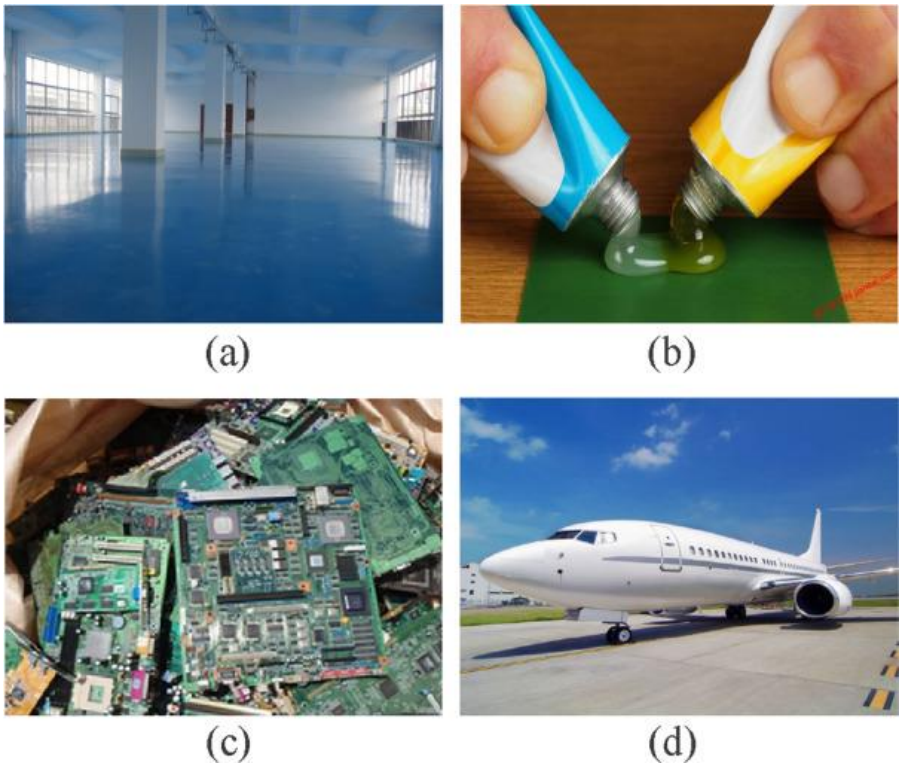

Figure 2. 2. Photos of epoxy resins used in (a) paints and coatings, (b) adhesives, (c) electronic materials, and (d) aerospace industry [148].

Paints and coatings

Epoxy resins are widely used as heavy duty anticorrosion coatings because of their exceptional properties, such as easy processing, high safety, excellent solvent and chemical resistance, toughness, low shrinkage on cure, mechanical and corrosion resistance, and excellent adhesion to many substrates [149]. Metal cans and containers are often coated with epoxy resins to prevent rusting, especially when packaging acidic foods like tomatoes. Epoxy resins are also used for high performance and decorative flooring applications such as terrazzo, chip, and coloured agglomerate flooring [150].

Adhesives

Epoxy adhesives are a major part of the class of adhesives called "structural adhesives" [151]. These highperformance adhesives are used in the construction of aircraft, automobiles, bicycles, boats, golf clubs, skis, snowboards, and other applications where high strength bonds are required. When used as adhesives in cryogenic engineering applications, it is necessary to optimize the epoxy shear strength at both cryogenic and room temperatures. Commercial epoxy adhesives are engineered for optimal toughness by incorporating phase separated thermoplastics, rubber particles, or rigid inorganic particles into the matrix. Typically, the adhesives are cured at elevated temperatures to increase their strength and activate chemical bonding at the substrate/adhesive interface [152].

Industrial tooling

Epoxy systems are used in industrial tooling applications to produce moulds, master models, laminates, castings, fixtures, and other industrial production aids [153]. This "plastic tooling" replaces metal, wood, and other traditional materials, and generally, improves the process efficiency while either lowering the overall cost or shortening the lead-time for many industrial processes [154]. Fiber reinforced epoxy composites have proven effective in repairing metallic components and tubular pipes. The composites also act as load bearing units in hydrogen storage cylinders.

Aerospace industry

Epoxy resins have been extensively used for structural adhesive applications in the aerospace industry because of their high adhesive properties and low cost. Epoxy resins reinforced with high strength glass, carbon, Kevlar, or boron fibers have the greatest potential for use as structural materials in aerospace industry [155].

Electronic materials

Epoxy resin formulations are important in the electronics industry and are employed in motors, generators, transformers, switchgear, bushings, and insulators [156]. Epoxy resins are excellent electrical insulators and protect electrical components from short circuiting, dust, and moisture. Metal filled polymers are extensively used for electromagnetic interference shielding. Epoxy moulding compounds are popularly used as encapsulation materials for semiconductor devices protect the integrated circuit devices from moisture, mobile ion contaminants, and adverse environmental conditions such as temperature, radiation, humidity, and mechanical and physical damage. Epoxy composites containing particulate fillers, such as fused silica, glass powder, and mineral silica have been used as substrate materials in electronic packaging applications [157].

Biomedical systems

Epoxy resins are widely used in biomedical applications [158]. Epoxy based materials have significant potential for biomedical applications such as embolic sponges, vascular grafts, and aortic heart valves, etc. Nanodiamond epoxy derivatives have found considerable application in biomedical systems because they exhibit a combination of extreme hardness, outstanding chemical inertness, low electrical and high thermal conductivities, wide optical transparency, and other unique properties [159].

Consumer applications

Epoxies are sold in hardware stores, typically as a pack containing separate resin and hardener, which must be mixed immediately before use. They are also sold in boat shops as repair resins for marine applications [160]. Epoxies typically are not used in the outer layer of a boat because they deteriorate by exposure to UV light. They are often used during boat

repair and assembly, and then overcoated with conventional or two-part polyurethane paint or marine varnishes that provide UV protection.

Marine applications

There are two main areas of marine use. Because of the better mechanical properties when compared to the more common polyester resins, epoxies are used for commercial manufacture of components where a high strength/weight ratio is required [161]. The second area is that, due to their gap filling properties, epoxies can be used as adhesives to many materials such as timber.

Biology

Watersoluble epoxies are commonly used for embedding electron microscope samples in plastic so they may be sectioned (sliced thin) with a microtome and then imaged [162].

Art

Epoxy resins, mixed with pigments, may be used as a painting medium, by pouring layers on top of each other to form a complete picture [163].

Petrochemical

Epoxies can be used to plug selective layers in a reservoir which is producing excessive brine. The technique is named "water shut-off treatment" [164].

Generally, in engineering structures, the strength and toughness of materials are two critical properties that determine the suitability and lifetime of the materials. A wide range of

particle reinforcements have been employed to enhance these two properties in polymers. Nanoparticles have a substantial interface in the polymer matrix and strongly affect the mechanical response of the polymer [165]. Therefore, nanomaterials have the potential to increase both strength and the toughness [166].

The enhancement in strength, stiffness and the fracture toughness by introducing graphene, CNTs, nanoclays and fibers to the epoxy matrix, together with other materials, such as the inclusion of different rubber particles, tailored according to the engineering needs, is a massive bonus for several nanocomposite applications. A lot of critical aspects such as the specific surface area, aspect ratio, filler loading, particle sizes, type of epoxy resin, functionalization and different techniques of the dispersion process have an effect on the performance of the resulting nanocomposite. The dispersion of the nanomaterials has been one of the major contributing factors as well as interfacial adhesion between the nanofillers and the epoxy matrix. Attaining a homogeneous dispersion is one of the main factors in achieving outstanding results [167].

Recently, graphene has attracted a lot of research interest, being at the forefront of nanotechnology [168]. Homogeneous dispersion is well achieved with graphene due to the planar structure, which eases the stress transfer during dispersion. Moreover, graphene requires only a low content ratio to enhance the nanocomposite whereas much higher loadings are required for other fillers [169].

Despite much progress has been achieved in the development of novel fillers for epoxy, challenges still exist in material selection and process design to fulfil the potential use of nanocomposites and improve the performance of epoxybased nanocomposites for advanced industrial applications.

Overall, current studies on epoxy based materials demonstrate that the incorporation of CNTs, graphene, nanoclay and fibers into the epoxy has the potential to significantly

improve the mechanical characteristics of epoxy resin [170]. However, there still exist underlying concerns that need to be fully explored in order to face the future challenges in this evolving field. Despite the fact that a large number of publications emphasize on different functionalisation methods and analyzing the mechanical characteristics of the nanocomposite, less effort has been placed on processing. Moreover, it is vitally important to develop tools and techniques for the quantitative analysis of the extent of the dispersion or agglomeration during the preparation stage for particles.

Graphene is an ideal reinforcement material with unique mechanical, thermal, and electrical properties. Graphene can be prepared using several methods, which are, mechanical exfoliation, chemical vapour deposition and chemical reduction of graphene oxide, etc [171]. Due to its unique properties, graphene is used as advanced filler in polymer matrices. By graphene addition in an epoxy matrix, strength, stiffness, aspect ratio, and other nanocomposite properties can be improved. For mechanical, electrical, and thermal applications, epoxy/graphene nanocomposites have been increasing the focus of attention. These composites are also used in various fields from biomedical to optical and petrochemical applications. The epoxy/graphene nanocomposites are also studied for aerospace and aeronautic relevance. The mechanical, electrical, and thermal properties are advantageous in the utilization of epoxy/graphene nanocomposites.

2.3 Graphene

2.3.1 Introduction to graphene

Since the historical observation of single-layer graphene by Andre Geim and Kostya Novoselov in 2004 [172], this atomically thin carbon film has received ever-increasing attention and became a rapidly rising star on the horizon of materials science [173]. For example, recently the European Commission has financed a 10-year research initiative, the European Graphene Flagship, which provides 1 billion Euro in funding and involves more than 140 academic and commercial institutions in 23 countries [174].

Graphene exhibits many specific and useful properties such as large surface area (2630 m^2/g) [175], excellent thermal conductivity (5000 W/m·K) [176], very high Young's modulus (1 TPa) [177], high value of white light transmittance as to 97.7% [178], and exceptionally high room temperature electron mobility of 2.5×10^5 cm^2/V s [179]. These fascinating properties have attracted extensive research interest in recent years with everincreasing scientific and technological impetus.

For example, as a conductive nanomaterial, graphene can be used for printed electronics beyond conventional siliconbased technologies [180]. For energy storage, Yang *et al.* [181] prepared a supercapacitor with a capacitance of 200-300 F/g. Kim *et al.* [182] used graphene as a transparent electrode and fabricated organic photovoltaic devices; Prasai *et al.* [183] incorporated graphene into organic coatings which significantly enhanced its corrosion resistance. A detailed sketch (Figure 2.3) outlines various types of synthesis routes along with an outline of the general applications of graphene.

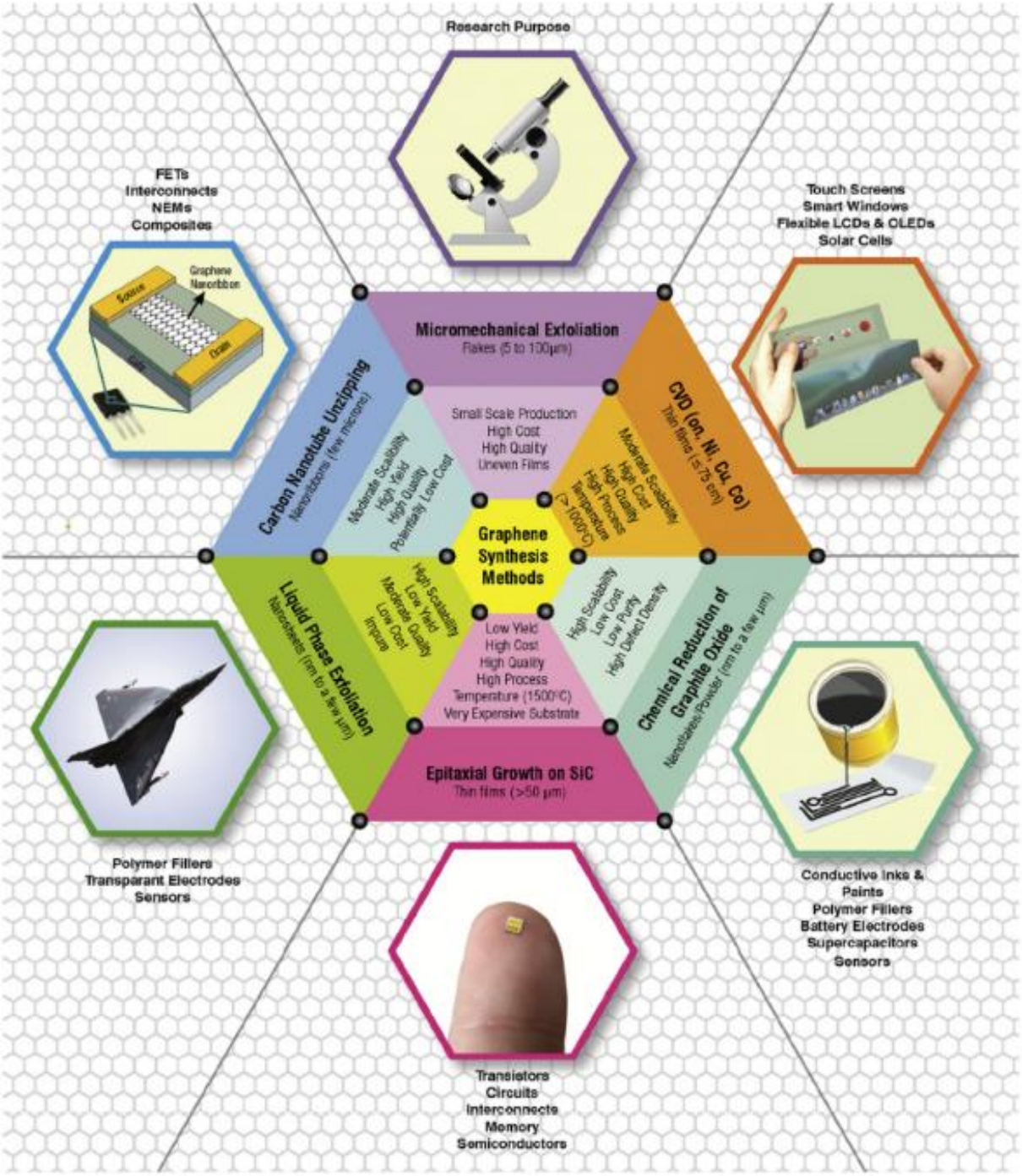

Figure 2. 3. Scheme depicting various conventional synthesis methods of graphene along with their important features, and their current and prospective applications [184].

2.3.2 Fabrication of Graphene

Efforts to exfoliate graphite down to its ultimate constituent can be dated back to 1960s. Fernandez *et al.* [185] extracted millimetre sized graphene sheets (as thin as 5 nm,

about 15 layers) from graphite crystals by micromechanical exfoliation for the very first time. However, it was then until 2004, by repeatedly cleaving a graphite crystal with a scotch tape to its limit, Andre Geim and Kostya Novoselov [172] isolated individual graphene layers, which led to the realization of a dreaming two-dimensional (2D) material and hence for various applications, marking the onset of successful fabrication of graphene.

Micromechanical exfoliation, the top-down method, is a simple peeling process as shown in Figure 2.4. Similarly, ultrasonication will also produce thin graphene sheets [186]. Currently, exfoliation of bulk graphite is the most commonly used method for the mass production of small graphene sheets [187]. This can be through direct exfoliation in a liquid, with or without the use of a surfactant [188], or in the solid state by edge functionalization [189], or by first inserting a chemical species between the graphene layers in graphite to weaken their interaction and then followed by thorough exfoliation [190].

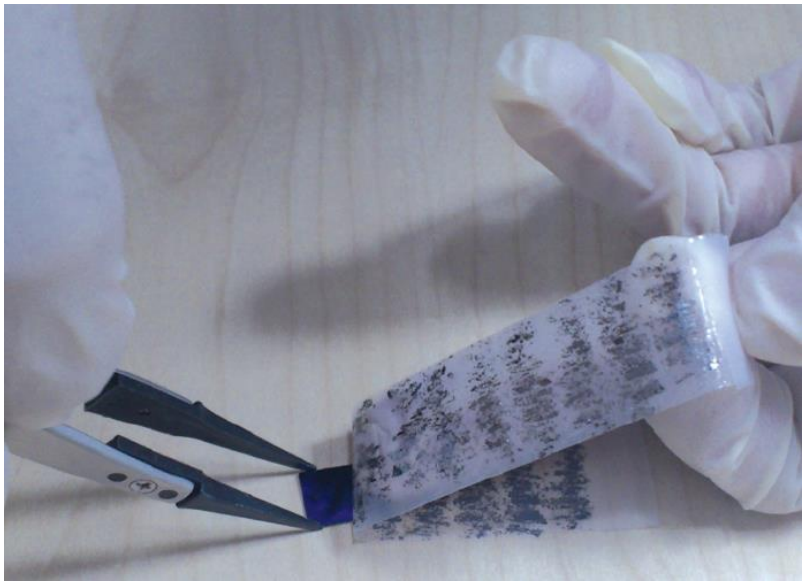

Figure 2. 4. Scotch tape method of graphene synthesis from graphite block [191].

Bottom-up approaches have also been developed such as Chemical Vapour Deposition (CVD) [192]. In a typical CVD process, a substrate is exposed to volatile

precursors in a reaction chamber, the precursors react and/or decompose on the substrate surface to produce the desired deposit [193]. For graphene production, silicon or a transition metal often serves as the substrate, the CVD chamber is vacuumed and heated, under a high temperature and the effect of catalyst, hydrocarbon gases are induced and decomposed. This process deposits a spread of carbon atoms onto the surface of the substrate, thus forming the graphene layers [194].

Another advanced method is the chemical reduction of exfoliated graphene oxide, which is an economical and very practical approach to synthesise graphene [195]. This process takes the advantage of π-π interactions of graphene oxide and aromatic organic molecules such as hydrazine (one of the most effective reductive agents), which can effectively return graphene oxide to its original state [196]. This method maintains graphene's electrical conductivity, flatness and optical properties, but it's not as same as pristine graphene and still contains some significant oxygen groups and a few irreversible lattice defects [197].

There are a number of other growth methods, some of these methods have certain advantages and should be investigated further, such as arc discharge method [198], template route method [199], electrochemical synthesis of graphene [200] and total organic synthesis of graphene [201]. Many studies have been directed towards developing techniques to create singlelayer graphene, however, to date, scalable production of single layer graphene is still at theexploration stage and there is no mature method to produce good quality graphene in mass quantity [202]. In general, mechanical exfoliation, CVD, chemical reduction, and epitaxial growth of graphene are among the most notable techniques in graphene production [203].

2.3.3 Graphene Oxide (GO)

GO is obtained from the exhaustive oxidation of graphite, and contains a range of oxygen functional groups with specific chemistry [204]. It is generally produced by the treatment of graphite using strong mineral acids and oxidizing agents, typically via treatment with $KMnO_4$ and H_2SO_4, as in the Hummers [205] method, or $KClO_3$ (or $NaClO_3$) and HNO_3 as in the Staudenmaier [206] or Brodie [207] methods, or some variation of these methods. There is no unambiguous model to describe the exact structure of GO because there is no single definitive analytical technique available to characterize this material. However, it is generally accepted that the carboxylic groups are mainly located at the edge, while the rest of functional groups (hydroxyl, epoxide, etc.) are present in highest concentration in the basal planes of the graphene layers [208]. Figure 2.5 shows a proposed structure of graphene oxide that is supported by solid-state nuclear magnetic resonance experiments on ^{13}C-labeled GO.

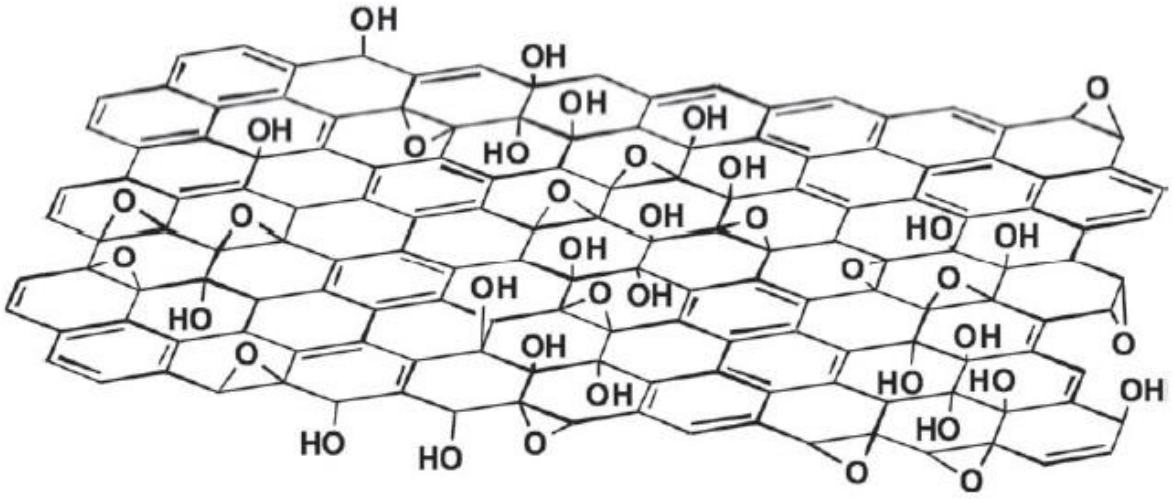

Figure 2. 5. A proposed schematic (Lerf-Klinowski model) of graphene oxide structure [209].

The oxygen functional groups on GO surface are polar and renders GO hydrophilic. GO can be dispersed in many solvents, and particularly well in water [210]. In addition, the most current and promising methods for large-scale production of graphene are based on exfoliation and reduction of graphene oxide [211].

2.3.4 Functionalization of Graphene

Pristine graphene is unsuitable for intercalation with large species, such as polymer chains, because graphene has a pronounced tendency to agglomerate in a polymer matrix [212]. As observed with other nanofillers, the maximum improvements in final properties can be achieved when the filler is homogeneously dispersed in the matrix and the external load is efficiently transferred through strong polymer/filler interfacial interactions [213]. Thus, dispersion and strong interaction between graphene and matrix play important role in the performance of matrix/graphene nanocomposites [214].

The chemical functionalisation of graphene is of significant interest because it can not only improve the solubility and processability, but can also enhance the interactions with the matrix [215-218]. The functional groups attached to graphene can be small molecules [219] or long polymer chains [220], for which various functionalisation approaches have been completed such as covalent and non-covalent functionalisation of graphene [221].

Covalent functionalisation is based on covalent linkage between graphene and other functional groups [222]. The structural alteration can take place at the end of the sheets and/or on the surface [223]. Covalent functionalisation is associated with rehybridisation of one or more sp^2 carbon atoms of the carbon network into the sp^3 configuration accompanied by simultaneous loss of electronic conjugation [224]. The covalent modification of graphene can be achieved in four different ways: nucleophilic substitution, electrophilic addition, condensation, and addition [225]. By conducting an epoxide ring-opening reaction, Yang *et al.* [226] covalently grafted 1-(3-aminopropyl)-3-methylimidazolium bromide onto the surface of graphene sheets. The modified graphene shows enhanced solubility in water, N, N-Dimethylformamide (DMF) and dimethyl sulfoxide (DMSO) at various concentrations, formed long-term stable and homogeneous dispersions.

Non-covalent functionalisation helps in networking or connecting the molecules without actually forming chemical bonds. However, this process requires the physical adsorption of suitable molecules on the graphene surface [227]. This can be achieved by wrapping molecules around the graphene by forming van der Waals bonds between functional groups and graphene, such as π -π interactions, electrostatic attraction, adsorption of surfactants and polymer wrapping [228-231]. For example, Song *et al.* [232] prepared epoxy/graphene nanocomposites with improved mechanical properties and thermal conductivities by non-covalent functionalization of graphene. The modified graphene shows good dispersibility in acetone, DMF, ethanol, pyridine, methanol, tetrahydrofuran (THF) and water, but only short-term stability in iso-propyl alcohol (IPA), dichlorobenzene (DCB), chloroform, dichloromethane and chlorobenzene, because the surface functional group 1-pyrenebutyric acid is not favoured compatible with those solvents.

2.4 Processing of Epoxy/Graphene Nanocomposites

Epoxy and its composites are versatile materials for many industrial fields, such as electrical applications, thermal applications, high-performance nanocomposites in automobiles, and aerospace applications but these composites have some limitations as well. As a new rising carbon allotrope, graphene showed an innovative path to overcome these limitations. The exploration of property enhancement of epoxy/graphene nanocomposites is rapidly advancing as evident in Figure 1.2, which shows the dramatic increase in epoxy/graphene nanocomposites research in recent years.

Obtaining a good distribution of the graphene-reinforcement is one of the greatest challenges in the preparation of epoxy/graphene nanocomposites. A welldispersed state ensures availability of the maximum surface area of filler, which will affect the neighbouring polymer chains and, consequently, the properties of the whole nanocomposite [233]. For

epoxy or any other matrix, dispersion significantly depends on the processing techniques. Significant research has been carried out on the manufacturing techniques for achieving a homogeneous and well-dispersed system [234-240]. The commonly used methods for epoxy/graphene nanocomposites are solution mixing, and recently, a newly emerged method called epoxy impregnation which will be discussed here.

2.4.1 Solvent Processing

The simplest and most widely used method for processing epoxy/graphene nanocomposites is to take advantage of the presence of functional groups attached to the graphene surface which enable the direct dispersion of graphene in water and many organic solvents. This contributes to strong physical or chemical interaction between the functionalised graphene and polymeric matrices [241]. A number of studies explain how the surface modification of graphene has been done by adding various functional groups such as amine [242], organic phosphate [243], silane [244], plasma [245] etc.

Functionalised graphene is normally dispersed in a suitable solvent by, for example, bath sonication, then mixed with epoxy resin, and then thesolvent is evaporated in a controlled condition [246]. The guiding principle is to select solvents compatible with the functional groups on the surface of graphene, ensuring that the functional group is compatible with the epoxy resin as well [247]. To achieve better dispersion of functionalised graphene, many solvents have been investigated. Rafiee *et al.* [248] prepared epoxy/graphene nanocomposites by dispersing graphene platelets in acetone using tip sonication, mixing graphene/acetone solution with epoxy resin and finally removing acetone by heating the mixture to 70 ℃. The prepared nanocomposites showed enhanced mechanical properties and resistance to fatigue crack growth at low graphene concentration (0.1 wt%). Fang *et al.* [249] dispersed graphene in DMF under bath sonication and used modified graphene with amine,

which provided a mechanical adhesion at the graphene-epoxy interface. The nanocomposites showed improved load transfer efficiency between graphene nanosheets and the matrix, accompanied by the enhanced dissipation capacity of nanocomposites for strain energy during fracture. Tang *et al.* [250] investigated the influence of reduced graphene oxide (r-GO) dispersion on the mechanical properties of epoxy resin. They found that with the assistance of ball milling in ethanol solution, the blends showed higher dispersibility, which resulted in higher strength and fracture toughness of epoxy resin as well as improved glass transition temperature (T_g) and electrical conductivity. In addition, they also found that the highly dispersed r-GO resulted in much more tortuous and fine, river-like structures on the fracture surface. This consumes fracture energy in comparison with the poorly dispersed r-GO, effectively improving the fracture toughness of the material. Chatterjee *et al.* [242] investigated the reinforcements of mechanical and thermal properties of a functionalised graphene filled epoxy nanocomposites. The amine functionalised expanded graphene nanoplatelets (GNP) were dispersed within epoxy resins using high-pressure processing followed by three roll milling in acetone. The resulting nanocomposite exhibited significant improvements in mechanical properties and thermal conductivity, indicating a favourable interaction at graphene/epoxy interface. Table 1 shows a summary of representative investigations on the solvent processing, the properties of the nanocomposites with or without graphene had been reported in each work, and the property enhancements by adding graphene have been summarized in the table.

Table 1. Different graphene dispersion method and the property enhancements.

Ref	solvent	filler	dispersion method	% increase in σ	% increase in E	% increase in K_{IC}	% increase in G_{IC}	a[x] increase in κ	folds increase in λ	increase in T_g (℃)	increase in T_d (℃)
[251]	acetone	m-GO	bath sonic + mechanical mix	18.8	42.2	85.7					
[252]	acetone	m-GO	bath sonic + mechanical mix + ball mill	63.2	12					1.6	
[253]	THF	m-G	mechanical mix	-11.1	21.5	103	236.1			11.7	
[254]	THF	m-G	bath sonic + mechanical mix	28	23.6	188.3	597	10			
[255]	acetone	m-GO	bath sonic + mechanical mix + ball mill	47.8	9.5	39	85.7				
[256]	acetone	r-GO	bath sonic + mechanical mix	46	10.9	63.3					
[257]	acetone	m-GO	bath sonic + mechanical mix + ball mill	61.4	16.5	33				3.9	30
[258]	DCM water	m-GO	mechanical mix	31.8						18	
[233]	DMF	m-G	bath sonic	46.2	31.7	127.2				4.9	4.8
[259]	DCM	m-GO	bath sonic + mechanical mix	47.3	21.7						
[260]	acetone	G	bath sonic + mechanical mix	20.2	19.3					11.4	
[261]	acetone	GO	bath sonic + mechanical mix	14.3	24					5.1	
[262]	DMF	m-G	bath sonic	24.4	14.4			7		9.3	4
[263]	acetone	G	bath sonic + mechanical mix	31.8	34.1	75.3		10		7.6	-2

[264]	acetone	GO	bath sonic + mechanical mix		11	76.9				11	
[265]	DCM	m-G	bath sonic	21.2	43.1			10	11		
[266]	water	r-GO	mechanical mix	468	68.7			10		19.6	19
[267]	water acetone	m-GO	bath sonic + mechanical mix	16.5	32	19.6	8.3				
[268]	ethanol	m-G	bath sonic + mechanical mix	47.9	103.3						
[269]	ethanol	m-GO	mechanical mix + ball mill	57.4	8.2						
[250]	ethanol	r-GO	bath sonic + ball mill	7.5	6.1	51.7		3		11.1	
[270]	THF acetone	m-G	bath sonic + mechanical mix	-0.23	0.267	124	292.8			12.2	
[271]	acetone	GO	mechanical mix + 3-roll calendaring	12.3	10	60	116			1.8	
[272]	DMF	m-G	bath sonic	97.2	11.4				-9	8	
[273]	MEK	G							26		
[274]	THF	m-G	bath sonic + mechanical mix	-17.1	21.5	122	205			12.4	
[275]	ethanol	m-Gi	bath sonic + mechanical mix	29.5	42						
[248]	acetone	G	tip sonic + shear mix	41.8	29.8	62.5	128				
[276]	water	r-GO						8			
[244]	water ethanol	m-Gi						7	29		
[277]	DMF	G	bath sonic	16.47	41.37	26.74	26.62			9.49	
[278]	DCB	G	bath sonic	21.12	41.37	26.31	25.16			10.49	
[279]		m-G	bath sonic	23.01	48.27	27.91	27.90			10.88	

As can be seen from table 1, a wide range of solvents have been used for the dispersion of graphene, such as THF, DMF, acetone, ethanol, water, dichloromethane (DCM), methyl ethyl ketone (MEK), etc. Dispersion techniques like tip sonication, bath sonication, mechanical mix, shear mix, and three roll calendaring have been widely adopted for homogeneous dispersion and most of these methods showed good results.

2.4.2 Resin Impregnation

This method refers to the impregnation of epoxy resin into the as-prepared graphene filter cake. It has not been widely reported in literature until recently as a method for preparing polymer nanocomposites. Im *et al.* [280] prepared a 60 wt% nanocomposite material by using this method for the very first time in 2012. They suspended GO particles in water under ultrasonication and then the prepared mixture was poured into a glass mould which was placed on a silicon oxide membrane. The mixture poured into the glass mould was filtered via vacuum filtration. After filtration, the filter cake which was peeled off from the SiO_2 membrane was annealed under heating to remove the residual water. Finally, the epoxy containing the curing agent was dropped onto the filter cake and cured under heating. This method infuses epoxy resin into the graphene sheet by capillarity driven wetting force and is appropriate for fabricating highly concentrated nanocomposites with reasonably high mechanical properties.

A similar approach has been used by Li *et al.* [281] to fabricate an 11.84 wt% epoxy/graphene nanocomposite. They first dispersed graphene platelets in the mixture of ethanol and water by ultrasonication and then removed the solvent by vacuum filtration. During the filtration process, self-assembly of the aligned graphene occurred (Figure 2.6), after which they immersed this aligned graphene into epoxy monomer and curing agent. By this method, they prepared a nanocomposite with aligned multilayer graphene in an epoxy

matrix. The nanocomposite showed a high thermal conductivity of 33.54 W/(m·K) at 90 °C. This remarkable improvement in thermal conductivity was due to the unique alignment structure formed during processing.

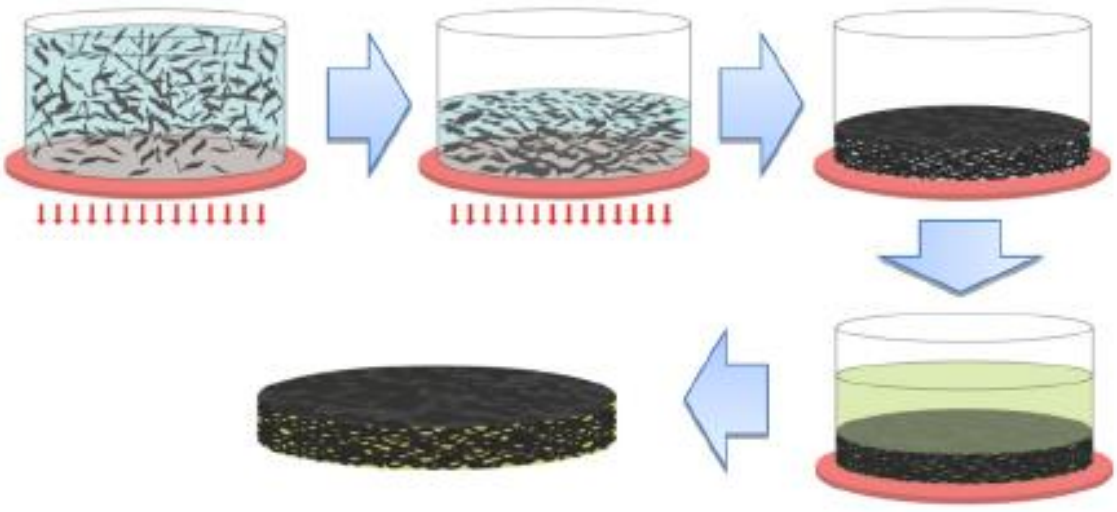

Figure 2. 6. Schematic diagram of the preparation of aligned epoxy/graphene [278].

Low filler percentage nanocomposites can also be prepared by this method. Jia *et al.* [282] reported the synthesis of a 0.1 wt% epoxy/graphene nanocomposite by impregnation of epoxy resin into a threedimensional (3D) graphene-nickel (Ni) foam via chemical vapour deposition, followed by curing of the polymer and etching of the Ni template. This nanocomposite with 0.1 wt% graphene delivered excellent fracture toughness, and the glass transition temperature increased 31 ℃ compared to solid epoxy. More than that, they reported this 3D interconnected graphene network serves as fast channels for charge carriers, giving rise to a remarkable electrical conductivity of the nanocomposite.

2.4.3 Other Methods

The most widely used method to prepare epoxy/graphene nanocomposites is through solvent processing. However, some derivative methods have also been adopted. Martin *et al.*

[283] dispersed graphene in an epoxy monomer by mechanical mixing. The mixture was then mixed with a photo initiator and cured by UV irradiation. They reported an enhancement in thermal and mechanical properties of the nanocomposite as a result of UV curing. Similarly, Sangermano *et al.* [284] prepared UV cured epoxy/graphene nanocomposites and similarly showed enhanced properties. Yu *et al.* [285] used a hot press in the curing procedure to fabricate the epoxy/graphene nanocomposite which showed several folds of increments in thermal conductivity. However, dispersing graphene in the epoxy matrix without using solvent is likely to be less efficient. Hsu *et al.* [286] mixed graphene, epoxy monomer and curing agent all together using three roll milling at room temperature. Uniformly dispersion of graphene was hindered by the high viscosity of the epoxy resin, therefore, mixing without a solvent might be considered as a less effective dispersion strategy.

2.5 Properties of Epoxy/Graphene Nanocomposites

2.5.1 Morphology

As property enhancements strongly correlate with nanocomposite microstructure [287], effective characterization of morphology is important to establish structure-property relationships for these materials.

Transmission electron microscope (TEM) images of these nanocomposites can provide direct observation of dispersed multilayer graphene platelets. Thicker platelets typically show adequate contrast against the epoxy matrix to be imaged without staining, whereas single layer platelets may be difficult to observe directly by TEM [288]. Studies on layered nanofiller based nanocomposites have suggested the existence of three general states of dispersion on short length scales: stacked, intercalated, or exfoliated, as shown in Figure 2.7.

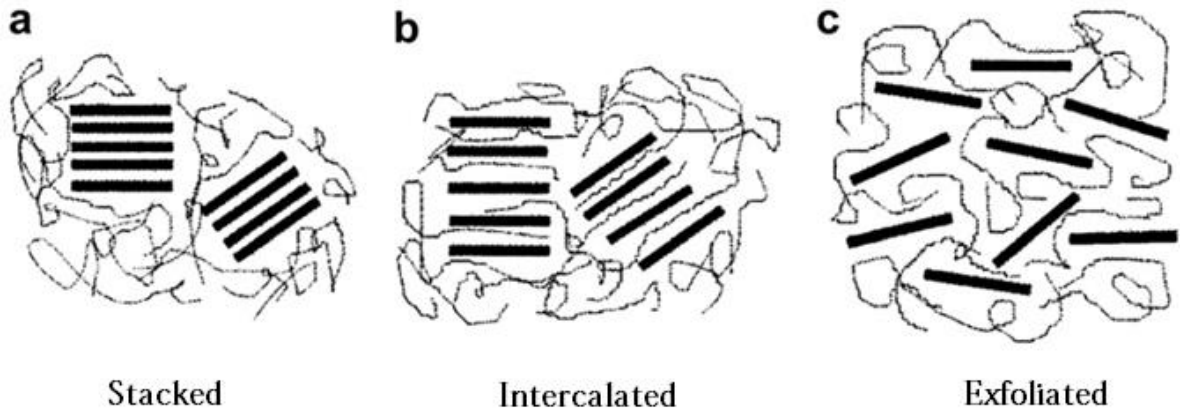

Figure 2. 7. Schematic showing three morphological states for layered nanofillers based nanocomposites [289]: (a) stacked, (b) intercalated, (c) exfoliated.

TEM is the most common method for assessing the state of dispersion. Immiscibility of the phases and/or insufficient exfoliation of the graphite or graphene platelet prior to mixing with epoxy can result in large agglomerates consisting of stacked graphene sheets when observed by TEM. Figure 2.8 shows an accurate measurement of the number of graphene layers in epoxy matrix.

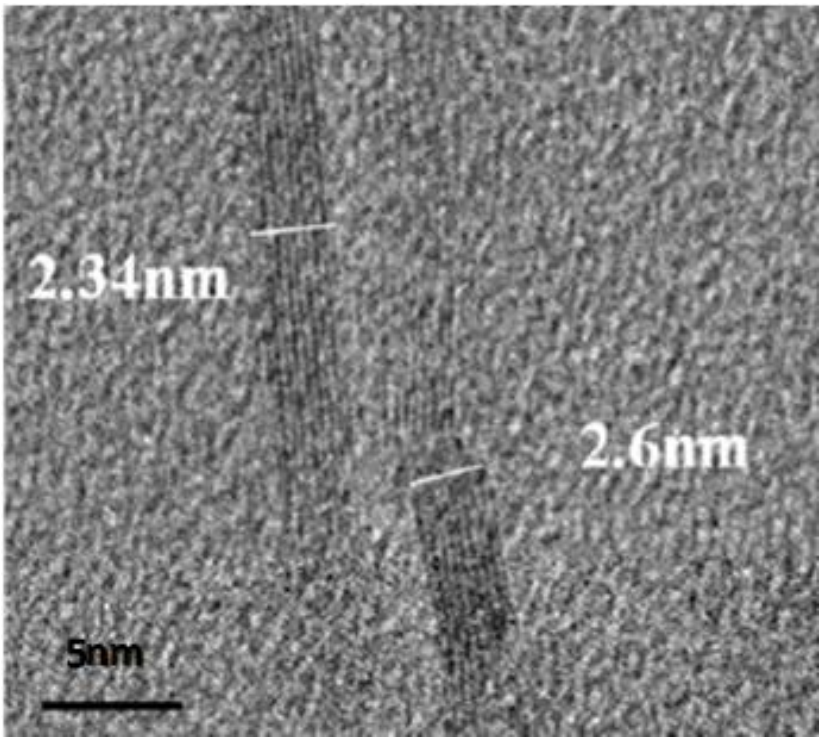

Figure 2. 8. TEM image of layered graphene in epoxy matrix [290].

The drawback of TEM is only a small area of the material can be observed, so cross-sectional analysis using scanning electron microscopy (SEM) has also been implemented to evaluate the dispersion of graphene as well as to examine the fracture surface for filler pull-out, which could give insight into the strength of interfacial adhesion [291]. However, SEM imaging cannot resolve the degree of exfoliation of the platelets and is, therefore, best utilized combined with TEM. Furthermore, atomic force microscope (AFM) and the corresponding height profile graph is an important technique to characterize the pristine or functionalised graphene. The AFM study can give the length and thickness of graphene sheets along with morphology (Figure 2.9). For AFM study, the sample is prepared by dispersing graphene in water or solvents and drop casting on a freshly cleaved mica surface. The dried sample is then observed through the instrument.

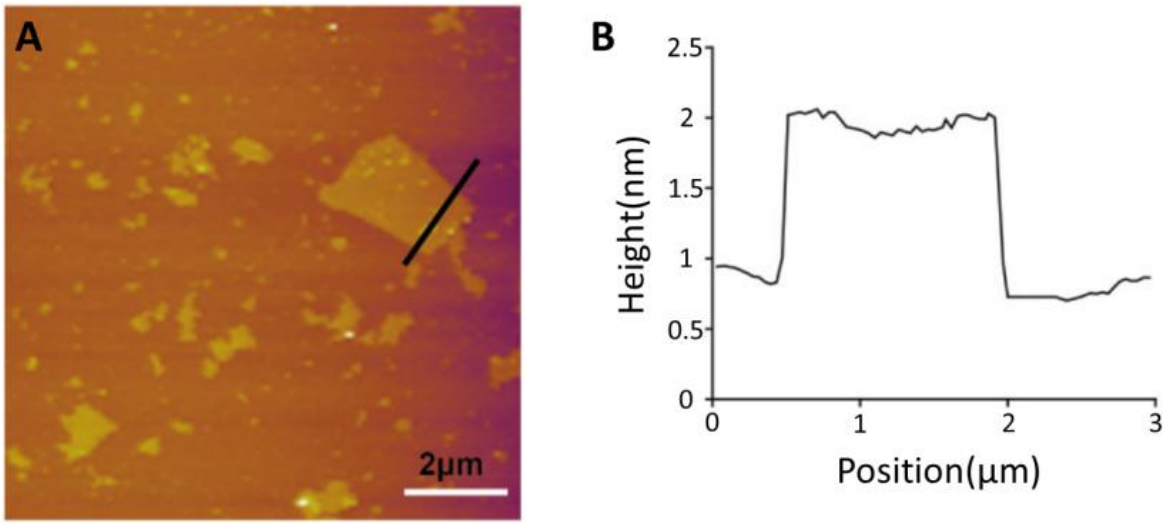

Figure 2. 9. (A) AFM images of graphene; (B) Height profile [292].

2.5.2 Mechanical Properties

As previously mentioned, graphene has excellent mechanical properties, namely, high Young's modulus, high tensile strength, low density, etc [293]. These exceptional properties make graphene an ideal candidate as a filler for nanocomposite materials. Most of the work

on epoxy/graphene nanocomposites is aimed at exploiting the remarkable mechanical enhancement effect of the graphene, coupled with the possibility to introduce further functionalities, such as electrical conductivity [294] or thermal stability [295].

Recently, Bortz *et al.* [271] conducted an investigation on the mechanical properties of epoxy/graphene oxide nanocomposites. The study showed the influence of graphene oxide concentration (0.1, 0.25, 0.5 and 1 wt%) on the fracture toughness and flexural strength of nanocomposites, which are presented in Figure 2.10. The graphs show that with the increase in graphene oxide concentration, the mechanical properties of nanocomposites increased as well. For example, at the concentration of 1 wt%, the nanocomposite showed more than one hundred percent increase in G_{IC}. Qi *et al.* [296] used thermotropic liquid crystalline epoxy to functionalize the graphene surface. The fabricated nanocomposites showed enhancement in tensile strength from 55.43 MPa to 78.96 MPa at 1 wt% accompanied by a nearly one hundred percent increase in impact strength. Similarly, Liu *et al.* [297] investigated the interphase of epoxy/graphene oxide and reported an increase in the modulus and toughness. Fracture toughness and flexural modulus were increased with increasing filler concentration which indicates the significant enhancement effect of graphene in epoxy matrices.

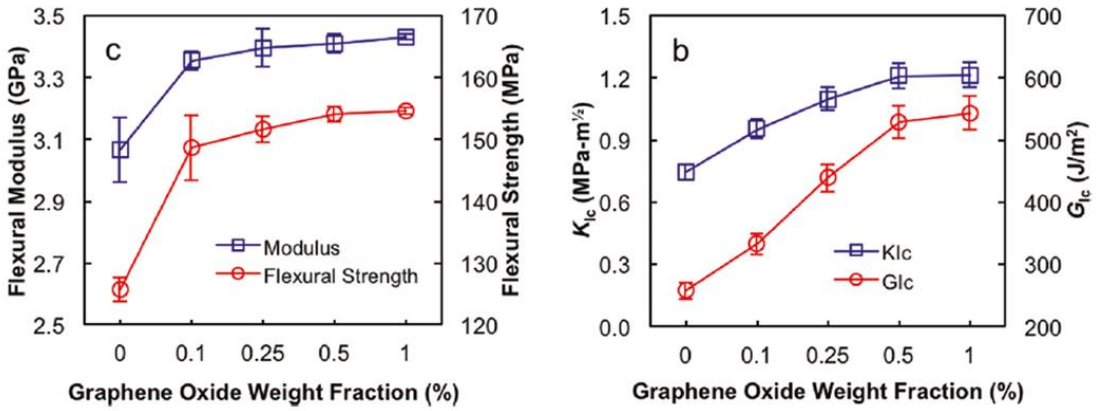

Figure 2. 10. Quasi-static mechanical properties of epoxy nanocomposites [271].

As discussed in previous sections, dispersion of graphene plays a very crucial role in the preparation of epoxy/graphene nanocomposites [298], for which many different techniques have been investigated. A homogenous dispersion could provide better load transfer to filler materials which results in better mechanical properties for the graphene nanocomposites [299]. For example, Li *et al.* [267] incorporated 0.5 wt% silane functionalized graphene into epoxy matrices by mechanical mixing and bath sonication and reported a 20% increase in elastic modulus and a 16% increase in tensile strength as compared to neat epoxy. Similarly, Rafiee *et al.* [248] reported a significant enhancement of Young's modulus at 0.1 wt% of epoxy/graphene nanocomposites processed by shear mixing and tip sonication. In well-dispersed nanocomposites, improved mechanical interlocking with polymer chains and graphene can be observed. Additionally, slipping of entrapped polymer molecules was suppressed, along with improved dispersion, tensile strength, and fracture toughness. Izzuddin *et al.* [270] reported that the presence of good adhesion between graphene and matrix were the main attributes for these increments. To form a strong interface, polyoxyalkyleneamine functionalised graphene was dispersed in epoxy matrices by bath sonication and mechanical mixing, and it was evident that the functionalisation treatment increased modulus and fracture properties of the nanocomposites. In their report, the samples with 0.489 vol% functionalised graphene, showed a 224% improvement in the fracture toughness when compared to the pure resin. Therefore, functionalisation of graphene has significant positive effects on the mechanical properties of epoxy nanocomposites.

2.5.3 Electrical Conductivity

Several studies relating to the electrical properties of polymer/graphene nanocomposites have been conducted [300]. The combination of graphene and polymer matrix offers new, attractive electrical properties and innovative conducting polymers. These

polymers can be used for various engineering applications, such as: electrical conducting adhesives, antistatic coating and films, electromagnetic interference shielding materials for electronic devices, thermal interface materials, etc. [301]. These conducting nanocomposites follow the principle of percolation theory which explains the transition from an insulator to a conductor in materials. The percolation threshold is the concentration at which the electrical conductivity of an insulating polymer matrix increases dramatically. A conductive continuous network of filler is created and electrons can be transported by direct contact among nanofiller particles; beyond this concentration, the conductivity of the nanocomposite increases marginally [302].

Electrical conduction in a nanocomposite is due to the formation of a continuous conductive network formed by the fillers. Therefore, the aligned nanofillers have higher probabilities to percolate at lower volumetric concentrations than spherical nanofillers [303]. Graphene becomes an ideal candidate to achieve this percolated network at low loading fractions due to its intrinsically high conductivity and its 2D structure. Wajid *et al.* [262] reported the ultra-low electrical percolation threshold at 0.088vol% in epoxy/graphene nanocomposites, by dispersing graphene with the assistance of tip sonication, mechanical mixing, and shear mixing. Similarly, Liang *et al.* [276] also reported a significant increase in the electrical conductivity by incorporating graphene in epoxy nanocomposite matrices through bath sonication and mechanical mixing. The conductivity was improved from 0.8 x 10^{-10} to 0.8 x 10^{-2} by incorporating 8 vol% reduced graphene oxide into epoxy. Such improvements are only possible when graphene is thoroughly de-bundled and homogeneously dispersed in the epoxy matrix. Monti *et al.* [304] dispersed graphene into epoxies to study the electrical conductivities. To improve dispersion, they processed the mixture through tip sonication and mechanical mixing, and used different solvents such as chloroform or THF. The highest electrical conductivity was observed for a sample with 3 wt%

graphene. It was also shown that the thermal conductivity increased with the increase of graphene concentration.

2.5.4 Thermal Conductivity

As opposed to the electrical conductivity, the thermal conductivity of epoxy/graphene nanocomposites has received less attention to date. Compared to electrical conductivity enhancements of several orders of magnitude, thermal conductivity enhancement by carbon nanofillers is not as significant [305]. However, a noteworthy increase in thermal conductivity can easily be obtained, as it has been reported that the 2D shape platelets like graphene nanosheets can improve thermal conductivity more effectively than 1D rod like carbon nanotubes (CNT) [244, 306]. As given by Kapitza resistance, the transfer of thermal energy is carried out by the free electron interaction and lattice vibration between the two contacted interfaces, poor coupling at the filler/polymer interfaces will significantly impact on thermal resistance [307]. Hence, a strong filler/polymer interface is required to achieve good thermal conductivity [308].

Veca *et al.* [306] applied alcohol and oxidative acid treatment with the assistance of extended and vigorous sonication to thermally expanded graphite. Carbon nanosheets were found well dispersed in the epoxy matrix with a thickness of less than 10 nm. The incorporation of 33 vol% carbon nanosheets could improve the in-plane thermal conductivity of epoxy nanocomposites to 80 W/(m·K). However, the cross-plane thermal conductivity was found to be only one-tenth to one-fifth of the average in-plane value. This highly anisotropic nature resulted from the 2D structure of the graphene sheets. Wang *et al.* [309] reported that 5% graphite oxide (prepared via thermal expansion) increased the thermal conductivity of epoxy to over 0.8 W/(m·K) and decreased the coefficient of thermal expansion by 31.7% below T_g. Ganguli *et al.*[244] found that 20 wt% silane functionalised, thermally expanded graphite

enhanced the thermal conductivity of epoxy from 0.2 to 5.8 W/(m·K). Interestingly, it was discovered that silane functionalisation could form covalent bonding with epoxies and improve the interfacial heat transfer between two components by reducing acoustic impedance mismatch in the interfacial area. However, excessive functionalisation also tends to reduce the intrinsic thermal conductivity of carbon materials. Figure 2.11 shows a larger contribution of graphene for the thermal conductivity of the epoxy matrix as compared to CNTs and carbon black.

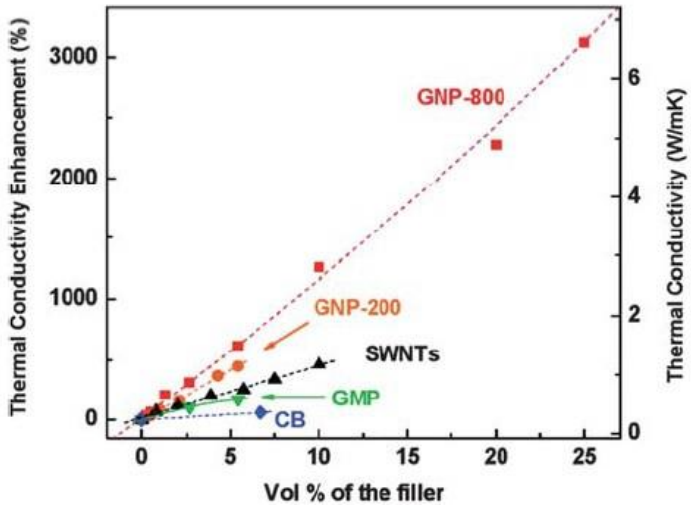

Figure 2. 11. Thermal conductivity enhancement of epoxy-based nanocomposites [310]. Utilized fillers: graphitic microparticles (GMP), GNPs exfoliated at 200 ℃ (GNP-200) and 800 ℃ (GNP-800), carbon black (CB) and SWNTs.

2.5.5 Thermal Stability

Several studies have evaluated the effect of graphene on the thermal properties in many polymer matrices, such as thermal degradation temperature [311], glass transition temperature [312], melting temperature [313], and polymer crystallinity of the nanocomposites [314]. However, there is no melting temperature for epoxy because of its thermosetting nature, therefore glass transition and thermal degradation behaviours are among the most important properties used to characterize the thermal stability of epoxy

nanocomposites. It is generally observed that graphene enhances the T_g of epoxy matrices [315]. This is due to the adhesion force between epoxy and graphene which reduces the mobility of epoxy chains on graphene surfaces. Contrarily, a decrease in T_g is expected for weakly adhering fillers and unstable interfaces facilitating the chain polymer mobility, thus lowering the T_g [316]. Li *et al.* [317] reported the increase in T_g of epoxy by hindering the segmental motion of polymer chains via mechanical interlocking and hydrogen bonding with surface oxygen functionalities. Similarly, a T_g increase of 14 ℃ in epoxy/graphene nanocomposites has been measured by Park *et, al.* [318] at 1 phr (parts per hundred resin) of graphene in epoxy matrices. This is an expected outcome of the strong filler-matrix adhesion and the conformational changes of the epoxy matrix at the epoxy/graphene interface.

Conversely, a significant volume of research reported the opposite trend and will be discussed here. It has been vastly reported that graphene reduces the glass transition or thermal degradation temperature of epoxy matrices and there is no unanimous agreement for this negative trend. Galpaya *et al.* [319] proposed the theory that the T_g of nanocomposites depends on the balance of two effects, i.e., influence on reaction conversion and molecular confinement. Graphene sheets are stiffer than epoxy matrix which could lead to significant confinement on the polymer chains. On the other hand, graphene sheets may impede the epoxy curing reaction. This could be explained by the functional groups on graphene surface reacting with the curing agent and/or epoxy resin, or graphene sheets covering the reactive sites in the resin due to its high surface area. If the latter plays the dominant role, this would be expected to reduce the polymer cross-link density and would also increase polymer chain mobility. Liao *et al.* [222] and Kim *et al.* [275] reported similar conclusions as well. According to them, the incorporation of graphene reduces the cross-link density of the epoxy matrix as well, which results in the decrease of T_g. Some research groups like Saur ń *et al.* [320], Liu *et al.* [321], and Guo *et al.* [243] reported that graphene acts as are active

plasticizer and has a plasticizing effect on epoxy resin, thus increasing the flexibility of chain segments of the epoxy matrix. Liu *et al.* [272] prepared an epoxy/imidazole functionalised graphene nanocomposite and reported that the short molecular chains of the functional group on the graphene surface are flexible and would result in an overall T_g decrease. There are also some other claims, such as Liu *et al.* [322] incorporated edge-functionalised graphene into epoxy resin and found that the T_g decreased because of the existence of graphene sheets that could result in increased flexibility of the network. Zhang *et al.* [323] prepared magnetic graphene reinforced epoxy nanocomposites and reported that the rigid structure of graphene nanoplatelets would cause extra enlarged free volume, which is detrimental to the thermal stability of the matrix.

Reportedly, thermal decomposition temperatures (T_d), which are characterized by the maximum weight loss rate in thermogravimetry, shift up 30 ℃ for epoxy nanocomposites by incorporating 0.5 wt% functionalised graphene [257]. Decomposition of graphene nanocomposites is substantially slower than neat epoxy, which is attributed to the restricted chain mobility of polymers near the graphene surface. Similarly, Prolongo *et al.* [324] reported that 0.5 wt% graphene nanoplatelets can push the thermal degradation temperature of epoxy from 377 ℃ to 397 ℃. Yousefi *et al.* [266] reported that both graphene oxide and reduced graphene oxide improved the thermal decomposition temperature of epoxy matrices. Figure 2.12 shows the shift in thermal gravimetric analysis (TGA) curves to higher temperatures, which means a higher thermal stability, due to the incorporation of graphene.

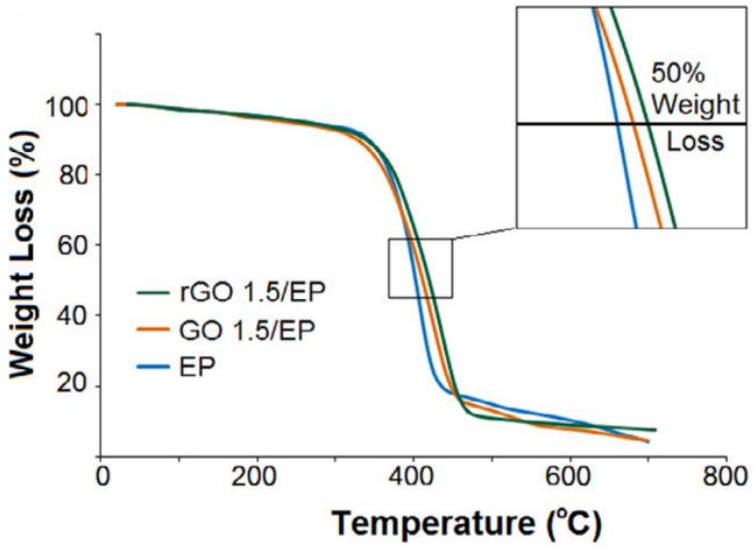

Figure 2. 12. TGA curves of epoxy nanocomposites containing GO and r-GO [266].

Wang *et al.* [325] *and* Xin *et al.* [326] incorporated functionalised graphene into epoxy matrices and reported a decrease in T_d. This was due to the presence of thermally unstable chemicals, which, on decomposition, lowered T_d when compared to monolithic epoxy. Feng *et al.* [263] used epoxy resin to modify graphene first, and then mixed with the epoxy matrix. They found that in some cases, the T_d of the nanocomposite decreased because the filler might cause defects in the polymeric networks during the curing.

In general, it is widely acknowledged that graphene could enhance the thermal stability of epoxy. However, there are still many controversies wherein many researchers reported a decrease in thermal properties of epoxy with the incorporation of graphene. The reason of such has not been fully explained and requires deeper understanding via extensive further research.

2.5.6 Flame Retardant Properties

Engineering materials are required to resist degradation during in an unlikely event of a fire in many critical applications like skyscrapers, boats, or aeroplanes [327]. In fact, some

studies reported that about 20% of victims of aeroplane crashes are killed not by the crash itself but by ensuing fires [328]. Materials used in aviation should be designed to inhibit, suppress, or delay the production of flames to prevent the spread of fire. Flame retardant materials are mainly based on halogen, phosphorus, inorganic, and melamine compounds [329], however, among these flame retardants, only inorganic fillers are normally nontoxic [330]. Current research on epoxy/graphene nanocomposites has been focused on improving the flame retardant properties such as the ease of ignition, limiting oxygen index, the rate of heat release, and the evolution of smoke and toxic gases by incorporating modified graphene, along with improving the physical properties of the epoxy matrix [331-333]. For example, Li *et al.* [334] used 2-(Diphenylphosphino)ethyltriethoxy silane modified graphene oxide, and then incorporated this modified graphene oxide into an epoxy matrix. They found that the limiting oxygen index increased from 20 to 36, which means a huge transition of material's mature from flammable to non-flammable. Jiang *et al.* [335] prepared epoxy/graphene-ZnS nanocomposites and reported that with the incorporation of ZnS decorated graphene, the carbon monoxide production rate for the nanocomposites is much lower than that of pure epoxy along with a decreased total smoke release. Wang *et al.* [10] prepared Ni-Fe Layered Double Hydroxide (LDH) modified graphene/epoxy nanocomposites. They found that with the incorporation of 2 wt% Ni-Fe LDH modified graphene, the time of ignition of epoxy matrix increased from 68s to 89s, the total heat release decreased from 113.1 MJ/m^2 to 44.2 MJ/m^2, and the fire growth index decreased from 13.3 $kW/m^2 \cdot s$ to 4.8 $kW/m^2 \cdot s$. Figure 2.13 shows the drastic decrease of heat release rate with the incorporation of graphene and Ni-Fe LDH modified graphene.

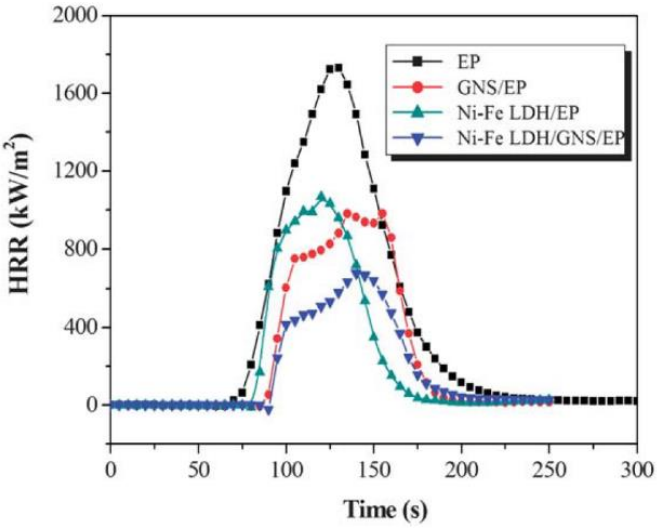

Figure 2. 13. Heat release rate versus time curves of epoxy and its nanocomposites [10].

Zhuo *et al.* [336] proposed a flame retarding mechanism for polymer matrix when filled with graphene. According to Zhuo *et al.* [336], the barrier effect of graphene plays a dominant role in flame retardancy. Graphene walls make excellent gas barriers, which delay the oxidative degradation of epoxy during a fire, moreover, the large surface area of graphene can induce a large amount of char which prevents the resin from suffering from heat fatigue.

In general, the addition of graphene into epoxy matrix results in improving flame retardancy and thermal stability of epoxy along with improved mechanical properties. Moreover, no environmental or toxicity issues have been reported for graphene and, therefore, it can be concluded that graphene has a great potential to be one of the most promising flame retarding fillers for nanocomposites in near future.

2.5.7 Synergic Effects with Other Fillers

Synergic effect or hybridisation means incorporation of two or more fillers together for enhanced functionality which is not possible to achieve with single filler alone. Recently, a tremendous research effort was undertaken to generate enhanced properties by synergistically combining different fillers as reported by Inam *et al.* [337]. The group

fabricated multiscale epoxy composites which showed enhanced mechanical properties with the combination of carbon nanotubes and carbon fibers. Chatterjee *et al.* [338] found that the CNT:GNP ratio is an interesting factor influencing the properties of the epoxy-based nanocomposites. At a nanofiller concentration of 0.5 wt%, highest CNT content (9:1) showed marked improvement in fracture toughness of 76%. Kumar *et al.* [339] suggested that by bringing together two nanofillers like CNT and GNP, they could form a co-supporting network. This net-like structure could shield the fillers from fracture and damage during processing, while still allowing full dispersion of both fillers during high power sonication, thus resulting in improved properties. Apart from the mechanical properties, the incorporation of carbon fillers into polymer matrices attained significance for the applications within which enhanced thermal and electrical conductivity were required together. Epoxy resins containing a binary mixture of GNP and single wall carbon nanotube (SWCNT) in 3:1 weight ratio have higher thermal conductivity than those reinforced with either individual fillers. Yu *et al.* [340] explained this synergistic effect by bridging interactions between GNP and SWCNT which can reduce the interfacial resistance for thermal conduction. Additionally, a remarkable synergetic effect between graphene platelets and multi-walled carbon nanotubes (MWCNTs) in improving the mechanical properties and thermal conductivity of epoxy nanocomposites was demonstrated by Yang *et al*. Both the tensile strength and thermal conductivity were increased by 35.4% and 146.9% respectively by using MWCNT/graphene fillers as compared to either filler for epoxy nanocomposites. They found that stacking of individual 2D graphene is effectively inhibited by introducing 1D MWCNTs. Long and tortuous MWCNTs can bridge adjacent graphene platelets and inhibit their agglomeration, resulting in a high contact area between the MWCNT/graphene structures and the polymer matrix [314].

In general, the exact mechanism responsible for this dramatic enhancement is not entirely understood. It is widely believed that molecular level interactions between the

nanomaterials and polymer matrices play a major role. The large interface area available for such interactions clearly holds the key for the dramatic enhancement in mechanical properties [341]. Table 2 lists some representative papers which adopt multi filler or hybridisation approach to modify the properties of the epoxy matrix.

Table 2. Synergic effect of graphene and other fillers in an epoxy matrix.

reference	filler	dispersion method	% increase in σ	% increase in E	% increase in K_{IC}	% increase in κ	% increase in λ	% increase in T_g	% increase in T_d
[342]	G + CNTs	bath sonic + mechanical mix				10			
[343]	G + capron	mechanical mix						31	
[344]	G + CNTs	bath Sonic	-23	-11.5		4			
[325]	GO + carbon fiber		15.1	20.2				9	
[345]	r-GO + CNTs	3-roll calendaring + shear mix						4	
[346]	GO + CNTs	bath sonic + mechanical mix							
[326]	G + glass fiber	shear mix	-16.3	-8.9				-9	-16
[338]	G + CNTs	bath sonic + 3-roll calendaring + high pressure homogenizer			78		84.2		
[280]	GO + CNTs	mechanical mix							
[314]	G + CNTs	bath sonic + shear mix + mechanical mix	0.9	23.1			23.8		

2.6 Summary

Graphene shows great potential as filler for the next generation of advanced nanocomposite materials. Numerous efforts have been made to prepare useful epoxy/graphene nanocomposites. However, the development and applicability of epoxy/graphene nanocomposites will be significantly related to the dispersion and the interfacial bonding of graphene in an epoxy matrix, which are the two most critical factors to determine the performance of these new nanocomposites. Thus, the key to preparing advanced epoxy/graphene nanocomposites is to improve the techniques for the dispersion of graphene and the engineering of the graphene-epoxy interface. This review provided a detailed introduction of epoxy/graphene nanocomposites and the critical analyses on recent research investigations. The following conclusions can be drawn from the existing reported research:

• Graphene has significant potential for epoxy-based composites. Extremely enhanced multi-functional properties can be achieved, subject to homogenous dispersion and strong interfacial interactions. Chemical functionalisation of graphene can also significantly improve the graphene-epoxy interfacial interactions.

• Solvent processing is the most widely adopted method to prepare epoxy/graphene nanocomposites. The high viscosity of epoxy may hinder the uniform dispersion of graphene and therefore, it is also difficult to adopt a solvent-free processing approach.

• Mechanical properties, electrical conductivity, thermal conductivity, thermal stability and flame retardant properties are generally increased with the incorporation of graphene.

• Graphene could increase the glass transition and thermal degradation temperatures of the epoxy nanocomposite. However, this needs to be further explored as some investigations have reported a negative trend.

In general, epoxy/graphene materials have remarkably high thermal and electrical

conductivities, as well as improved mechanical strength and thermal stability. Because of these excellent properties, graphene reinforced epoxy nanocomposites possess great potential to be used in automotive, electronics, aerospace and etc. However, further work is still required to understand this particular area fully before such applications can be materialised.

3 Experimental

3.1 Materials

3.1.1 Epoxy Matrix System

The epoxy matrix used in this study consists of EPOPHEN^{TM} EL5 bisphenol A based liquid epoxy (EP) and EPOPHEN^{TM} EHA57 diamine hardener (HD), purchased from Polyfiber UK Ltd. This epoxy system is a multi-purpose resin offering good all-round properties with the epoxy group content of 4.76-5.25 mol/kg. The viscosity of the epoxy resin and the hardener are 12000-15000cps and 45cps respectively at room temperature. To prepare cured epoxy (EP+HD), the mix proportions are 50 parts by weight of hardener to 100 parts by weight of liquid epoxy.

3.1.2 Graphene

Graphene was purchased from Graphene Laboratories Inc. USA, (product name: AO-3). The graphene nanoplatelets have a specific surface area of 80m^2/g, an average lateral size of 4.5μm, and an average thickness of 8nm. Figure 3.1 shows the SEM images of the as received graphene nanoplatelets.

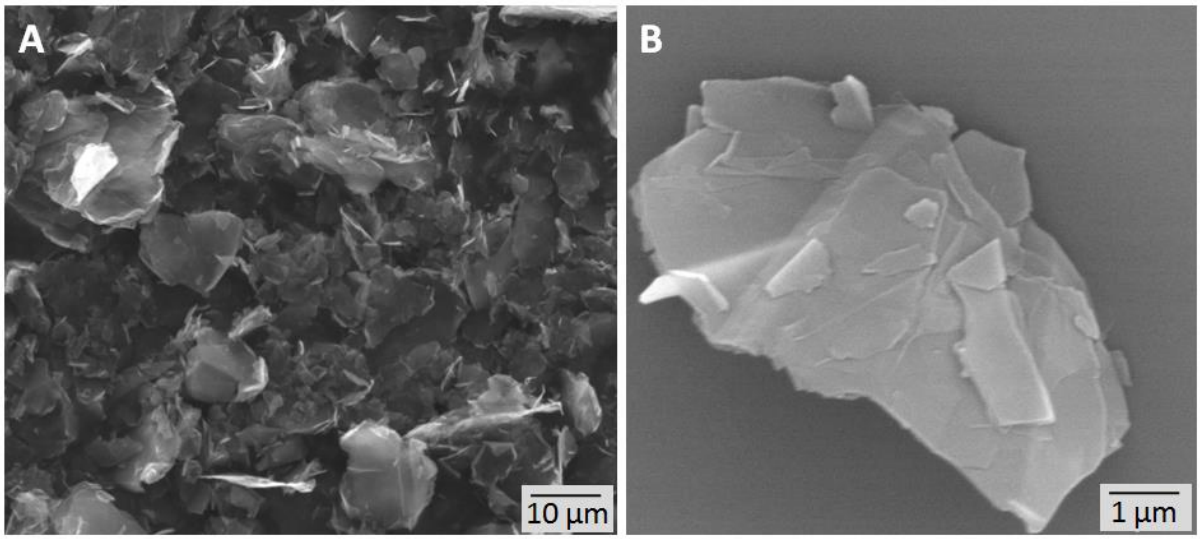

Figure 3. 1. SEM images of graphene nanoplatelets: (A) Graphene clusters; (B) one single piece of graphene nanoplatelet.

3.2 Sample Preparation

Firstly, graphene was dispersed in a solvent with bath sonication, then epoxy monomer was added, the mixture was then heated with magnetic stirring to remove the solvent. Subsequently, the mixture was cooled down to room temperature and the hardener was added, vacuum degassing was then carried out to remove the entrapped air bubbles. Lastly, the mixture was mold casted and epoxy/graphene nanocomposites had been made. Figure 3.2 shows the schematic of the sample preparation. However, for each experimental part, the sample preparation processes are slightly different and will be introduced in each chapter separately.

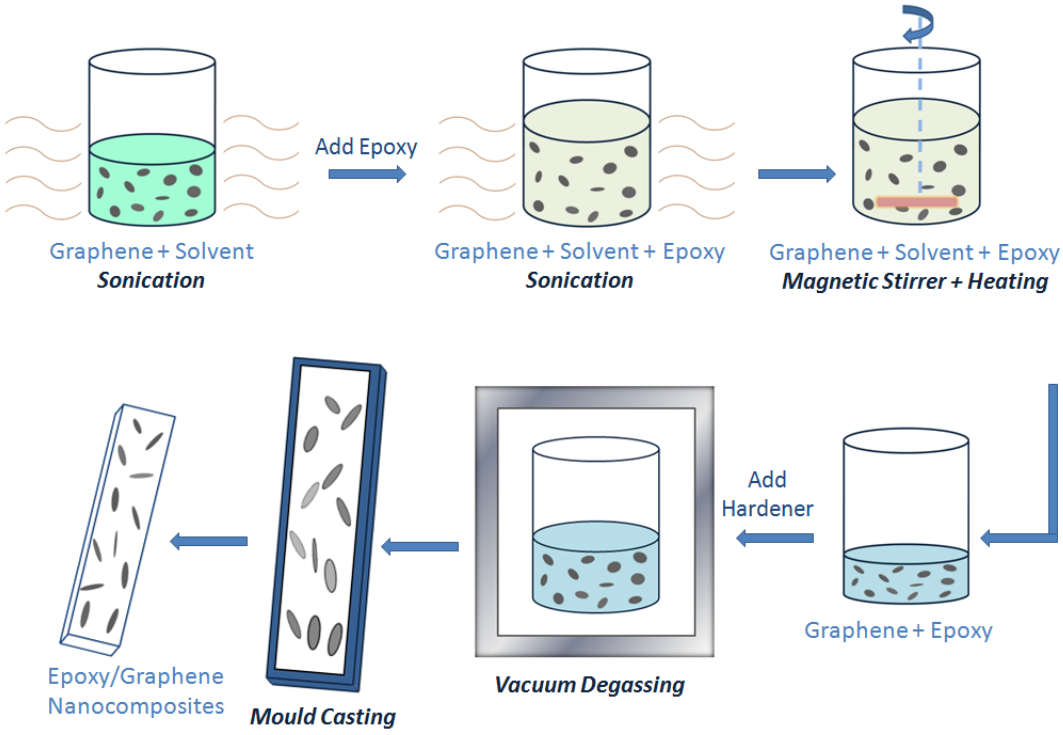

Figure 3. 2. Schematic of the preparation of nanocomposites.

3.3 Characterization

3.3.1 Tensile Test

Tensile tests were conducted on a Universal Testing Machine (Instron 3382), the crosshead speed was kept at 2mm/min for all tests. The tensile tests were conducted according to ASTM D638 (Type V geometry) with the specimen thickness of 4mm. Tensile strength (σ) was calculated using Equation (1),

$$\sigma = \frac{F}{A} \tag{1}$$

where F is the load applied on the material at the fracture point and A is the cross-sectional area through which the force is applied. Tensile modulus (E) was calculated using Equation (2),

$$E = \frac{\sigma}{\varepsilon} \tag{2}$$

where σ is the tensile strength and ε is the extensional strain. Six specimens were tested for all sets of conditions and mean values were then reported.

3.3.2 Flexural Test

Three-point bend flexural tests were also conducted on Universal Testing Machine (Instron 3382), the crosshead speed was kept at 2mm/min for all tests. A rectangular specimen was used to determine the flexural strength and flexural modulus according to ASTM D790, the specimen dimensions were 3 × 12.7 × 70mm. The flexural strength σ was calculated using Equation (3),

$$\sigma = \frac{3FL}{4wh^2} \tag{3}$$

where F is the load applied on the material at the fracture point, L is the length of the support span, w is the width and h is the thickness of specimen. The flexural modulus was calculated using Equation (4),

$$E = \frac{L^3 F}{4wh^3 d} \quad (4)$$

where d is the deflection due to the load and F is the load applied at the middle of the beam. Six specimens were tested for all sets of conditions and mean values were then reported.

3.3.3 Fracture Test

Fracture toughness tests were conducted on the Universal Testing Machine (Instron 3382), the crosshead speed was kept at 2mm/min for all tests. A single-edge-notch three-point bending (SEN-TPB) specimen was used to determine Mode-I fracture toughness (K_{1C}) according to ASTM D5045, the specimen dimensions were 3 × 6 × 56mm with a crack length of 3mm. The K_{1C} was calculated using Equation (5),

$$K_{1C} = \frac{P_{max} f(\frac{a}{w})}{BW^{1/2}} \quad (5)$$

where P_{max} is the maximum load of the load-displacement curve, $f(a/w)$ is the constant related to the sample geometry and was calculated using Equation (6), B is sample thickness, W is sample width, and a is crack length (kept between 0.45 W and 0.55 W). The critical strain energy release rate (G_{1C}) was calculated using Equation (7) where E is the Young's modulus obtained from the tensile tests (MPa), and v is the Poisson's ratio of the polymer, taken to be 0.35.

$$f\left(\frac{a}{w}\right) = \frac{\left[\left(2 + \frac{a}{w}\right)\{0.0866 + 4.64\left(\frac{a}{w}\right) - 13.32\left(\frac{a}{w}\right)^2 + 14.72\left(\frac{a}{w}\right)^3 - 5.6(\frac{a}{w})^4\}\right]}{(1 - \frac{a}{w})^{3/2}} \quad (6)$$

$$G_{1C} = \frac{{K_{1C}}^2 (1 - v^2)}{E} \quad (7)$$

The schematics of the testing specimens are shown in Figure 3.3.

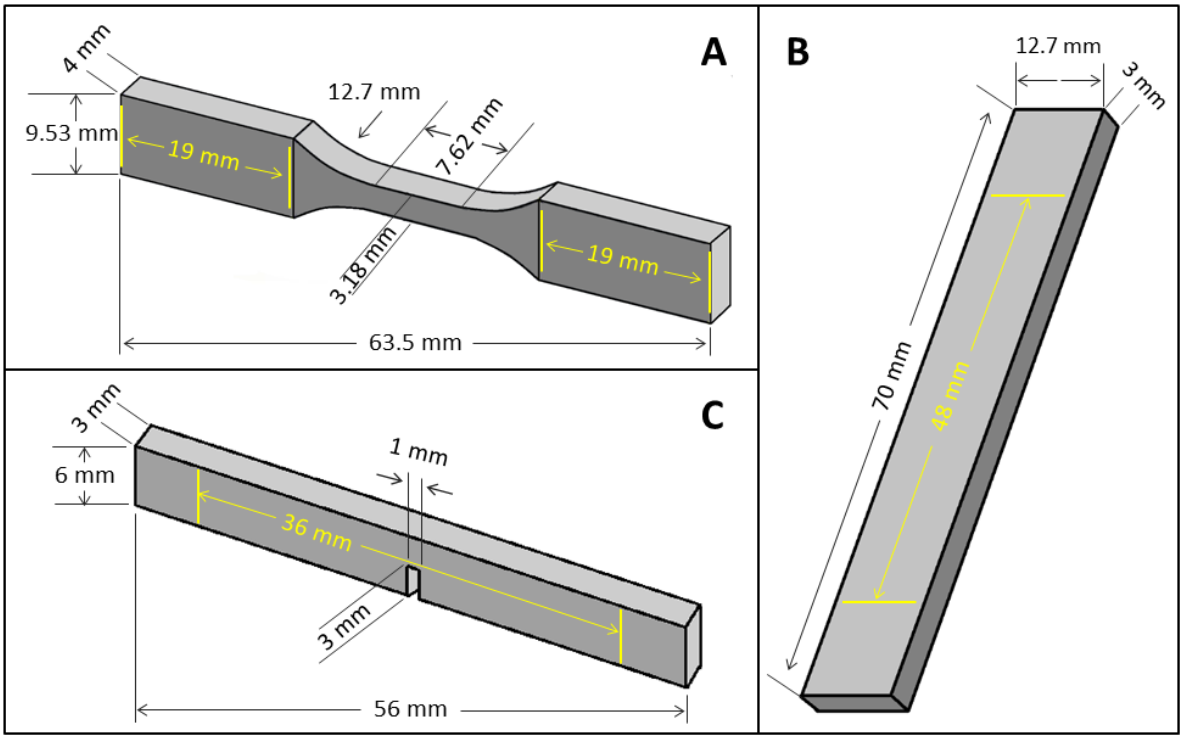

Figure 3. 3. Schematics of mechanical test specimens: (A) Tensile; (B) Three-point bend; and (C) Fracture toughness.

3.3.4 Vickers Hardness Test

Vickers hardness (*HV*) was tested by Buehler Micromet II, a load of 200g was applied for 10 seconds on each sample. The *HV* was calculated using Equation (8),

$$HV = \frac{F}{A} \tag{8}$$

where F is the force applied to the surface of the sample and A is the surface area of the resulting indentation. Six specimens were tested for all sets of conditions and mean values were then reported.

3.3.5 DMA Test

Dynamic Mechanical Analyzer (DMA) (Model 8000, Perkin Elmer) was used to determine the storage modulus (E') and loss factor tan δ. Rectangular specimens with

dimensions of 2.5 × 8 × 30mm were tested in single cantilever mode. All tests were carried out using the temperature sweep method (temperature ramp from 30 to 150 ℃ at 5 ℃/min) at a constant frequency of 1Hz. The glass transition temperature (T_g) was taken as the temperature value at the peak of tan δ curves.

3.3.6 TGA Test

Thermogravimetric analysis (TGA) of the nanocomposites was carried out with a TA Instruments Q500 thermal analyzer. The temperature range was from room temperature to 600 ℃ at a ramp rate of 5 ℃/min under N_2 atmosphere. Sample weight was around 5-10mg.

3.3.7 SEM Test

Scanning electron microscopy (SEM) analysis was carried out by an FEI Quanta 200 electron microscope on the fracture surface of nanocomposites with an electron beam of 5 kV to evaluate the fracture modes in the samples. A layer of gold with 10nm thickness was applied on the fracture surface using Emscope sputter coater model SC500A.

3.3.8 FTIR Test

Fourier Transform Infrared Spectroscopy (FTIR) was carried out at room temperature by the FTIR spectrophotometer (Perkin Elmer, L1185247). The sampling area of the chamber was pre-rinsed with acetone. FTIR was used to verify the surface chemical groups of graphene.

3.3.9 XRD Test

X-ray diffraction (XRD) test was carried out with a Siemens D-5000 diffractometer using a Cu Kα radiation source (λ = 0.154 06 nm) with a step size of 0.02 ° to examine the structure of the epoxy/graphene nanocomposites.

3.3.10 UV-Vis Test

Light transmittance in the UV-Visible spectroscopy (HITACHI U-3000) has been used to quantify the reagglomeration of graphene in the epoxy system through a series of controlled experiments. Tests were always carried out immediately after the sonication of each dispersion. Standard polystyrene cuvettes with an optical path length of 10mm were used for transmittance measurements. The light transmittance of the graphene dispersions were recorded at a fixed wavelength of 450nm.

3.4 Experimental variables

To carry out this study, different parameters had been investigated, the experimental variables are listed in Table 3. Detailed experimental methods will be introduced in each chapter separately.

Table 3. Lists of experimental variables.

<table>
<tr><td rowspan="4">Chapter 4</td><td>Sonication time</td><td rowspan="4">Chapter 7
Part I</td><td>DMF-100</td></tr>
<tr><td>Storage time</td><td>DMF-300</td></tr>
<tr><td>Concentration</td><td>DMF-500</td></tr>
<tr><td>Sonication temperature</td><td>DMF-1500</td></tr>
<tr><td rowspan="3">Chapter 5</td><td>Hand Mix</td><td rowspan="3">Chapter 7
Part II</td><td>DCB</td></tr>
<tr><td>Tip Sonication</td><td>Ethanol</td></tr>
<tr><td>Bath Sonication</td><td>DMF</td></tr>
<tr><td rowspan="4">Chapter 6</td><td>0.1wt%</td><td rowspan="2">Chapter 8</td><td>SDS</td></tr>
<tr><td>0.3wt%</td><td>GA</td></tr>
<tr><td>0.5 wt%</td><td colspan="2" rowspan="2"></td></tr>
<tr><td>1 wt%</td></tr>
</table>

4 Dispersion and Reagglomeration of Graphene in Epoxy System

4.1 Introduction

In practical terms, graphene is not suitable to disperse in epoxy just by simple mixing. This is due to graphene's pronounced tendency to reagglomerate in the matrix due to the strong van der Waals force between separately dispersed graphene sheets [347, 348]. The maximum improvement in final properties could only be achieved when graphene is homogeneously dispersed in the matrix and external stresses are efficiently transferred through a strong graphene-epoxy interface [269, 349]. This can also be seen for other polymer nanocomposites where it is critical to achieve homogenisation and thorough dispersion. Therefore, the dispersion state of graphene in the matrix plays a crucial role in achieving superior properties from graphene/epoxy nanocomposites.

In this part, pristine graphene was dispersed in a two-component epoxy system without using any solvent. The effect of sonication time, storage time, graphene concentration and sonication temperature on the dispersion and reagglomeration of graphene in epoxy resin, hardener and their mixtures have been extensively analysed here.

4.2 Experimental

Graphene samples were weighed in Sartorius MC210S analytical balance (with the readability of 0.01mg) and dispersed in epoxy resin by hand mixing for 5 seconds gently, and then sonicated through a bath sonicator (Grant MXB6) for uniform dispersion.

For studying the influence of sonication time on the dispersibility, 0.005wt% dispersions were sonicated for different durations from 6 minutes to 60 minutes at 20℃. Another part of dispersion was sonicated for 30 minutes, and then stored for 10 days for studying the reagglomeration against storage time. For studying the influence of the

concentration on the dispersibility, different concentrations from 0.005wt% to 0.1wt% of samples were made, and then sonicated for 30 minutes at 20 ℃. For studying the influence of sonication temperature on the dispersibility, 0.005wt% dispersions were sonicated for 6 minutes from 20 ℃ to 60 ℃. Graphene-hardener, graphene-epoxy dispersions were prepared by the same method accordingly. All samples were degassed at -0.1MPa to remove the entrapped air bubbles. The materials and characterization techniques were described in chapter 3.

4.3 Result and Discussion

4.3.1 Reagglomeration as a Function of Sonication Time

Sonication is the most widely adopted method to disperse graphene in a liquid matrix and has proved to be of high efficiency. Figure 4.1 shows graphene dispersion in epoxy resin and hardener before and after sonication.

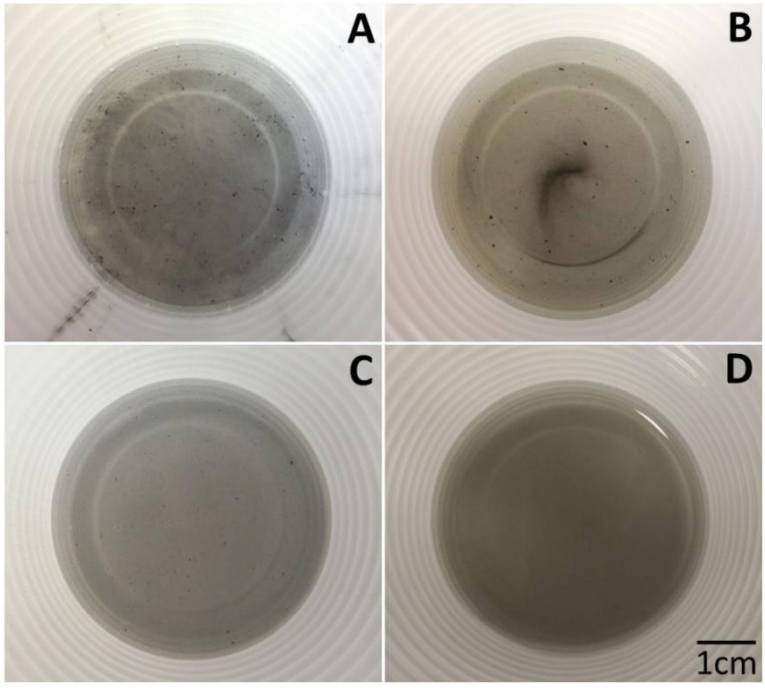

Figure 4. 1. Graphene in epoxy resin and hardener: (A) graphene-epoxy resin before sonication; (B) graphene-hardener before sonication; (C) graphene-epoxy resin after sonication; and (D) graphene-hardener after sonication.

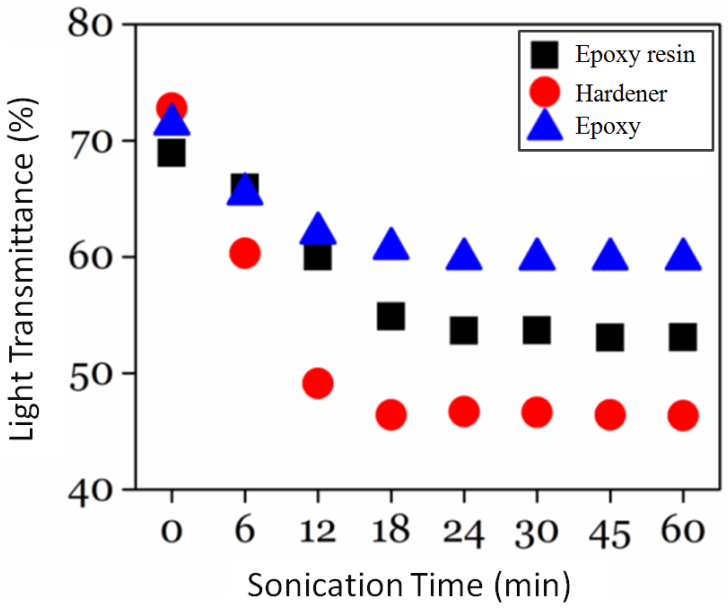

Figure 4. 2. Light transmittance of graphene dispersion against sonication time.

The light transmittance of graphene dispersion against storage time is shown in Figure 4.2. The graphs show a significant drop in the transmittance for the graphene dispersion in hardener within the first 12 minutes. This high magnitude slope suggests a much higher tendency of graphene to disperse in hardener. Before sonication, graphene agglomerates lowered light absorbance because of the shielding effects of the bundles [31]. After sonication, the agglomerates were dispersed into small agglomerates/flakes causing higher light absorption or lower light transmittance. A similar trend was also observed for the graphene dispersion in epoxy resin, where light transmittance also decreased with the sonication time. However, the magnitude of the slope is much lower than that of hardener due to the high viscosity of epoxy resin, making it more difficult for graphene to disperse. It is noteworthy that when compared to 15 percent drop in epoxy resin and 26 percent drop in hardener, there is just 11 percent drop in the transmittance for graphene dispersion in epoxy. This lower decrement in light transmittance suggests non-uniform dispersion, which is due to the curing of the resin while mixed with hardener. After mixing liquid resin with hardener,

the resin started to cure immediately. The fast gelling and curing process left only limited time for graphene dispersion. This time period was not sufficient to disperse graphene uniformly. Therefore, selection of epoxy with longer curing durations is desirable for preparing epoxy/ graphene nanocomposites.

This dispersion of graphene is further analysed by optical microscopy. Large agglomerates before sonication were clearly seen from the sample, as shown in Figure 4.3 (A) and (B). After sonication for 60 minutes, the agglomerates were unlocked into small flakes, as shown in Figure 4.3 (C) and (D).

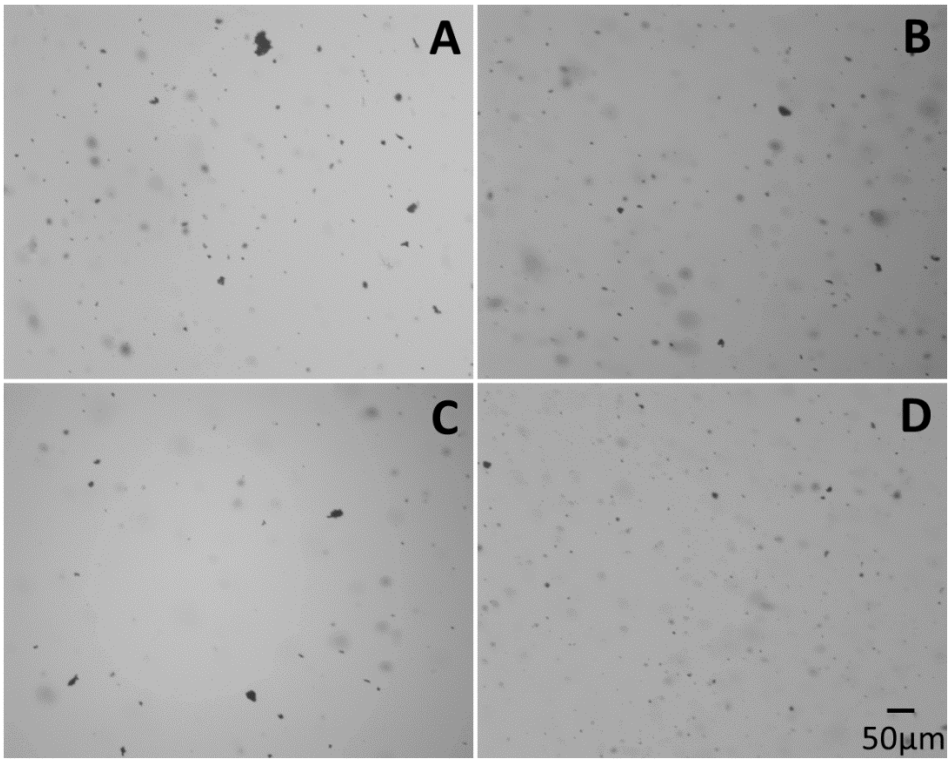

Figure 4. 3. Optical microscopic analyses: (A) graphene-epoxy resin before sonication; (B) graphene-hardener before sonication; (C) graphene-epoxy resin after sonication; and (D) graphene-hardener after sonication.

This qualitative result shows that the dispersion of graphene in the mixture of epoxy resin and hardener together has the lowest efficiency because of the curing of the resin. As the resin cures, the molecular chain of the resin become fixed and hinders graphene from any further dispersion. Due to the high viscosity and sticky nature of epoxy resin, the dispersion of graphene in epoxy resin is more difficult, whilst the dispersion of graphene in hardener is easier and possesses higher efficiency.

4.3.2 Reagglomeration as a Function of Storage Time

Graphene has a tendency to agglomerate in the low viscous matrix due to the strong van der Waals force. It is therefore necessary to understand its reagglomeration behaviour in order to gain meaningful knowledge about the stability of the dispersion.

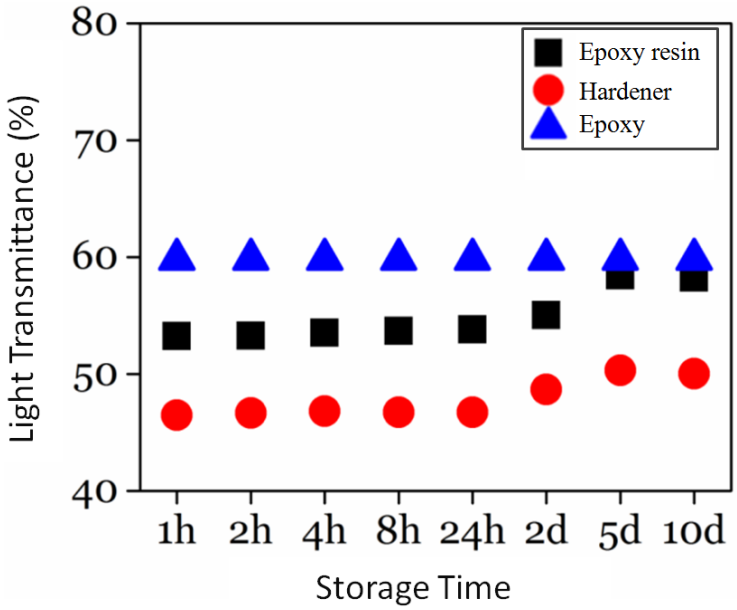

Figure 4. 4. Light transmittance of graphene dispersion against storage time.

Figure 4.4 shows the light transmittance of graphene dispersion against storage time. Within the first 5 days, the behaviour of graphene in epoxy resin and hardener were similar.

Both dispersions showed slight increments in light transmittance, which were 5% and 4% in epoxy resin and hardener respectively. These increments indicate that some level of reagglomeration took place during this time, but only a limited amount. During 5 to 10 days, the light transmittance did not change, indicating that the dispersions were stable over this time period. The light transmittance of graphene dispersion in epoxy stayed constant, because the system became stable after the resin was fully cured within 24 hours.

Optical microscopy further confirmed the stability of the dispersion. Figure 4.5 (A) and (B) shows the graphene dispersion in epoxy resin and hardener tested within 1 minute after sonication, Figure 4.5 (C) and (D) show the dispersion after 10 days storage. It can be seen that there were no obvious changes in the dispersion state, indicating that the dispersions were in general stable during this time period.

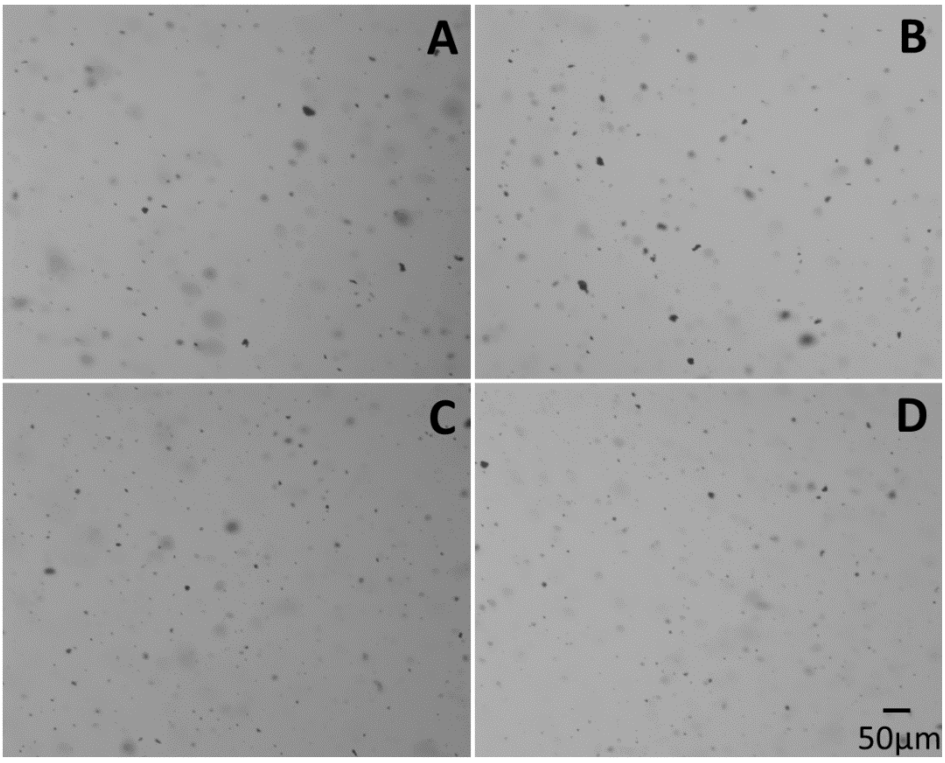

Figure 4. 5. Optical microscopic analyses: (A) graphene-epoxy resin storage for 1min; (B) graphene-hardener storage for 1min; (C) graphene-epoxy resin storage for 10 days; and (D) graphene-hardener storage for 10 days.

4.3.3 Reagglomeration as a Function of Graphene Concentration

Five series of graphene dispersion with concentrations between 0.005% and 0.1% were prepared. Figure 4.6. shows the changes in the transparency of the graphene dispersions at different concentrations. As evident in the image below, suspensions with higher concentration levels showed lower light transmission when compared to low concentration suspensions. Samples with a concentration higher than 0.025 wt% were visually all black with no light transmission.

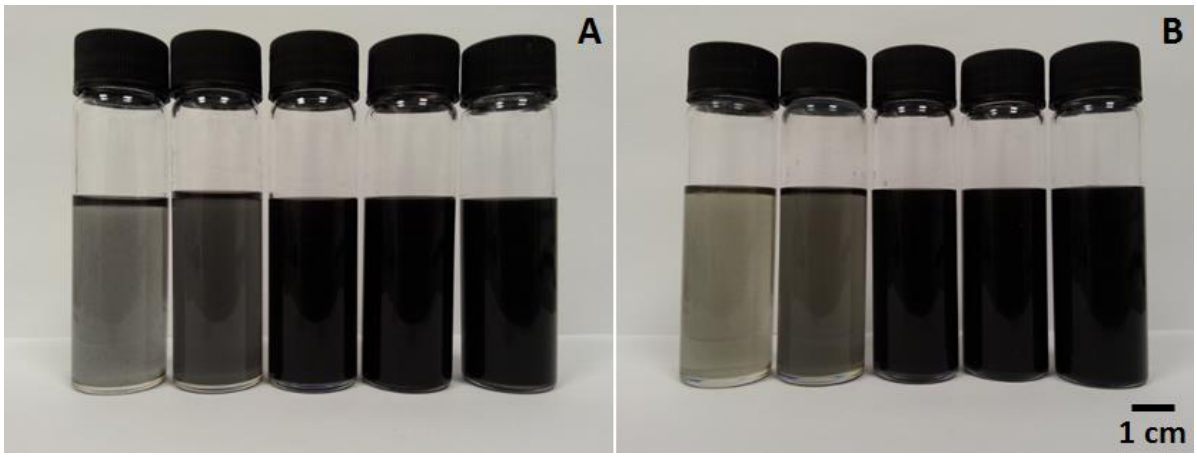

Figure 4. 6. Qualitative analysis of (A) graphene-epoxy resin; and (B) graphene-hardener (concentration from left to right: 0.005wt%; 0.0125wt%; 0.025wt%; 0.05wt%; 0.1wt%).

As mentioned in section 4.3.1, at low concentration, the light transmittance decreased with the decreasing of agglomerate size. Figure 4.7 shows the measured light transmittance against concentration. The light transmittance decreased with the increase of concentration.

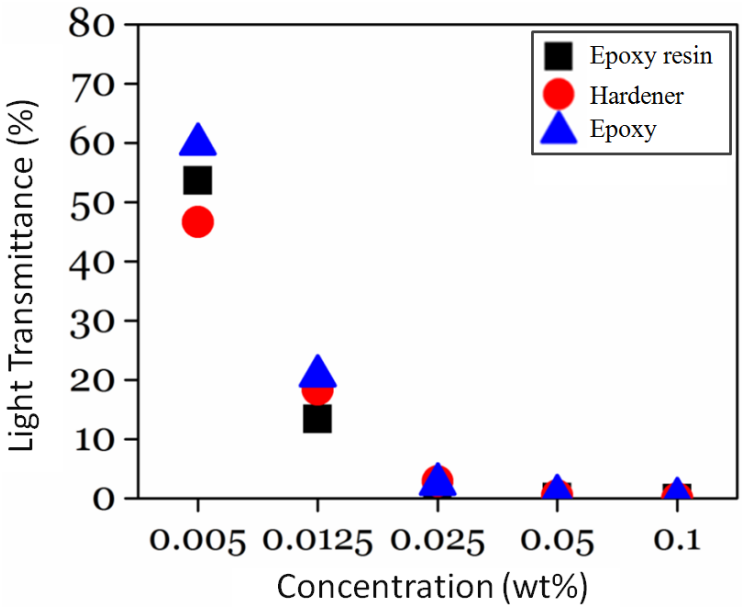

Figure 4. 7. Light transmittance of graphene dispersion against concentration.

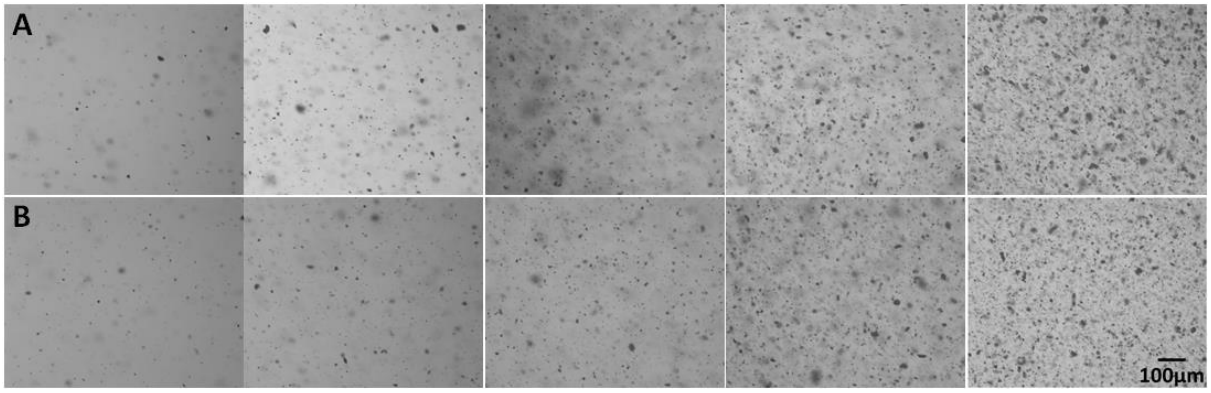

Figure 4. 8. Optical microscope image of graphene dispersion with increased concentration in (A): epoxy resin; (B): hardener.

Figure 4.8 depicts the optical photograph of graphene dispersion in epoxy resin and hardener with increased concentration after sonicating for 30 mins. It can be seen that the graphene was dispersed due to the effects of the sonication. Reagglomeration behaviour cannot be seen directly here. As the inter-particle distance between dispersed graphene is small at higher concentration, this then makes the graphene sheets easier to attract each other and therefore it can be deduced that the reagglomeration behaviour can be more pronounced at higher concentrations. Besides reagglomeration, higher graphene concentration also means

increased difficulty for uniform dispersion [32], which further hinders the stability of the dispersion.

4.3.4 Reagglomeration as a Function of Sonication Temperature

High temperature accelerates the chemical reactions as well as the mobility of the molecules in a liquid system, which would make graphene nanoplatelets easier to disperse. Five series of samples were prepared with sonication temperatures from 20 to 60 ℃ and sonication for 6mins. The results are shown in Figure 4.9. For graphene-hardener dispersion, the light transmittance was 60.32% at 20 ℃ after 6 minutes sonication, however, it reached 46.42% at 50 ℃ within 6 minutes. This value could only be achieved after 18 minutes sonication at 20 ℃, as shown in Figure 4.2 (section 4.3.1). Similarly, the light transmittance of graphene-epoxy resin dispersion was 53.21% at 60 ℃ after 6 minutes sonication, which was only achieved after 24 minutes at 20 ℃ (Figure 4.2). For graphene-epoxy dispersion, longer sonication duration will lead to the curing of the resin, which would hinder any dispersion. Under higher temperature, sonication at 50 ℃ for 6 minutes was enough to reach uniform dispersion state as confirmed in Figure 4.9.

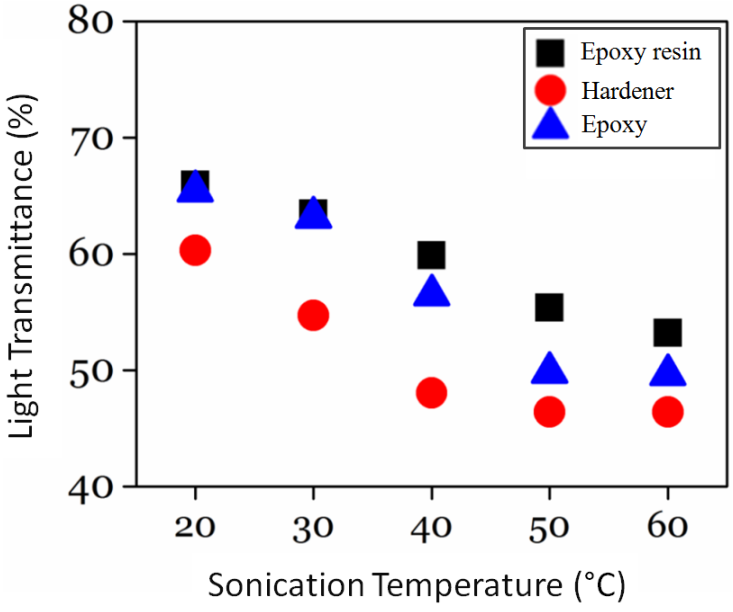

Figure 4. 9. Light transmittance of graphene dispersion against sonication temperature.

These results confirm that the dispersion is strongly dependent on the sonication temperature. Theoretically, an appropriate dispersion is achieved by providing the right energy to the system, which is normally accomplished by sonication. However, for fine powders or strongly bonded agglomerates, higher temperatures are preferred for an increased mobility of chemical species and effective de-bundling of agglomerates.

4.4 Summary

Dispersion of graphene in matrix plays a crucial role for the performance of nanocomposites. Reagglomeration, i.e. agglomeration with the passage of time, has often been underestimated and even ignored. In this work, the reagglomeration of graphene in a two-component epoxy system was measured using optical transmittance spectroscopy. The results showed that the temperature and viscosity significantly contributed to the dispersion of graphene. Graphene tends to disperse easily under high temperatures in a low viscosity system. Besides this, lower concentration levels produced a lower reagglomeration profile (size and trend) and vice versa. On the contrary, some researchers remark that low viscosity and high temperature may accelerate reagglomeration because graphene shows more mobility in the low viscosity system, and a higher temperature helps the formation of physical bonds like the van der Waals force present between graphene sheets. Although there exists some dispute, it is in general consensus that temperature, viscosity, and concentration are the most critical parameters and should be adjusted for the preparation of a stable epoxy/graphene composition and subsequently its nanocomposites.

5 Effects of Processing Techniques on the Properties of Nanocomposites

5.1 Introduction

To disperse graphene into epoxy matrix, a variety of processing methods have been applied. For example, bath sonication has been used to disperse graphene in epoxy by Qiu *et al.* [217], Wan *et al.* [257], Ren *et al.* [311] and Shen *et al.* [350].When using bath sonication, the resulting material shows positive property enhancements and uniform graphene dispersions. Tip sonication has also been used a lot, and shows positive results [262, 351-355]. As the simplest and most convenient method, hand mixing has also been widely applied to prepare epoxy/graphene nanocomposites, such as shown by Kim *et al* [275], Yue *et al.* [342], Shokrieh *et al.* [356] and Ribeiro *et al.* [357].

Various methods have been selected to prepare epoxy/graphene nanocomposites. In general, the large interfacial area created by graphene can affect the behaviour of the surrounding polymer chains even at low-level graphene contents [358, 359]. Subsequently, improved mechanical properties, higher thermal degradation temperatures and glass transition temperatures can be obtained for the nanocomposites when graphene is uniformly dispersed [264]. Therefore, the graphene dispersion is a key point to determine the final properties of the epoxy/graphene nanocomposites [360]. In general, different processing methods result in different levels of graphene dispersions, and thus it is very important to understand the effectiveness of these methods. However, the dispersion effectiveness of these methods is rarely compared in literature.

In this part, three different processing methods were applied to process epoxy/graphene nanocomposites. The mechanical properties, DMA, TGA and SEM images of the nanocomposites were tested to evaluate their dispersion levels in relation to the processing methods used.

5.2 Experimental

Four sets of samples were prepared. One set of samples was prepared as a control sample using neat epoxy only, while another three sets of 0.3 wt% epoxy/graphene nanocomposites were prepared by using the different processing methods discussed previously, namely, bath sonication, tip sonication and hand mixing.

For the samples prepared by bath sonication, graphene was first dispersed in epoxy hardener and bath sonicated for thirty minutes using an Ultra 7000 sonicator, epoxy monomer was then added with hand stirring for 5 minutes followed by a further 5 minutes of bath sonication. Vacuum degassing was then carried out to remove the entrapped air bubbles.

Next, the mixtures were mould casted and cured at room temperature for 6 hours followed by 6 hours post-curing at 80℃. Tip sonication and hand mixing were used to prepare nanocomposites according to the same method of bath sonication. Tip sonication was applied with a Sonics CV334 sonicator. The materials and characterization techniques were described in chapter 3.

5.3 Results and Discussion

5.3.1 Tensile Test

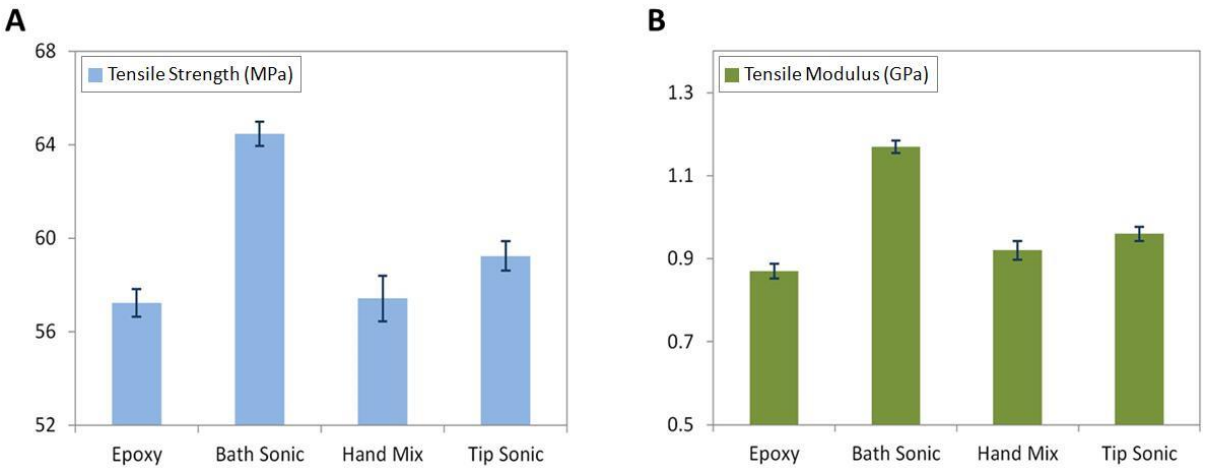

Figure 5. 1. Tensile properties of nanocomposites: (A) Tensile strength; (B) Tensile modulus.

As shown by Figure 5.1(A), epoxy showed the lowest tensile strength, which was 57.23MPa.After introducing graphene, all sets of samples showed increased tensile strength. The samples prepared by bath sonication showed the maximum increase, with the tensile strength of 64.46MPa. Tip sonicated samples showed a medium increase in the tensile strength, with the value of 59.24MPa. Hand mixed samples showed the minimum increase in tensile strength, which was 57.42MPa.

The tensile modulus of the nanocomposites is shown in Figure 5.1(B). Epoxy showed the lowest tensile modulus with 0.87GPa, while the minimum increase in the tensile modulus was observed in hand mixed samples with 0.92GPa, samples prepared with bath sonication showed the highest tensile modulus, which was 1.17GPa. Tip sonicated samples showed a value of 0.96 GPa.

The general increase in tensile properties was due to the incorporation of graphene. The uniformly dispersed graphene formed a continuous network in the matrix, which supported the network of the matrix and allowed the release of any concentrated stress, thus enhancing the tensile properties. The more uniformly dispersed, the higher the property enhancement would be. The results showed that bath sonication could disperse graphene at the highest efficiency, tip sonication produced medium dispersion. However, hand mixing showed the lowest efficiency to produce a fine and homogeneous graphene dispersion.

5.3.2 Flexural Test

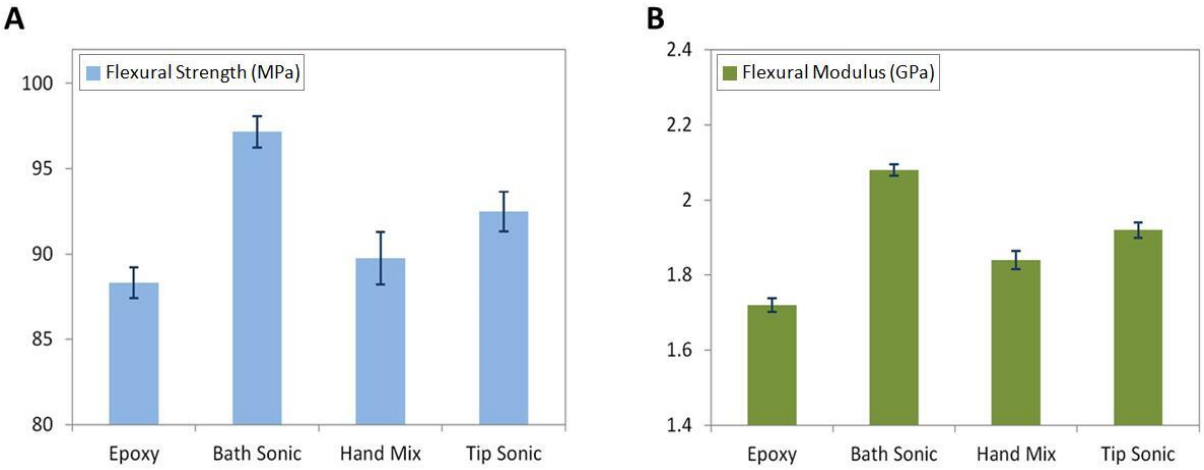

Figure 5. 2. Flexural properties of nanocomposites: (A) Flexural strength; (B) Flexural modulus.

The variation in flexural strength is shown in Figure 5.2(A). Epoxy showed the lowest flexural strength, which was 88.32MPa. After introducing graphene, the flexural strength increased in general. The maximum flexural strength was observed at 97.17 for bath sonicated samples. Tip sonicated samples showed an intermediate increase, with the flexural strength of 94.48MPa. The lowest flexural strength was observed in hand mixed samples, with the value of 89.76MPa.

For flexural modulus, as shown in Figure 5.2(B), the lowest value was also observed in epoxy samples, which was 1.72GPa. In case of bath sonicated samples, the flexural modulus increased to 2.08GPa, which presented the greatest flexural modulus. Hand mixed samples showed the lowest flexural modulus, which was 1.84GPa. Tip sonicated samples showed the value of 1.92GPa.

In general, the incorporation of graphene resulted in higher flexural properties. While bath sonication produced the best dispersion of graphene in the matrix, hand mixing showed the lowest increment in the flexural properties, which was due to the non-uniform dispersion of graphene.

5.3.3 Fracture Test

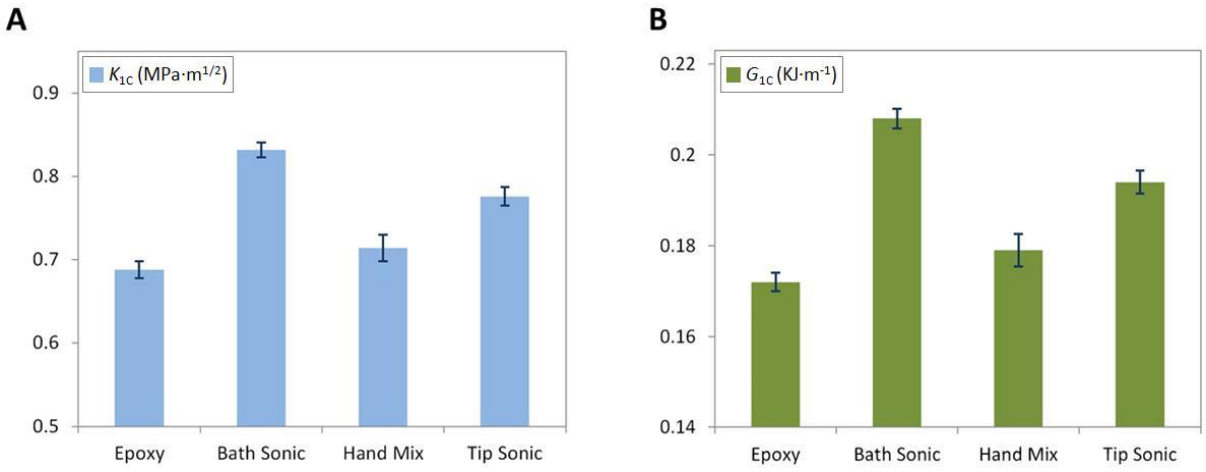

Figure 5. 3. Fracture properties of nanocomposites: (A) Fracture toughness (K_{1C}); (B) Critical strain energy release rate (G_{1C}).

A similar trend in K_{1C} and G_{1C} can be observed and is shown in Figure 5.3. Epoxy showed the lowest K_{1C} and G_{1C} values, which showed the fragile nature of the material. After introducing graphene, both K_{1C} and G_{1C} increased.

The maximum increment in K_{1C} was observed in Figure 5.3(A) in case of bath sonicated samples, which increased from 0.688MPa·m$^{1/2}$ to 0.832MPa·m$^{1/2}$. For tip sonicated samples, the K_{1C} also showed improvement due to the enhanced dispersion of graphene in epoxy matrix. Hand mixed samples showed a lower level of improvement when compared to that of tip sonicated and bath sonicated samples, which was 0.714MPa·m$^{1/2}$.

G_{1C} is shown in Figure 5.3(B). Neat epoxy showed the lowest G_{1C} value, which was 0.172KJ·m^{-1}. After introducing graphene, the maximum G_{1C} was obtained at 0.208KJ·m^{-1} in case of bath sonicated samples. Tip sonicated samples showed increased G_{1C} as well, which was 0.194KJ·m^{-1}.Hand mixed samples showed the lowest increments in G_{1C} value, which was 0.216KJ·m^{-1}.

In general, after introducing graphene, the fractural properties increased. This was due to the reinforcement effect of graphene. The graphene in the epoxy matrix improved the energy absorbing capacity, and as a result improved the fracture toughness of nanocomposites. Bath sonicated samples produced the best dispersion, and consequently the nanocomposites showed the highest fracture properties. Among all these three processing methods, hand mixing showed the lowest dispersing efficiencies.

5.3.4 Hardness Test

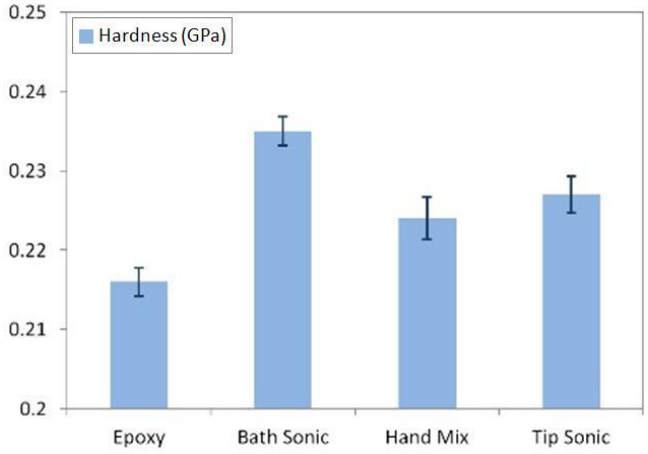

Figure 5. 4. Hardness of nanocomposites.

The Vickers hardness of nanocomposites are shown in Figure 5.4. Neat epoxy showed the lowest hardness of 0.216GPa. With the incorporation of graphene, the hardness of the nanocomposites significantly improved, particularly in the case of the bath sonicated samples, where the hardness increased to 0.235GPa. Lower levels of improvement were observed in case of tip sonicated samples, with 0.217GPa of the hardness. The minimum increment in the hardness was observed in hand mixed samples, with the value of 0.179GPa.

The increase of hardness can be attributed to the reinforcement effect of graphene in the epoxy matrix. As a rigid material, graphene restrains the mobility of the epoxy molecular chain, thus increasing the hardness of nanocomposites. Moreover, uniformly dispersed

graphene can shorten the distance among cross-linking points, which could increase the cross-linking density of the epoxy network, and this can provide a positive influence in the improvement of desired properties. In general, bath sonication showed the highest efficiency in producing a homogeneous graphene dispersion.

5.3.5 DMA Test

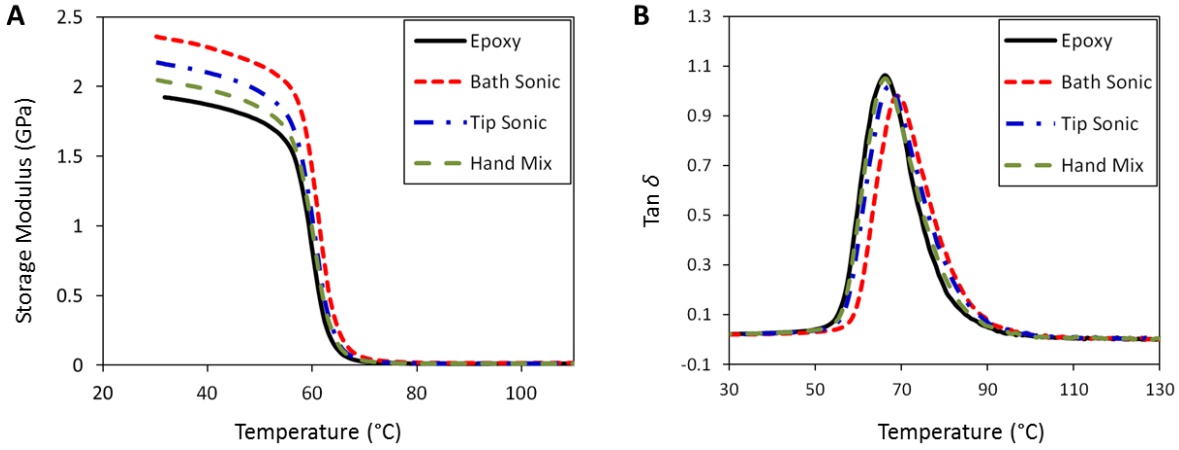

Figure 5. 5. DMA results of nanocomposites: (A) Storage Modulus; (B) Tan δ.

Figure 5.5(A) shows the storage modulus (E') as a function of temperature for epoxy/graphene nanocomposites. As can be seen from the figure, the storage modulus of neat epoxy was 66.08GPa. After introducing graphene, all sets of samples showed increased storage modulus, indicating that graphene as a filler had increased the storage modulus of epoxy effectively. Among all the nanocomposites, hand mixed samples showed the lowest increment in storage modulus, which was 2.04GPa. Tip sonicated samples showed a medium increase in the storage modulus with the value of 2.17GPa. Bath sonicated samples showed the highest increment in storage modulus, which was 2.35GPa.

Glass transition temperature (T_g) characterizes the segmental motion of polymers and was taken as the temperature value at the peak of tan δ curves as shown in Figure 5.5(B). In the figure, it shows that the tan δ peak was observed at 66.08 ℃ for neat epoxy. After

introducing graphene, T_g shifted to higher temperatures. This was attributed to the fact that graphene had restricted the chain mobility of epoxy, therefore leading to the increase in T_g. Amongst these increments, bath sonicated samples showed the highest T_g of 69.28 ℃, indicating the highest processing efficiency by bath sonication. Samples prepared by hand mixing showed the T_g value of 66.41 ℃, and indicated the lowest dispersing efficiency.

5.3.6 TGA Test

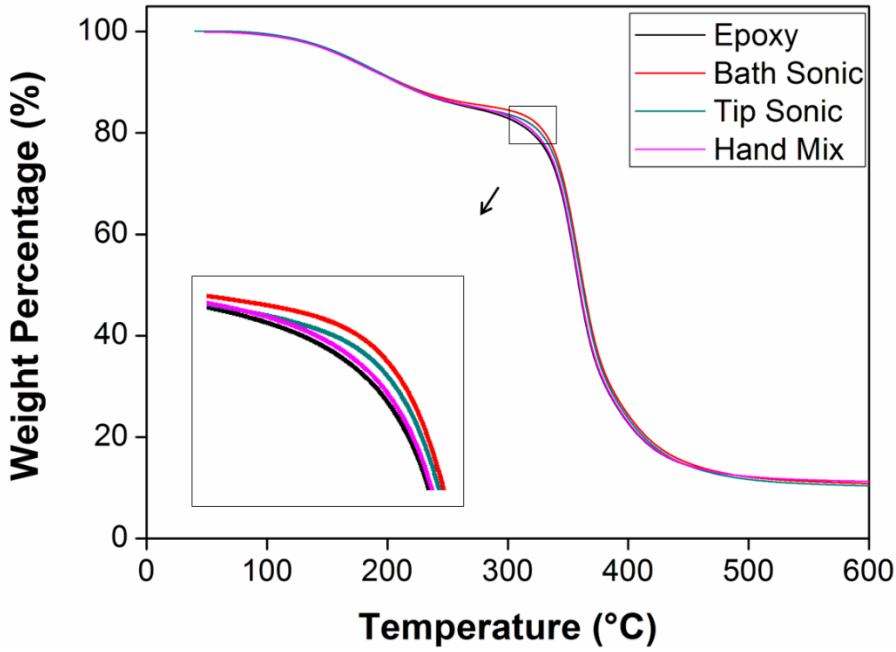

Figure 5. 6. TGA curves of nanocomposites.

Thermal decomposition is one of the fundamental thermal properties and is critical for practical applications. Figure 5.6 shows the TGA curves of the nanocomposites in a nitrogen atmosphere. All the samples had a similar two stage weight loss, indicating that all samples had a similar thermal degradation mechanism. The first weight loss from 100 ℃ to 230 ℃ was attributed to the decomposition of small molecules on the side chain. The second weight loss, which occurred from 250 ℃ to 500 ℃, showed the decomposition of the main polymer chain. As can be seen from the figure, neat epoxy showed the highest decomposition rate, indicating

that this material was the most unstable under heating. After introducing graphene, bath sonicated samples showed the lowest decomposition rate, indicating the highest thermal stability of the graphene samples. The reason for this stability can be explained by the fact that the graphene had increased the cross-linking density of the nanocomposites. Generally, the cross-linking density refers to the concentration of cross-linked bonds per volume. As for typical polymer nanocomposites, the higher the cross-linking density is, the stronger the polymer chains bond each other, therefore improving the nanocomposites' capacity to withstand heat. Compared with the structures of the epoxy samples, where DMF prepared samples tend to shorten the distance among cross-linking points, and thus increase the cross-linking density of the resultant network. Among all the nanocomposites, hand mixed samples showed the highest decomposition rate, which evidenced the lowest dispersion efficiency. The increase in the thermal stability of bath sonicated sample can, once again, be attributed to the uniform dispersion of graphene.

5.3.7 SEM Test

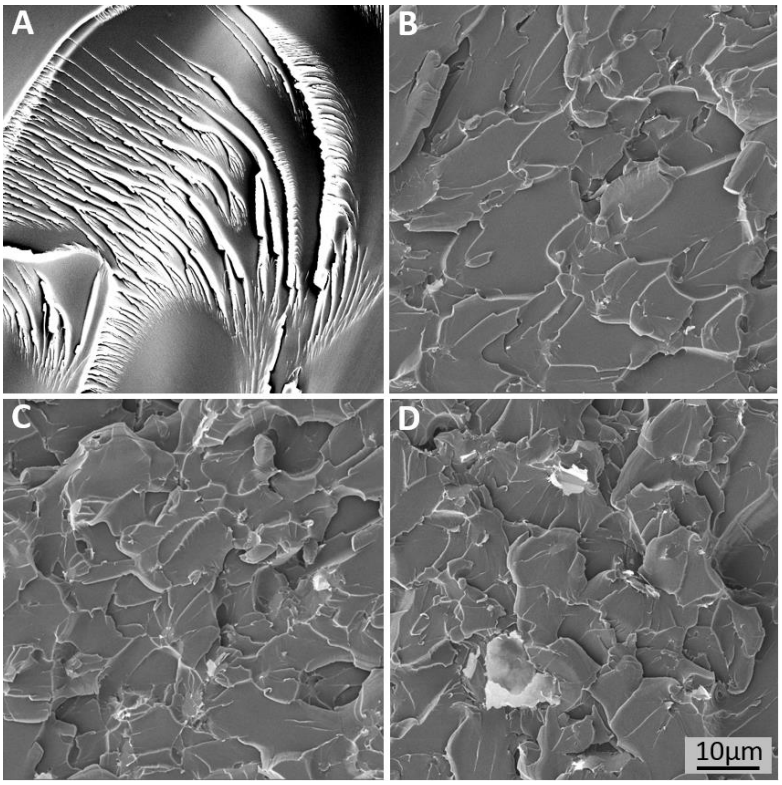

Figure 5. 7. SEM images of fracture surfaces of (A) Neat epoxy; (B) Bath sonicated; (C) Tip sonicated and (D) hand mixed.

The fracture surfaces were studies by SEM and are shown in Figure 5.7. As can be seen from Figure 5.7(A), river-like fracture patterns can be observed on the epoxy surface, which show the brittle nature of the material and poor resistance to crack initiation and propagation. For nanocomposites prepared with graphene, the fracture pattern had changed and showed the sheet-sheet delaminating pattern. For bath sonicated samples, as shown in Figure 5.7(B), clear fracture patterns can be seen and reveal the better dispersion of graphene. The uniformly dispersed graphene could bridge growing cracks, thus stabilising and preventing any further deterioration causing larger and more harmful cracks, consequently enhancing the properties of the material. However, for tip sonicated and hand mixed samples,

as shown in Figure 5.7(C) and (D), some poorly dispersed graphene can still be seen on the surface. The poorly dispersed graphene formed defects in the nanocomposites, which acted to concentrate the stresses locally, eventually causing a localised weakness, thus decreasing the properties of the nanocomposites.

In general, samples prepared by bath sonication showed the best dispersion of graphene. Tip sonication showed medium dispersion efficiency, and hand mixing showed the lowest dispersion efficiency.

5.4 Summary

For epoxy/graphene nanocomposites, graphene must be dispersed homogeneously in epoxy matrix for the best of the desired property enhancements. However, because of the van der Waals force between separately dispersed graphene, graphene tends to reagglomerate in the matrix. Therefore, to achieve uniform dispersion, various processing methods have been applied.

In this work, 0.3wt% epoxy/graphene nanocomposites were prepared and bath sonication, tip sonication and hand mixing were applied to investigate their dispersing efficiencies of graphene in epoxy matrix. Mechanical properties, TGA, DMA and SEM image of nanocomposites were tested. Nanocomposites prepared by bath sonication showed the highest property enhancements, indicating that bath sonication had the highest processing efficiency. Tip sonication prepared samples showed medium property enhancements, however, SEM images showed that large poorly dispersed graphene can still be seen on the samples prepared by hand mixing, indicating that hand mixing is not sufficient to disperse graphene uniformly in the matrix.

6 Effects of Graphene Contents on the Properties of Nanocomposites

6.1 Introduction

Graphene has been found as a promising reinforcement material for polymers due to its extremely high aspect ratio, unique graphitised planar structure, outstanding mechanical properties, thermal conductivity and electrical conductivity [361, 362]. The large surface area of graphene increases the contact area with the matrix, and thus reinforce the matrix [363, 364]. Extensive research has been carried out to enhance the properties of epoxy by using graphene. For example, Bortz *et al.* [271] conducted an investigation on the mechanical properties of epoxy/graphene nanocomposites. Their results showed that, generally, with the incorporation of graphene, the mechanical properties of nanocomposites improved. Liu *et al.* [365] dispersed graphene in acetone and prepared epoxy/graphene nanocomposites, and also reported an increase in the mechanical properties. Li *et al.*[317] prepared epoxy/graphene nanocomposites, they reported the increase in glass transition temperature of epoxy by hindering segmental motion of polymer chains via mechanical interlocking. By incorporating graphene into epoxy, Wan *et al.* [257] reported higher thermal decomposition temperatures of nanocomposites, which was attributed to the restricted chain mobility of polymers near the graphene surface.

In general, with the incorporation of graphene, the properties of nanocomposites increase. However, the problem of reagglomeration also occurs with the incorporation of graphene, as graphene tends to reagglomerate in liquid matrices at high concentrations.

In this part, epoxy/graphene nanocomposites were prepared with different graphene loadings. Mechanical properties, DMA, TGA and SEM images of nanocomposites were tested to evaluate the properties of the nanocomposites.

6.2 Experimental

Five sets of samples were prepared. One set of sample was prepared for reference using neat epoxy only, while another four sets were prepared using different contents of graphene, which were 0.1 wt%, 0.3 wt%, 0.5 wt% and 1 wt% respectively. The samples were marked as G-0.1, G-0.3, G-0.5 and G-1 accordingly.

A certain amount of graphene was first dispersed in epoxy hardener and bath sonicated for half an hour, an epoxy monomer was then added with hand stirring for 5 minutes followed by 5 minutes of bath sonication, vacuum degassing was then carried out to remove the entrapped air bubble. Subsequently, the mixtures were mouldcasted and cured at room temperature for 6 hours followed by 6 hours post-curing at 80℃. The materials and characterization techniques were described in chapter 3.

6.3 Results and Discussion

6.3.1 Tensile Test

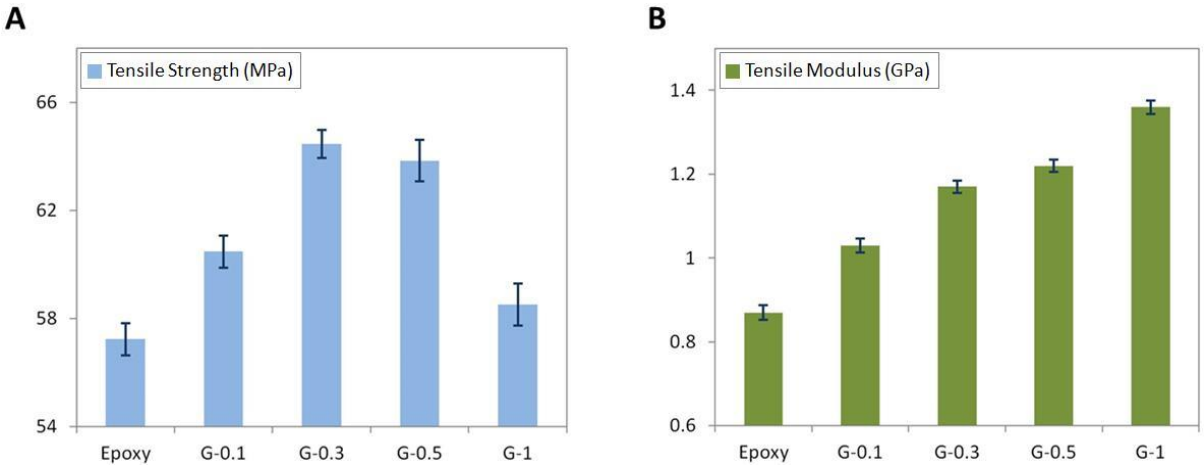

Figure 6. 1. Tensile properties of nanocomposites: (A) Tensile strength; (B) Tensile modulus.

As shown in Figure 6.1(A), epoxy showed the lowest tensile strength, which was 57.23MPa. After graphene was introduced, all samples showed increased properties in tensile strength. When the graphene content was increased, the tensile strength of the

nanocomposites first increased, then decreased. G-0.1 exhibited a tensile strength of 60.47MPA, while the maximum increase in tensile strength was shown by G-0.3, which was 64.46MPa. However, with further increasing of graphene contents, the tensile strength of nanocomposites decreased.G-0.5 showed the tensile strength of 63.84MPa, while G-1 showed a tensile strength of only 58.51MPa.

For tensile strength, the values showed increments when the graphene loading was lower than 0.3wt%, this was due to the reinforcement effect of graphene. Graphene in the matrix formed a continuous network, thus released the stress concentration. However, after further increasing of the graphene contents, the tensile strength decreased. This was due to the non-uniform dispersion of graphene at high concentrations. Non-uniformly dispersed graphene formed defects in the matrix, and thus increased the stress concentration leading to a decrease of the properties.

The tensile modulus of the nanocomposites is shown in Figure 6.1(B). Epoxy showed the lowest tensile modulus, which was 0.87GPa.With the increase of graphene contents, the tensile modulus of nanocomposites increased. G-0.1 showed the lowest increment in tensile modulus, with the value of 1.03GPa. G-0.3 and G-0.5 showed the tensile modulus of 1.17GPa and 1.22GPa, respectively. The maximum increase in tensile modulus is shown by G-1, with the value of 1.36GPa.

Tensile modulus enables the calculation of the changes in the dimension of a material under tensile loads. A solid material deforms when a load is applied to it, tensile modulus predicts how much a material extends under tension. As can be seen from the results, the incorporation of graphene enables an ability to withstand tensile deformation.

The general increase of tensile properties was due to the incorporation of graphene. In general, considering both the strength and modulus, it is suggested that graphene content should be kept lower than 0.3wt% for the best dispersion and reinforcement effect.

6.3.2 Flexural Test

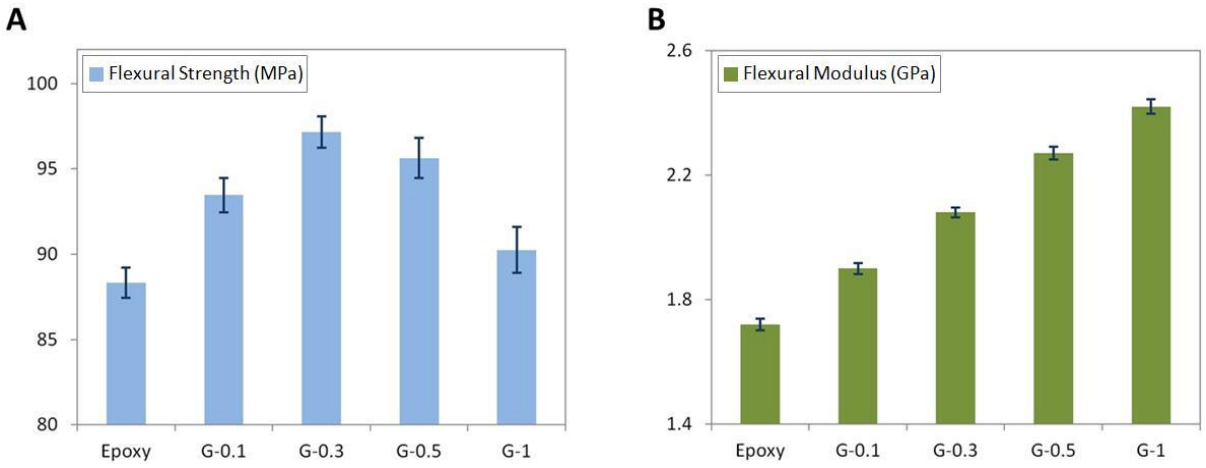

Figure 6. 2. Flexural properties of nanocomposites: (A) Flexural strength; (B) Flexural modulus.

The variation in flexural strength is shown in Figure 6.2(A). Epoxy showed the lowest flexural strength, which was 88.32MPa. After introducing graphene, the flexural strength first increased, and then decreased. G-0.1 showed the flexural strength of 93.46MPa, the maximum flexural strength was observed at 97.17MPa for G-0.3 samples. However, with the further increasing of the graphene contents, the flexural strength decreased. G-1 showed the flexural strength of 90.24MPa, which was lower than that of G-0.3 and G-0.5 samples.

For flexural modulus, as can be seen from Figure 6.2(B), the lowest value was also observed in epoxy samples, which was 1.72GPa. The flexural modulus increases with the concentration of graphene, G-1 samples showed the maximum flexural modulus of2.42GPa. G-0.1, G-0.3 and G-0.5 samples showed medium increase.

In general, for flexural properties, a similar trend was observed when compared to the tensile properties. The modulus increased with the graphene concentration. However, if too much graphene were used, e.g., 0.5wt% or 1wt%, the strength decreased, which was due to the non-uniform dispersion of graphene.

6.3.3 Fracture Test

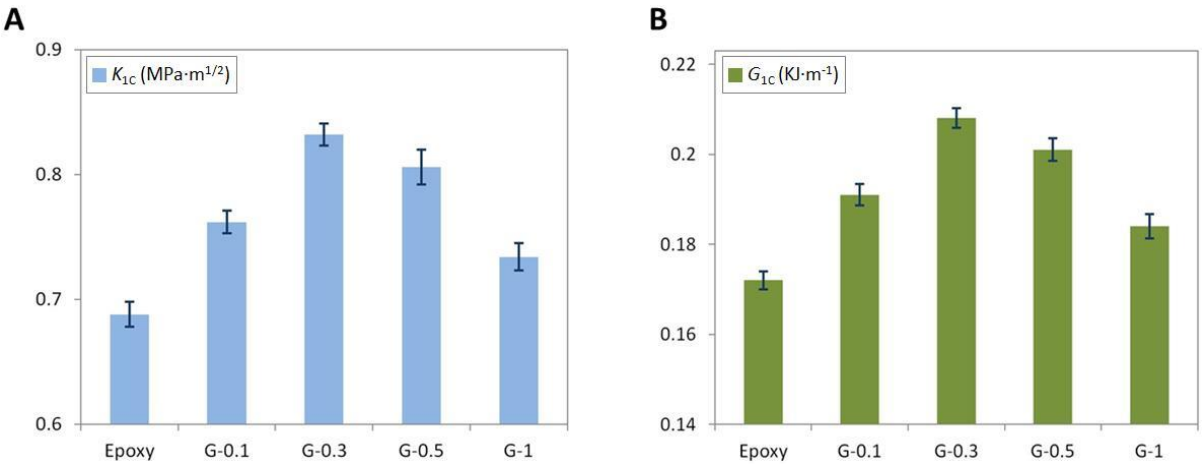

Figure 6. 3. Fracture properties of nanocomposites: (A) Fracture toughness (K_{1C}); (B) Critical strain energy release rate (G_{1C}).

From Figure 6.3, with the incorporation of graphene, the K_{1C} and G_{1C} increased first and then decreased. The maximum increment in K_{1C} was observed in Figure 6.3(A) in case of G-0.3 samples, which increased from 0.688MPa·m$^{1/2}$ to 0.832MPa·m$^{1/2}$. For G-0.1 samples, the K_{1C} also showed a medium increase compared to that of the neat epoxy samples, which was due to the incorporation of graphene. However, when compared to G-0.3 samples, G-0.5 and G-1 samples showed lower increments, with the K_{1C} value of 0.806MPa·m$^{1/2}$ and 0.734MPa·m$^{1/2}$, respectively.

A similar trend was also observed in the G_{1C}, which is shown in Figure 6.3(B). Neat epoxy showed the lowest G_{1C} value, which was 0.172KJ·m^{-1}. After introducing graphene, G-0.1 samples showed increased G_{1C} with the value of 0.191KJ·m^{-1}. The maximum G_{1C} was obtained at 0.208KJ·m^{-1} in case of G-0.3 samples. G-0.5 and G-1 samples showed lower increments when compared to that of G-0.3 samples, with the G_{1C} value of 0.201KJ·m^{-1} and 0.184KJ·m^{-1}, respectively.

In general, with the increasing of graphene contents, the fracture properties increased. This was due to the reinforcement effect of graphene in epoxy matrix. The incorporation of

graphene improved the energy absorbing capacity, as a result improving the fracture toughness of the nanocomposites. However, with the further increasing of graphene contents, e.g., 0.5wt% or 1wt%, the K_{1C} and G_{1C} values of nanocomposites decreased. This was due to the non-uniform dispersion of graphene. High concentration of graphene tends to reagglomerate in the matrix.

6.3.4 Hardness Test

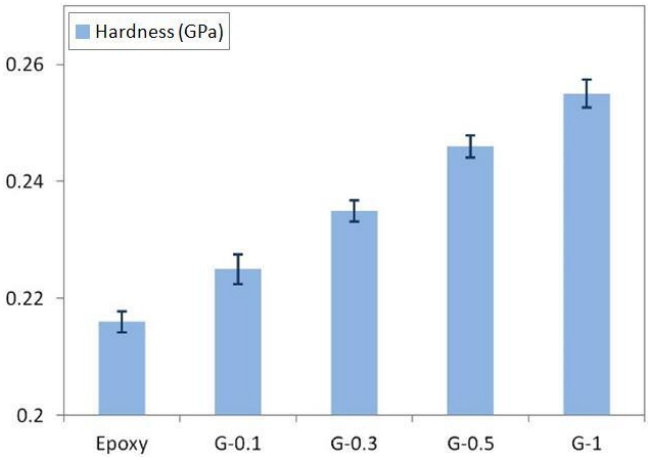

Figure 6. 4. Hardness of nanocomposites.

The Vickers hardness of the nanocomposites is shown in Figure 6.4. Epoxy showed the lowest hardness of 0.216GPa. With the incorporation of graphene, the hardness of the nanocomposites increased, particularly in case of G-1 samples, the hardness increased to 0.255GPa. Medium increments were observed for G-0.1, G-0.3 and G-0.5 samples.

The increase of hardness can be attributed to the reinforcement effect of graphene in the epoxy matrix. As a rigid material, the incorporation of graphene increased the hardness of the epoxy significantly.

6.3.5 DMA Test

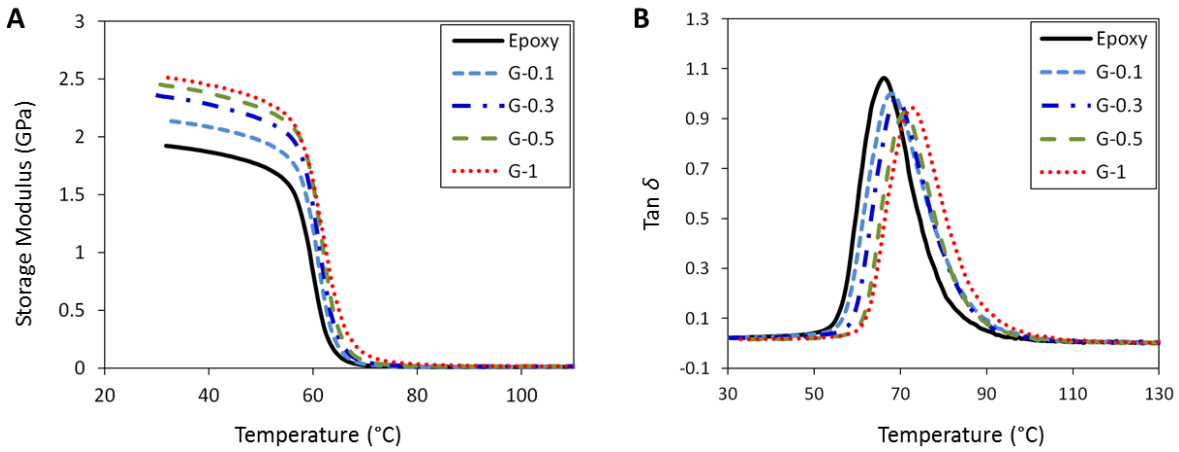

Figure 6. 5. DMA results of nanocomposites: (A) Storage Modulus; (B) Tan δ.

Figure 6.5(A) shows the storage modulus (E') as a function of temperature for epoxy/graphene nanocomposites. As can be seen from the figure, the storage modulus of Epoxy was 1.92GPa. With the increasing of the graphene contents, the storage modulus of nanocomposites increased accordingly. G-1 showed the highest storage modulus, which was 2.51GPa.

Glass transition temperature (T_g) characterizes the segmental motion of polymers and was taken as the temperature value at the peak of tan δ curves as shown in Figure 6.5(B). In the figure, it shows that the tan δ peak was observed at 66.08 ℃ for neat epoxy. After graphene was introduced, T_g shifted to a higher temperature. Among all of the increments, G-1 samples showed the highest T_g of 72.43 ℃, which was more than 6 ℃ higher when compared to that of neat epoxy. The reason for this increment in T_g can be attributed to the fact that the incorporation of graphene had restricted the molecular mobility of the epoxy matrix, and thus increased the T_g values.

6.3.6 TGA Test

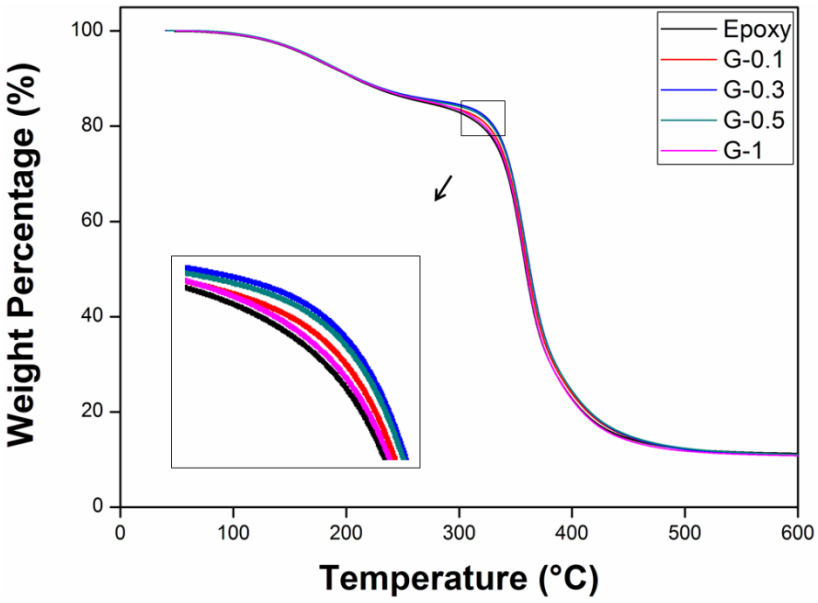

Figure 6. 6. TGA curves of nanocomposites.

Thermal decomposition is one of the fundamental thermal properties and is critical for practical applications. Figure 6.6 shows the TGA curves of the nanocomposites in a nitrogen atmosphere. All samples had a similar two stage weight loss, indicating that all samples had a similar thermal degradation mechanism. The first weight loss from 100 ℃ to 230 ℃ was attributed to the decomposition of small molecules on the side chain. The second weight loss occurred from 250 ℃ to 500 ℃ which showed the decomposition of the main polymer chain. Neat epoxy showed the highest decomposition rate. When compared to neat epoxy, G-0.1, G-0.3, G-0.5 and G-1 samples showed lower decomposition rate, indicating a higher thermal stability of the nanocomposites. The reason for this phenomenon can be explained by the fact that uniformly dispersed graphene had increased the cross-linking density of the nanocomposites. Generally, the cross-linking density refers to the concentration of cross-linked bonds per volume. As for typical polymer nanocomposites, the higher the cross-linking density is, the stronger the polymer chains bond each other, therefore improving the nanocomposites' capacity to withstand heat. Compared to the structures of neat epoxy

samples, nanocomposites prepared with graphene tend to shorten the distance among cross-linking points, and thus increase the cross-linking density of the resultant network. Among all the nanocomposites, G-0.3 samples showed the lowest decomposition rate, and indicated the best property enhancement. However, among all the nanocomposites, G-1 samples showed the highest decomposition rate under heating, which was caused by the reagglomeration of graphene. A high concentration of graphene in the matrix tends to reagglomerate and formed defects, and thus decreased the properties of nanocomposites.

6.3.7 SEM Test

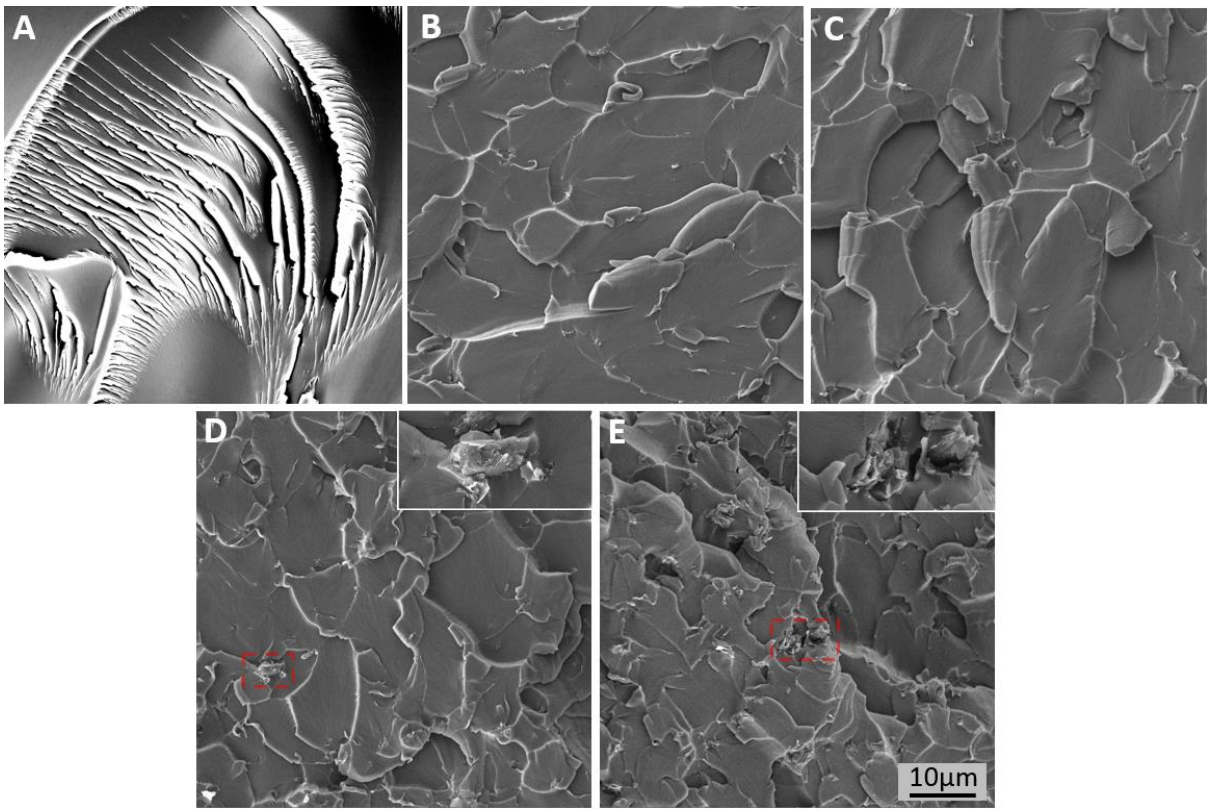

Figure 6. 7. SEM images of fracture surfaces of (A) Neat epoxy; (B) G-0.1; (C) G-0.3; (D) G-0.5and (E) G-1.

The fracture surfaces were studied by SEM and are shown in Figure 6.7. As can be seen from Figure 6.7(A), a river-like fracture pattern can be observed on the epoxy surface,

which illustrates the brittle nature of the material and its poor resistance to crack initiation and propagation. For nanocomposites prepared with graphene, the fracture pattern changed to a sheet-sheet delaminating pattern. For G-0.1 and G-0.3 samples, as shown in Figure 6.7(B and C), clear fracture patterns can be observed which reveal the better dispersion of graphene. The uniformly dispersed graphene could share external stress and can restrict deterioration in the matrix, such as any advancing cracks, which, ultimately improves the mechanical properties. However, for G-0.5 and G-1 samples, as shown in Figure 6.7(D) and (E), some poorly dispersed graphene can be seen on the surface. The poorly dispersed graphene formed defects in the nanocomposites, which act to concentrate the stresses locally, eventually causing a localized weakness, and thus decreasing the properties of the nanocomposites.

In general, the incorporation of graphene had changed the fracture mechanism of the matrix. Graphene can be dispersed efficiently in the epoxy matrix at low loadings. However, reagglomeration occurs at graphene concentration of 0.5 wt% and 1 wt%.

6.4 Summary

Graphene as a filler could enhance the properties of epoxy efficiently. In general, with the incorporation of graphene, the properties of nanocomposites increase. However, because of the strong van der Waals force on the graphene surface, graphene tends to reagglomerate in the matrix especially at high concentrations.

This work investigated the influence of graphene contents on the properties of an epoxy matrix. 0.1 wt%, 0.3 wt%, 0.5 wt% and 1 wt% epoxy/graphene nanocomposites were made. The results showed that uniformly dispersed graphene in epoxy can be obtained at low graphene concentrations. The uniformly dispersed graphene resulted in better performance of the material. 0.3 wt% epoxy/graphene nanocomposites showed the highest strength and fracture toughness. With the increase of the graphene content, the modulus and hardness

increased as well. However, high contents of graphene lead to reagglomeration in the matrix, and subsequently, the strength and fracture toughness decreased when the graphene contents were higher than 0.5wt%.In addition, uniformly dispersed graphene was quite effective to improve the T_g and thermal stability of epoxy resin when compared to poorly dispersed graphene. 0.3wt% nanocomposites showed the highest T_g and thermal stability. In consideration of the general properties of the nanocomposites, 0.3wt% graphene loading is therefore recommended for this epoxy system.

7 Effects of Solvents on the Properties of Nanocomposites

Part I: Effect of Solvent Dosage

7. 1 Introduction

Using solvents as dispersing medium has been widely accepted and regarded as the simplest method to distribute isolated graphene homogeneously in nanocomposite materials. For example, in some studies [297, 319, 366-368] graphene was dispersed in acetone and resulted in improved final properties of nanocomposites, with a concentration of graphene dispersion at 1g/L. In some studies [266, 346, 369-374] graphene was dispersed in water, ethanol, tetrahydrofuran (THF), dichloromethane (DCM), N, N-Dimethylformamide (DMF) at 1g/L, and resulted in improved final properties. Some research [261, 375, 376] demonstrated dispersal of graphene with solvents like DMF, ethanol, and acetone at 1g/2L. Furthermore, in some works [312, 355, 377], graphene was dispersed in solvents at concentrations of 1g/3L or even 1g/10L. Large amounts of solvents were used in this process because it is generally recognized that solvents help to disperse graphene. In other studies, solvents have been used, but without reporting the quantity of solvent usage. For example, some work [378, 379] reported using DMF in the processing of epoxy/graphene nanocomposites, and final materials showed enhanced mechanical properties and resistance to fatigue crack growth. Some work [380-382] reported usage of ethanol and the nanocomposites showed improved load transfer efficiency as well as improved glass transition temperature. Other solvents like isopropanol [383], THF [384, 385], butanone [273, 386], acetone [387], dichloromethane [388] have also been reported in the processing of epoxy/graphene nanocomposites. However, in these works, it is not specified how much of the solvents were used. Therefore, these studies cannot be referred to in the solvent usage of epoxy/graphene nanocomposites preparation.

To understand the relationship among solvent dosage, graphene dispersion state, and the properties of epoxy/graphene nanocomposites, 0.3wt% nanocomposites have been prepared with different dosages of DMF, which are 100ml, 300ml, 500ml, and 1500ml respectively. As the DMF dosage is different, it is expected that the dispersion and reagglomeration behaviour of graphene in epoxy matrices would be different.

7.2 Experimental

Five sets of nanocomposites filled with 0.3wt% graphene were prepared. One set of sample was prepared for reference using neat epoxy only, marked as G-0.3. Another four sets were prepared with different dosages of DMF.

0.45g graphene was first dispersed in a specified dosage of DMF (100ml, 300ml, 500mls, and 1500ml, marked as D-100, D-300, D-500 and D-1500 respectively) and then bath sonicated for thirty minutes. Epoxy monomer was then added to the dispersion and sonicated for another thirty minutes. To remove the DMF, the mixtures were heated to 150 ℃ with stirring. It is important to clarify that the mixture with 100ml of DMF was only heated for four hours, mixtures with 300ml and 500ml DMF were heated for eight hours, and the mixture with 1.5L DMF was heated for sixteen hours to ensure full evaporation of the solvent. Next, the mixtures were cooled down to room temperature and the hardener was added via hand stirring for five minutes followed by five minutes of bath sonication. Vacuum degassing was then carried out to remove the entrapped air bubbles. Subsequently, the mixtures were mould casted and cured at room temperature for six hours followed by six hours post-curing at 80 ℃. The materials and characterization techniques were described in chapter 3. The sample preparation process was shown in Figure 3.2.

7.3 Results and Discussion

7.3.1 Tensile Test

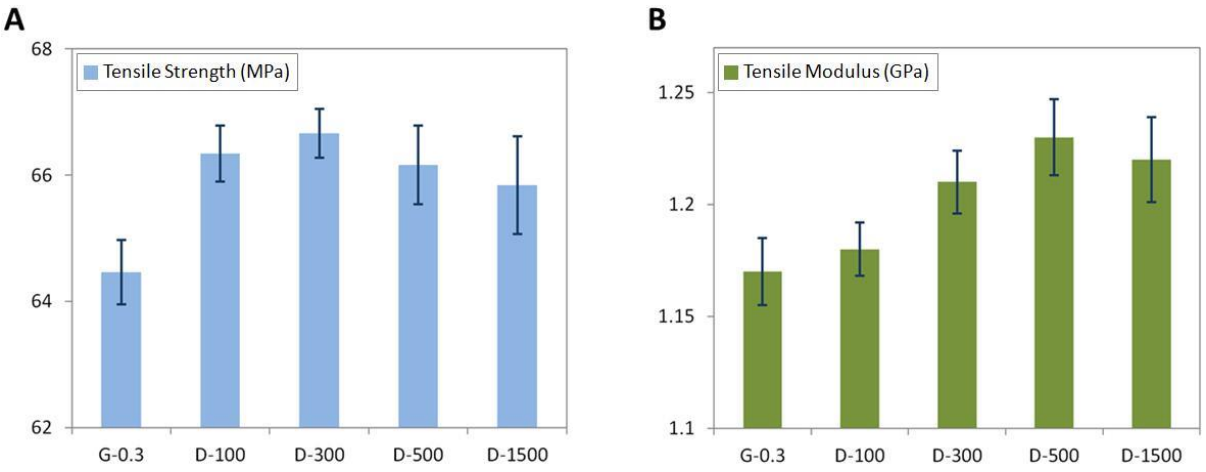

Figure 7. 1. Tensile properties of nanocomposites: (A) Tensile strength; (B) Tensile modulus.

As shown by Figure 7.1(A), G-0.3 showed the lowest tensile strength, which was 64.46MPa, all samples prepared with DMF showed increased properties in tensile strength. With increasing of DMF dosage, the tensile strength of nanocomposites increased first and then decreased. D-100 showed the tensile strength of 66.34MPA, the maximum increase in the tensile strength was shown by D-300, which was 66.66MPa. With further increasing of DMF dosage, the tensile strength of nanocomposites decreased. D-500 samples showed the tensile strength of 66.16MPa. D-1500 showed 65.84MPa in tensile strength.

The tensile modulus of the nanocomposites is shown in Figure 7.1(B). G-0.3 showed the lowest tensile modulus of 1.17GPa.The minimum increase in the tensile modulus was observed in the case of D-100 samples, which was 1.18GPa.Samples prepared with 500ml DMF showed the highest tensile modulus, which was 1.23GPa. With further increasing of DMF dosage, D-1500 showed lower tensile modulus compare to that of D-500 samples.

The general increase in tensile properties was due to the incorporation of graphene. Uniformly dispersed graphene tends to shorten the distance among cross-linking points, and thus increased the cross-linking density of the resulting network. Additionally, the uniformly

dispersed graphene formed a continuous network in the matrix, which supported the network of the matrix and released the stress concentration, also further enhancing the mechanical properties. Thus, the usage of solvents increased the properties of nanocomposites in general. However, if too much solvent was used, e.g., 1500ml DMF in this work, lower properties were observed when compared to samples prepared with less solvents, e.g., 500ml DMF. This decrease can be ascribed to the reagglomeration of graphene, which was caused by the large dosage of DMF. As large dosages of DMF require longer time to be evaporated off, this results in a higher tendency of reagglomeration.

7.3.2 Flexural Test

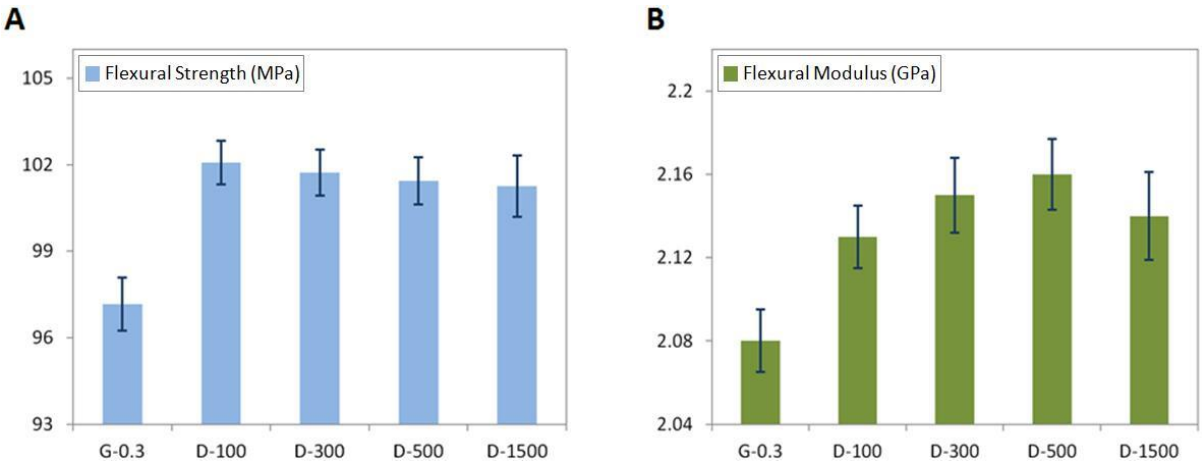

Figure 7. 2. Flexural properties of nanocomposites: (A) Flexural strength; (B) Flexural modulus.

The variation in flexural strength is shown in Figure 7.2(A). G-0.3 showed the lowest flexural strength, which was 97.1MPa. After introducing DMF, the flexural strength generally increased. Maximum flexural strength was observed at 102.08MPa for D-100 samples. However, with further increases of DMF dosages, the flexural strength decreased. D-1500 showed the minimum increase in flexural strength, which was 101.26MPa.

For flexural modulus, as shown in Figure 7.2(B), the lowest value was also observed in G-0.3 samples, which was 2.08GPa. In case of D-500 the flexural modulus increased to 2.18GPa, which was the maximum flexural modulus for this series of tests. However, D-1500 samples showed lower flexural modulus compare to that of D-500 samples, which was 2.14GPa.

In general, the improved dispersion of graphene by using DMF resulted in higher flexural properties. However, if too much solvent was used, e.g., 1500ml DMF, the flexural properties decreased.

7.3.3 Fracture Test

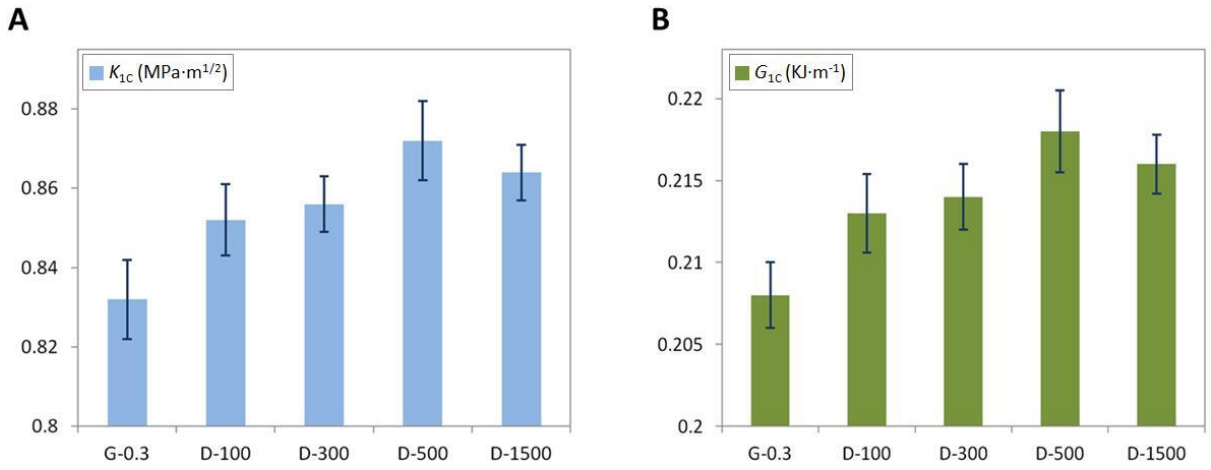

Figure 7. 3. Fracture properties of nanocomposites: (A) Fracture toughness (K_{1C}); (B) Critical strain energy release rate (G_{1C}).

Figure 7.3 shows that with an increase in DMF dosage, the K_{1C} and G_{1C} increased first and then decreased. The maximum increment in K_{1C} was observed in Figure 7.3(A) in case of D-500 samples, which increased from 0.832MPa·m$^{1/2}$ to 0.872MPa·m$^{1/2}$. For D-100 and D-300 samples, the K_{1C} also showed medium increments due to the enhanced dispersion of graphene in the epoxy matrix. D-1500 samples showed lower increments compared to that of D-500 samples, with the K_{1C} value of 0.864MPa·m$^{1/2}$.

A similar trend was also found in the G_{1C}, which was shown in Figure 7.3(B). G-0.3 samples showed the lowest G_{1C} value, which was 0.208KJ·m^{-1}. After introducing DMF, the maximum G_{1C} was obtained at 0.218KJ·m^{-1} in D-500 samples. D-100 and D-300 samples showed increased G_{1C} as well, which were 0.213KJ·m^{-1} and 0.214KJ·m^{-1}, respectively. D-1500 showed lower increments compare to D-500 samples, which was 0.216KJ·m^{-1}.

In general, when increasing the DMF dosage, the fractural properties increased. This was due to the enhanced dispersion of graphene in the epoxy matrix. The uniformly dispersed graphene improved the energy absorbing capacity, which also improved the fracture toughness of nanocomposites. However, with further increases in DMF dosages, e.g., 1500ml DMF, the K_{1C} and G_{1C} values of nanocomposites decreased. This was due to the over-dosage of DMF. Large dosages of DMF caused reagglomeration of graphene in this process.

7.3.4 Hardness Test

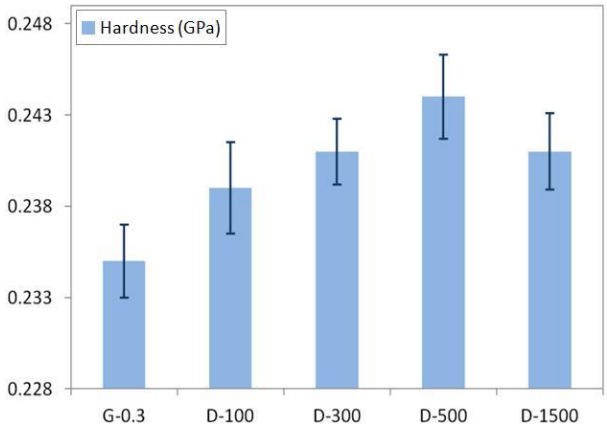

Figure 7. 4. Hardness of nanocomposites.

The Vickers hardness of nanocomposites are shown in Figure 7.4. G-0.3 samples showed the lowest hardness of 0.235GPa. With the usage of DMF, the hardness of nanocomposites significantly improved, particularly with the D-500 samples, the hardness increased to 0.244GPa. D-100 and D-300 samples also showed average increments in the

hardness, which were 0.239GPa and 0.241GPa, respectively. However, compare to that of D-500 samples, only lower improvement was observed for D-1500 samples, with a hardness of 0.241GPa.

The increase in hardness can be attributed to the good dispersion of graphene in the epoxy matrix. As described above, uniformly dispersed graphene shortens the distance among cross-linking points, which increases the cross-linking density of the epoxy network, and then plays a positive role to improve the mechanical properties. On the other hand, graphene in a liquid matrix tends to reagglomerate over time. As larger dosages of DMF require a longer time to evaporate, this results in a higher tendency of reagglomeration.

7.3.5 DMA Test

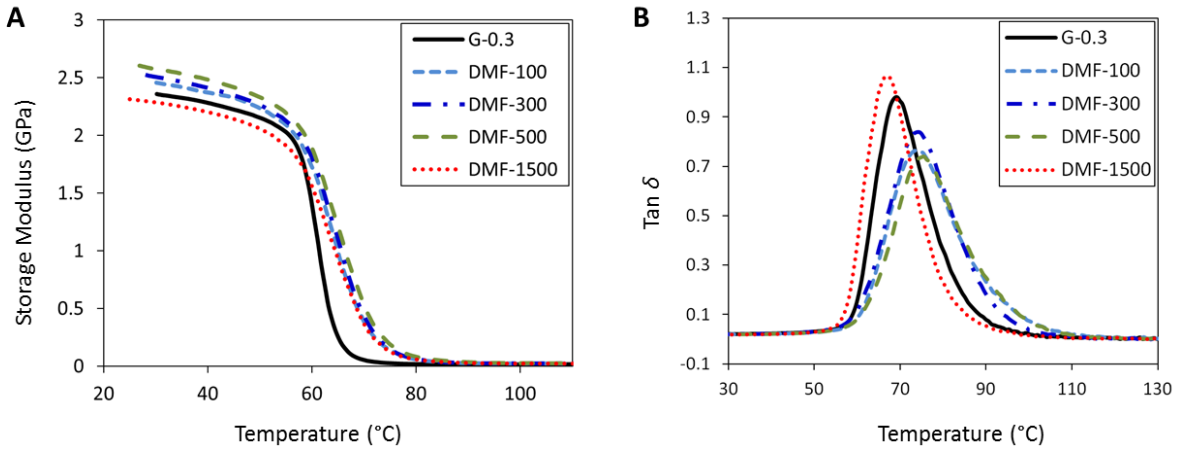

Figure 7. 5. DMA results of nanocomposites: (A) Storage Modulus; (B) Tan δ.

Figure 7.5(A) shows the storage modulus (E') as a function of temperature for epoxy/graphene nanocomposites. As can be seen from the figure, the storage modulus of G-0.3 was 2.35GPa. D-100, D-300, and D-500 samples showed an increased storage modulus, valued 2.45GPa, 2.52GPa, and 2.60GPa, respectively. However, D-1500 samples showed the minimum storage modulus, which was 2.31GPa.

Glass transition temperature (T_g) characterizes the segmental motion of polymers and was taken as the temperature value at the peak of tan δ curves as shown in Figure 7.5(B). As seen in this figure, tan δ peak was observed at 69.28 ℃ for G-0.3 samples. For D-100, D-300, and D-500 samples, T_g shifted to higher temperatures. This can be ascribed to the fact that the uniformly dispersed graphene restricted molecular mobility of the epoxy matrix, thus leading to the increased T_g value. Among these increments, 500ml DMF prepared nanocomposites showed the highest T_g of 75.57 ℃, which was more than 6 ℃ higher than that of G-0.3 samples. The increase of 5 ℃ in T_g were obtained for D-100 and D-500 samples. The reason for this increase can be explained by the effect of graphene on the cross-linking structure of the nanocomposites. As for a typical polymer nanocomposite, the higher the cross-linking density, the stronger the polymer chains bond with each other, therefore resulting in higher T_g of the nanocomposites. However, D-1500 samples showed the T_g of 65.78 ℃, which was even lower than that of G-0.3 samples. The likely reason for this decrease was that graphene in a liquid matrix tends to reagglomerate over time. Larger dosages of DMF require a longer time to be evaporated and therefore tends to result in a higher tendency of reagglomeration. Compared with the structure of good-dispersed samples, graphene agglomerates lead to the decrease of T_g.

7.3.6 TGA Test

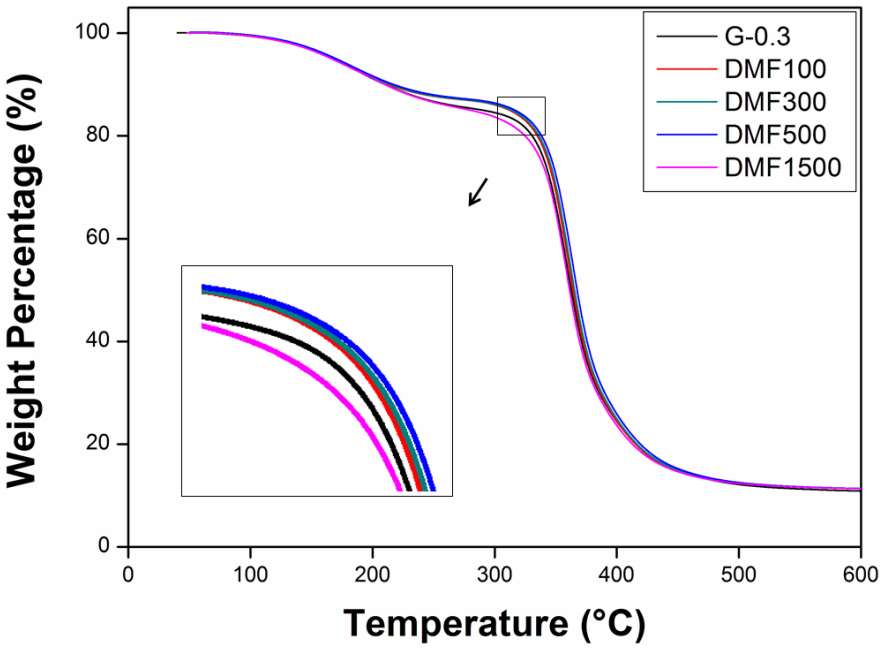

Figure 7. 6. TGA curves of nanocomposites.

Thermal decomposition a fundamental thermal property and is critical for practical applications. Figure 7.6 shows the TGA curves of the nanocomposites in a nitrogen atmosphere. All samples had a similar two stage weight loss, indicating that all samples had a similar thermal degradation mechanism. The first weight loss, from 100 ℃ to 230 ℃ was attributed to the decomposition of small molecules on the side chain. The second weigh loss occurring from 250 ℃ to 500 ℃ showed the decomposition of the main polymer chain. G-0.3 samples showed a medium decomposition rate. As compare to G-0.3 samples, D-100, D-300, and D-500 samples showed lower decomposition rates, indicating that the uniformly dispersed graphene had increased the thermal stability of nanocomposites.

The reason for this phenomenon can be explained by the fact that graphene had increased the cross-linking density of the nanocomposites. Generally, the cross-linking density means the concentration of cross-linked bonds per volume. As for typical polymer nanocomposites, the higher the cross-linking density is, the stronger the polymer chains bond

with each other, therefore improving the nanocomposites' capacity to withstand heat. Compared to the structure of G-0.3 samples, the DMF prepared samples had a tendency to shorten the distance among cross-linking points, and thus increased the cross-linking density of the resulting network. On the other hand, the uniformly dispersed graphene formed a continuous network in the matrix, which reduced the volatilization rate of the decomposition products. However, if too much DMF was used, e.g., 1500ml in this work, non-uniformly dispersed graphene decreased the properties of nanocomposites, therefore D-1500 samples showed the highest decomposition rate under heating.

In general, the increased thermal stability of D-100, D-300, and D-500 samples resulted in a higher heat capacity of nanocomposites, which was due to the uniform dispersion of graphene.

7.3.7 SEM Test

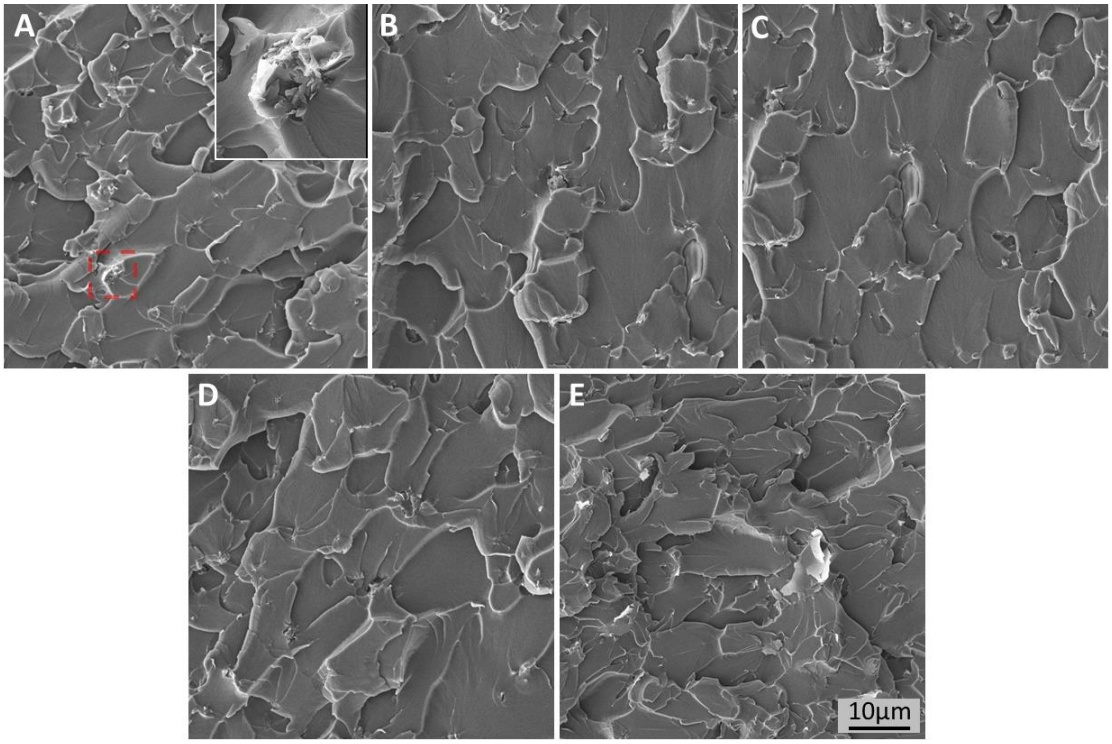

Figure 7. 7. SEM images of fracture surfaces of (A) G-0.3; (B) D-100; (C) D-300; (D) D-500, and (E) D-1500.

The fracture surfaces were studies by SEM and are shown in Figure 7.7. For G-0.3 samples, as shown in Figure 7.7(A), some poorly dispersed graphene can be seen on the surface. This poorly dispersed surface featured a poor interfacial interaction between the epoxy matrix and graphene, and showed the brittle nature of material, as well as the poor resistance to crack initiation and propagation. Compared with G-0.3, the fracture surfaces for the 100ml, 300ml and 500ml DMF prepared samples were relatively smooth, as shown in Figure 7.7(B), (C), and (D). The clear fracture pattern showed the fracture mechanism of sheet-sheet delamination for the nanocomposites, and revealed that the usage of a certain amount of DMF can generate a uniform dispersion of graphene. The uniformly dispersed graphene in the matrix formed a continuous network, which released the stress concentration effectively. Additionally, uniformly dispersed graphene could bridge growing cracks, thus stabilising and preventing any further deterioration from causing larger and more harmful cracks, consequently enhancing the properties of nanomaterials. However, for 1500ml DMF prepared samples, as shown in Figure 7.7(E), some large graphene agglomerates could be seen on the fracture surface. These agglomerates formed defects in the nanocomposites, which acted to concentrate the stresses locally, eventually causing a localized weakness, which caused large cracks and decreased the properties of the nanocomposites.

7.3.8 XRD Test

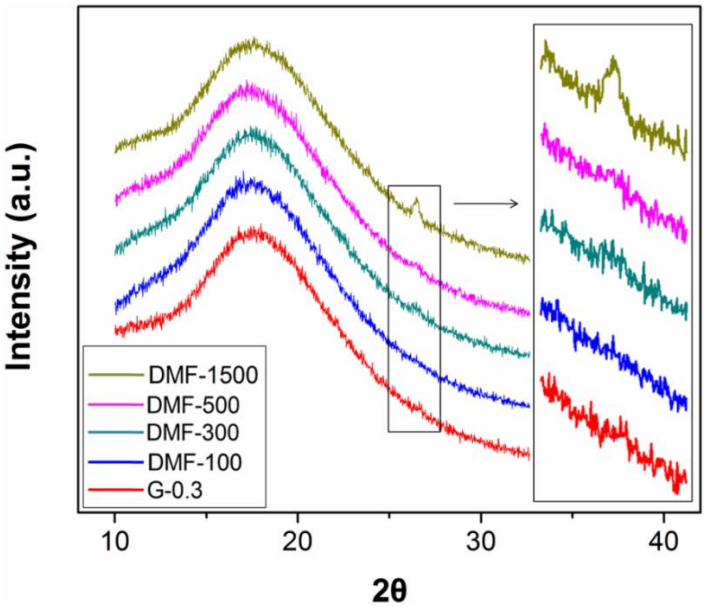

Figure 7. 8. XRD patterns of nanocomposites.

Finally, XRD was used to characterize the structure of the epoxy/graphene nanocomposites. As shown by Figure 7.8, all the samples exhibited a wide diffraction from 11-28 °, which was caused by a scattering of the X-ray beam by cured epoxy molecules and revealed the amorphous feature of matrix. However, for samples prepared with 1500ml DMF, there was a sharp shoulder peak of 2θ at 26.5 °, which is characteristic of the structure of graphite.

This graphitic structure could only be caused by the agglomeration of graphene during the processing. This result clearly showed that the use of large dosage of DMF induced reagglomeration of graphene, which lead to the decrease in the properties.

7.4 Summary

DMF was used to investigate the effects of solvent dosage on the preparation and the properties of epoxy/graphene nanocomposites. This research provides guidelines for the usage of DMF in the preparation of epoxy/graphene nanocomposites, and could also be a

reference for other polymer composites where the use of solvents is required in the processing. Mechanical properties, TGA, DMA, SEM, and XRD were tested in this work and the results show that large dosage of solvents are responsible for decreasing the final properties of the nanocomposites. The long processing times, higher temperatures, and low viscosity of solvents are responsible for the promotion of the reagglomeration of graphene. These findings will have profound implications in nanocomposite manufacturing, as large amounts of solvents could be avoided from economic and health and safety perspectives. Additionally, the processing time could be shortened, and environmental pollution could be controlled more effectively by reducing the amount of evaporated solvents. These results help in optimisation and are having positive implications on the practical processing technology of nanocomposites. Although the relationship between solvent dosage and the consequent processing of epoxy/graphene nanocomposites has been demonstrated in this report for the first time, it has not given the critical value for the best condition of dispersibility and processability. Therefore, more work needs to be conducted to fully understand the best usage of solvents.

7 Effects of Solvents on the Properties of Nanocomposites

Part II: Effect of Different Solvents

7.5 Introduction

Solvents are widely used as a dispersant to overcome the van der Waals force between graphene nanosheets, and generate homogeneous dispersions. For example, ethanol [389-391] has been widely adopted as a dispersant for graphene materials, and showed good dispersion characteristics and stability. Dimethyformamide (DMF) [392] is also well recognised for polymer researchers as a good dispersant. When using DMF, a lot of research reported enhancements in the final properties of epoxy/graphene nanocomposites.

DCB was also reported as a good dispersant for graphene for the following reasons: Firstly, DCB is a commonly used reaction solvent for fullerenes and is known to form stable SWNT dispersions [393]. Secondly, DCB is a convenient dispersant and is compatible with a variety of chemicals. Thirdly, DCB, being aromatic, can interact with graphene via π-π stacking [394]. Fourthly, it has been reported [395, 396] that solvents with high values of the dispersion component (δ_d) of the Hildebrand solubility parameter are the best for producing homogeneous and agglomerate-free dispersions of graphene. DCB shows a high δ_d of 19.2MPa$^{1/2}$. As for these regards, DCB tends to be suitable to produce stable graphene dispersion.

However, although DCB shows some advantages, the use of DCB to prepare epoxy/graphene nanocomposites is not yet fully realised by the polymer community. Research indicates that, to date, there has been no exclusive study investigating the use of DCB as a dispersant for epoxy/graphene nanocomposites. In this work, o-dichlorobenzene has been used for the first time to prepare epoxy/graphene nanocomposites. Another two commonly used solvents, DMF (δ_d = 17.4MPa$^{1/2}$) and ethanol (δ_d = 15.8MPa$^{1/2}$) have been used as comparative samples in this work.

7.6 Experimental

Four sets of 0.3wt% nanocomposites were prepared. For reference, one set of samples using no solvent was prepared and marked as G-0.3. Another three sets of samples were prepared by DCB, DMF and ethanol, respectively.

Graphene nanoplatelets were first dispersed in a solvent (DCB, DMF and ethanol, respectively), bath sonicated for thirty minutes, and then an epoxy monomer was added to the dispersion and sonicated for further thirty minutes. To remove the solvent, the mixtures were heated with stirring. Then the mixtures were cooled down to room temperature and the hardener was added with hand stirring for five minutes followed by five minutes of bath sonication. Vacuum degassing was then carried out to remove the entrapped air bubbles. Subsequently, the mixture was mold casted and cured at room temperature for six hours followed by post-curing at 80 ℃ for six hours. The materials and characterization techniques were described in chapter 3. The sample preparation process was shown in Figure 3.2.

7.7 Results and Discussion

7.7.1 Visual Stability of Colloids

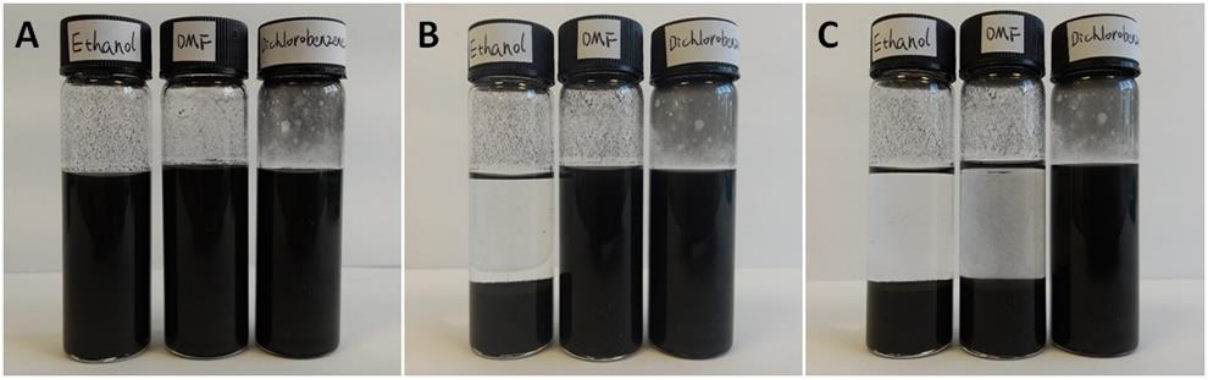

Figure 7. 9. Visual stability of graphene suspensions, (A). 5min after sonication; (B). 2h after sonication and (C). 12h after sonication.

Successful fabrication of the nanocomposites depends crucially on maintaining a stable dispersion of the graphene before polymer curing. Figure 7.9 shows the colloidal suspension for graphene in DCB, DMF and ethanol after sonication at different time intervals. The picture shows that the graphene settled down in ethanol within two hours after sonication, the graphene-DMF suspension also reagglomerated significantly and settled down within twelve hours of sonication. However, stable dispersion could only be achieved by DCB, suggesting that DCB is the best substance for preparing uniformly dispersed epoxy/graphene nanocomposites.

7.7.2 Tensile Test

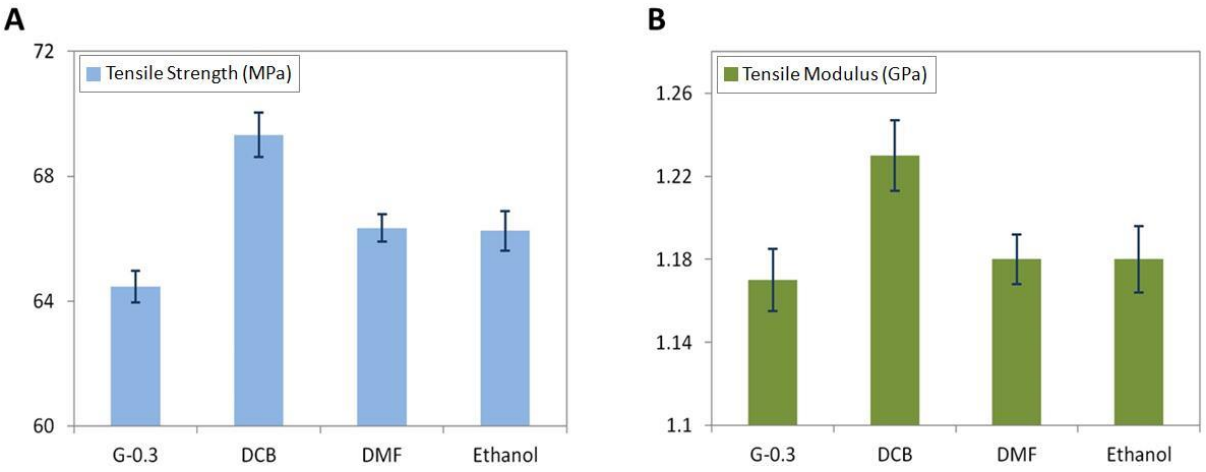

Figure 7. 10. Tensile properties of nanocomposites: (A) Tensile strength; (B) Tensile modulus.

As shown by Figure 7.10(A), G-0.3 showed the lowest tensile strength, which was 64.46MPa. After introducing the solvents, all the samples showed increased tensile strength properties. The maximum increase in the tensile strength was shown by DCB samples, which was 69.32MPa. DMF and ethanol samples showed medium increases in tensile strength, which were 66.34MPa and 66.25MPa, respectively.

The tensile modulus of the nanocomposites is shown in Figure 7.10(B). G-0.3 showed the lowest tensile modulus of 1.17GPa. Both DMF samples and ethanol samples showed the tensile modulus of 1.18GPa. Samples prepared with DCB showed the highest tensile modulus, which was 1.23GPa.

The general increase of tensile properties was due to the good distribution of graphene by using solvents. Uniformly dispersed graphene could shorten the distance among cross-linking points, and thus increased the cross-linking density of the resultant network. Besides that, graphene in the matrix formed a continuous network, thus releasing the stress concentration and enhancing the mechanical properties. In general, the usage of solvents could increase the properties of nanocomposites. Among all these samples, DCB samples showed better tensile performance than DMF and ethanol samples, indicating that DCB had higher dispersion efficiencies than that of DMF and ethanol.

7.7.3 Flexural Test

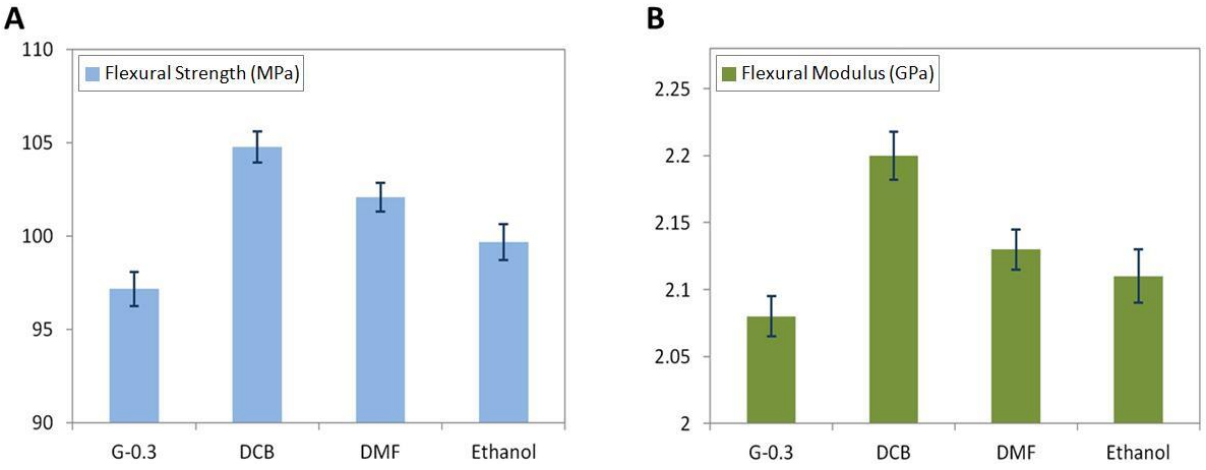

Figure 7. 11. Flexural properties of nanocomposites: (A) Flexural strength; (B) Flexural modulus.

The variation in flexural strength is shown in Figure 7.11(A). G-0.3 showed the lowest flexural strength, which was 97.1MPa. After introducing the solvents, the flexural

strength generally increased. The highest flexural strength was observed at 104.77MPa for DCB samples. DMF sample showed an average increase in flexural strength, which was 102.08MPa, and ethanol samples showed the minimum increase, with a flexural strength of 99.67MPa.

For flexural modulus, as shown in Figure 7.11(B), the lowest value was also observed in G-0.3 samples, which was 2.08GPa. In case of the DCB samples the flexural modulus increased to 2.2GPa, showing the greatest increase. DMF showed the flexural modulus of 2.13GPa. Compared to that of DCB and DMF samples, ethanol samples showed lower flexural modulus, which was 2.11GPa.

To sum up, the usage of solvents resulted to higher flexural properties. Among all the solvents, DCB samples showed the best property enhancement.

7.7.4 Fracture Test

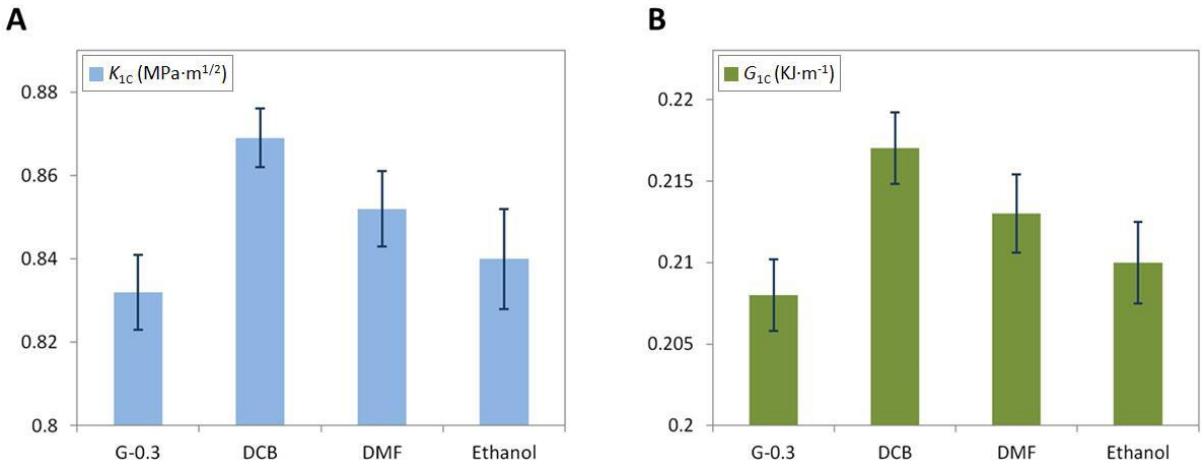

Figure 7. 12. Fracture properties of nanocomposites: (A) Fracture toughness (K_{1C}); (B) Critical strain energy release rate (G_{1C}).

From Figure 7.12 both the K_{1C} and G_{1C} increased after the solvents were introduced. The maximum increment in K_{1C} was observed in Figure 7.12(A) and was generated by the DCB samples, which increased from 0.832MPa·m$^{1/2}$ to 0.869MPa·m$^{1/2}$. For the DMF samples,

the K_{1C} also showed increased values due to the enhanced dispersion of graphene in the epoxy matrix, with the K_{1C} value of 0.852MPa·m$^{1/2}$. Ethanol samples showed a lower improvement compared to that of the DMF samples, which was 0.84MPa·m$^{1/2}$.

A similar trend was also found in the G_{1C}, which was shown in Figure 7.12(B). G-0.3 samples showed the lowest G_{1C} value, which was 0.208KJ·m^{-1}. After introducing DCB, the highest G_{1C} was obtained at 0.217KJ·m^{-1}. DMF samples showed increased G_{1C} as well, which was 0.213KJ·m^{-1}.Ethanol samples showed lower levels compared to that of DMF samples, which was 0.21KJ·m^{-1}.

In general, after the solvents were introduced, the fractural properties increased. This was due to the enhanced dispersion of graphene in epoxy matrix. The uniformly dispersed graphene improved the energy absorbing capacity, improving the fracture toughness of nanocomposites as a result. In general, DCB showed better dispersion efficiency than that of DMF and ethanol.

7.7.5 Hardness Test

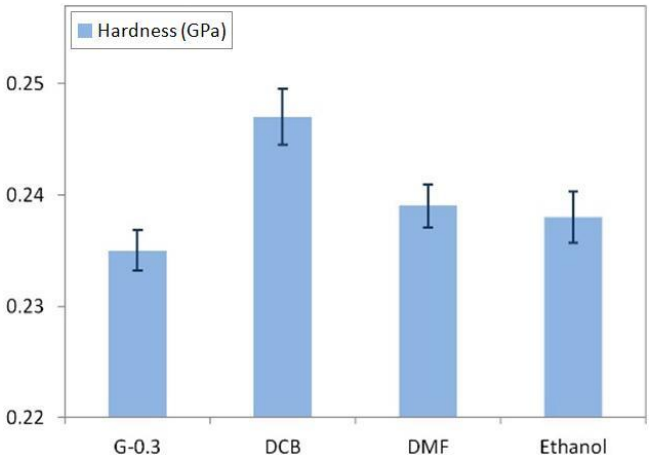

Figure 7. 13. Hardness of nanocomposites.

The Vickers hardness of nanocomposites are shown in Figure 7.13. G-0.3 samples showed the lowest hardness of 0.235GPa. After solvents were introduced, the hardness of

nanocomposites significantly improved, particularly in DCB samples, where the hardness increased to 0.247GPa. However, lower increments were observed in DMF and ethanol samples, which were 0.239GPa and 0.238GPa, respectively.

The increase of hardness can be attributed to the good dispersion of graphene in the epoxy matrix. As described above, uniformly dispersed graphene shortened the distance among cross-linking points, which increased the cross-linking density of the epoxy network, and played a positive role in improving the mechanical properties. Among these solvents, DCB showed the best dispersion efficiency, DMF second and lastly, ethanol.

7.7.6 DMA Test

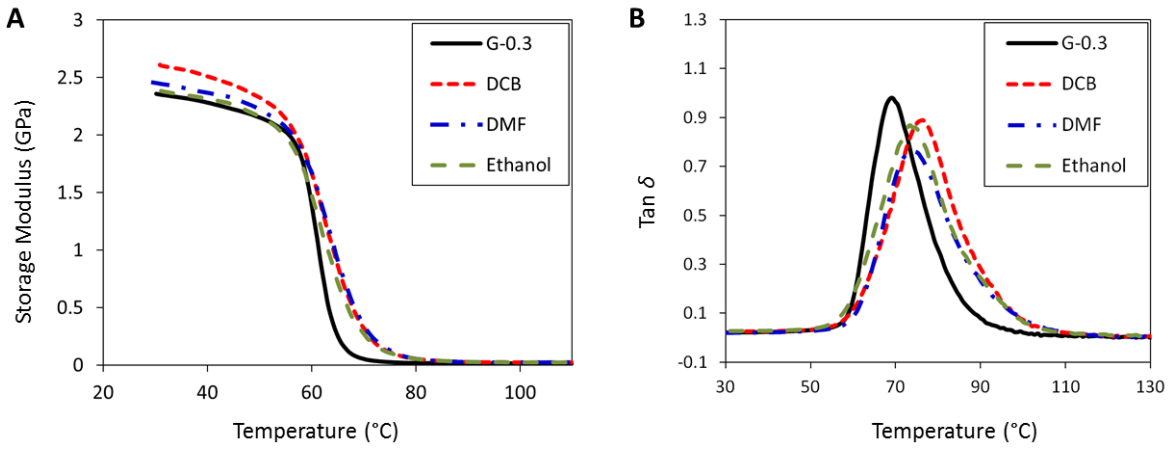

Figure 7. 14. DMA results of nanocomposites, (A). storage modulus and (B). tan δ.

Figure 7.14(A) shows the storage modulus (E') as a function of temperature for epoxy/graphene nanocomposites. As shown in the figure, throughout the temperature range investigated, the storage modulus of samples prepared with solvents increased significantly when compared to the samples prepared with no solvent. Specifically, DCB prepared samples showed 2.61GPa in the storage modulus, which was the highest increase, while G-0.3 showed the storage modulus of 2.35GPa. DMF and ethanol samples showed the storage modulus of 2.45GPa and 2.38GPa, respectively.

Glass transition temperature (T_g) characterizes the segmental motion of polymers and was taken as the temperature value at the peak of tan δ curves as shown in Figure 7.14(B). In the figure, the tan δ peak was observed at 69.28 ℃ for G-0.3 samples. For nanocomposites prepared with DCB, DMF, and ethanol, T_g shifted to higher temperatures, which can be ascribed to the fact that the uniformly dispersed graphene restricted the chain mobility of epoxy, thus leading to increased T_g values. Among these increments, DCB prepared samples showed the highest T_g of 76.57 ℃, which was more than a 7 ℃ increase compared to that of G-0.3 samples. Only a slight increase (~4 ℃) in T_g was obtained for samples prepared with DMF and ethanol. As described above, the uniformly dispersed graphene can increase the cross-linking density of the epoxy network, and plays an important role in improving the T_g.

7.7.7 TGA Test

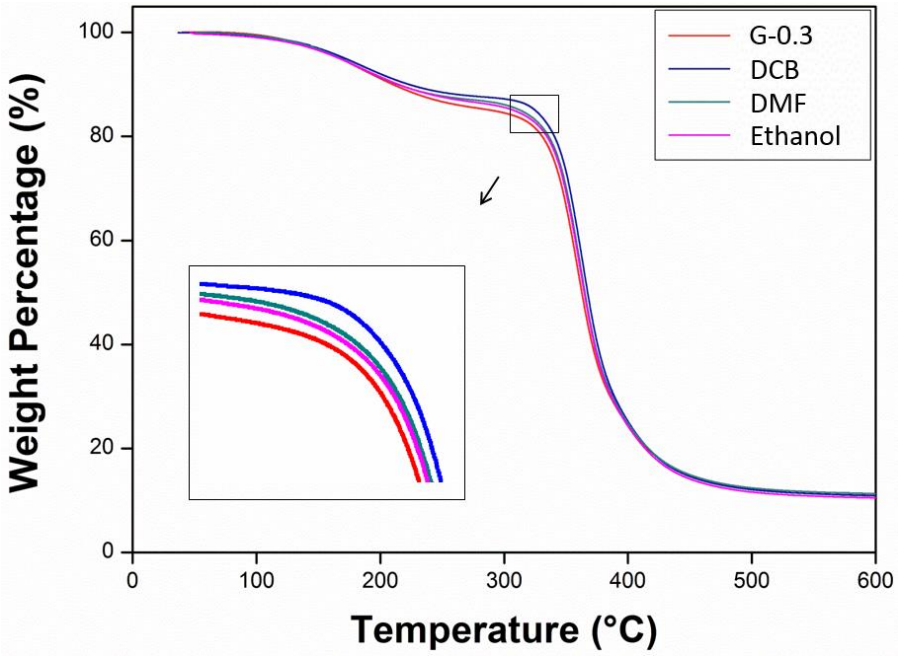

Figure 7. 15. TGA curves of the nanocomposites.

Thermal decomposition is a fundamental thermal property and is critical for practical applications. Figure 7.15 shows the TGA curves of the nanocomposites in a nitrogen

atmosphere. All samples showed a similar two stage weight loss, indicating that all samples had a similar thermal degradation mechanism. The first weight loss from 100 ℃ to 230 ℃ was attributed to the decomposition of small molecules on the side chain. The second weigh loss occurred from 250 ℃ to 500 ℃, showing the decomposition of the main polymer chain. As can be seen from the figure, DCB samples showed the lowest decomposition rate, indicating that DCB samples were more stable than DMF and ethanol samples.

This phenomenon can be explained by the fact that graphene increased the cross-linking density of the nanocomposites. Generally, the cross-linking density means the concentration of cross-linked bonds per volume. As for typical polymer nanocomposites, the higher the cross-linking density, the stronger the polymer chains bond with each other, therefore improving the nanocomposites' capacity to withstand heat. Compared with the structures of DMF and ethanol samples, DCB prepared samples tend to shorten the distance among cross-linking points, and thus increased the cross-linking density of the resulting network. On the other hand, the uniformly dispersed graphene formed a continuous network in the matrix, which reduced the volatilization rate of the decomposition products.

In general, the increased thermal stability of DCB samples resulted in a higher heat capacity of nanocomposites and a better barrier effect of the graphene network, which was due to the uniform dispersion of graphene.

7.7.8 SEM Test

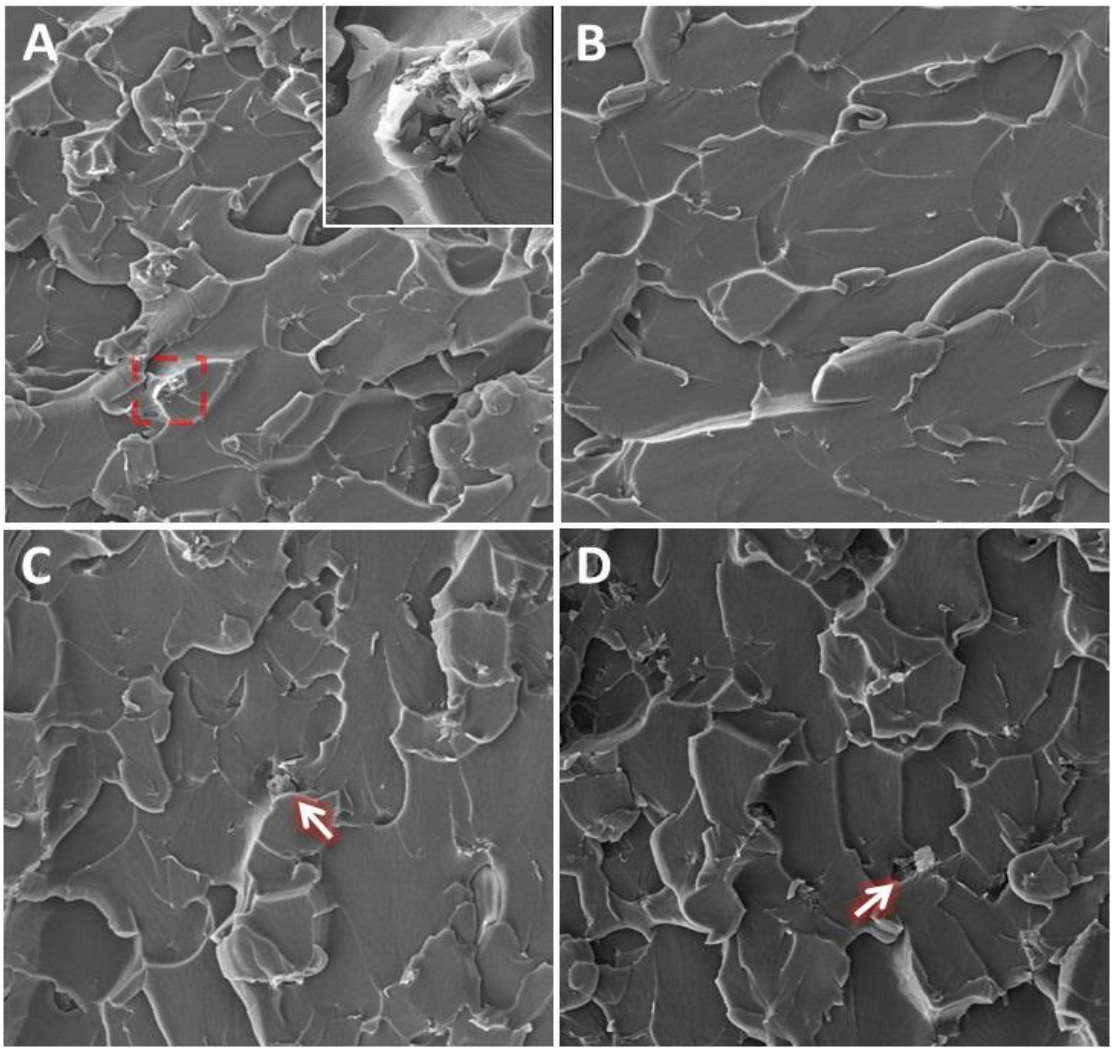

Figure 7. 16. SEM images of fracture surfaces of (A) G-0.3; (B) DCB samples; (C) DMF samples, and (D) ethanol samples.

The fracture surfaces were studied using SEM and are shown in Figure 7.16. For G-0.3 samples, as shown in Figure 7.16(A), graphene agglomerates were sparsely located on the surface, the inset of Figure 7.16(A) showed the typical morphology of one of these graphene agglomerates. The relatively rough surface of this fractured sample shows the brittle nature of the material and poor resistance to crack initiation and propagation. When compared with the G-0.3 samples, the fracture surface for the DCB samples was relatively smooth, as shown in Figure 7.16(B). These fracture patterns showed the fracture mechanism of the sheet-sheet

delamination of this material, and revealed that the usage of DCB could produce a better dispersion of graphene. However, for the DMF and ethanol prepared samples, as shown by the arrows in Figure 7.16(C) and (D), some poorly dispersed graphene can still be seen on the surface. These agglomerates formed defects in the matrix, which acted to concentrate the stresses locally, eventually causing a localised weakness, which causes decreased properties in the nanocomposites.

7.8 Summary

A prerequisite for the exploitation of graphene in epoxy nanocomposites is the homogeneous dispersion and distribution of the graphene in the matrix. The extraordinarily high specific surface area of graphene results in very high van der Waals forces between them, inducing a strong tendency to reagglomerate. The selection of the dispersion medium is very important for the final properties of the nanocomposite.

Therefore, DCB was used to test its effectiveness on the epoxy/graphene nanocomposites preparation. Colloidal dispersion stability, mechanical properties, TGA, DMA, and SEM images of nanocomposites were tested. The results showed that DCB was eligible to produces stable graphene dispersion. However, DMF and ethanol showed lower dispersing efficiencies. Nanocomposites prepared with DCB also showed higher mechanical properties and better thermal stability compared to those prepared with DMF and ethanol.

In general, it is concluded that DCB was found to be more effective than DMF and ethanol for making homogeneous graphene dispersions. The usage of DCB can brings the nanocomposites with outstanding mechanical properties and improves their thermal stability. This finding is significant in practice and gives guidelines of DCB usage in epoxy/graphene nanocomposite preparation, and could also be translated to other polymer composites where using of solvents is required in the processing.

8 Effects of Different Surfactants on the Properties of Nanocomposites

8.1 Introduction

Surface functionalisation of graphene has been widely adopted to resolve the problem of agglomeration [216]. As the most commonly used amphiphilic water-soluble dispersants, Sodium Dodecyl Sulphate (SDS) and Gum Arabic (GA) show good potential to de-bundle nanofillers from their agglomerates. For SDS, negatively charged sulphate groups coat on graphene and provide electrostatic repulsion, and thus prevent agglomeration [212, 397]. For GA, the long polymer chains of GA physically get adsorbed between graphene which disperses them by steric repulsion [398]. Therefore, SDS and GA has been widely used to disperse graphene. For example, Amoli *et al.* [358] prepared an electrically conductive adhesive by using SDS. A stable graphene dispersion was achieved using this method and the resultant material showed significant electrical conductivity at noticeably low graphene content. Hajian *et al.* [399] prepared poly vinyl butyral/graphene nanocomposite using SDS, the prepared nanocomposites showed good toughness and flexibility. Furthermore, SDS has also been used to prepare graphene nanocomposites in poly vinyl alcohol [400], polyurethane [401] and polystyrene [402] matrices. For GA, by exfoliating graphite in GA aqueous solution, high yielding and stable dispersion of graphene was achieved [403-405]. GA has also been reported to disperse graphene and produce hydrogel [229], poly ethylene oxide [406] nanocomposites, etc.

However, although SDS and GA have been widely used to disperse graphene, their dispersion effect for graphene is still not yet fully studied. In this work, SDS and GA have been selected to compare their dispersion effect for graphene in epoxy matrix for the first time. Nanocomposites were made, mechanical properties, glass transition temperature (T_g), thermal decomposition behaviour and fracture surface morphology were tested to compare the effect of SDS and GA on the properties of epoxy/graphene nanocomposites.

8.2 Experimental

Three sets of 0.3wt% nanocomposites were prepared. One set of samples was prepared with unmodified graphene, marked as G-0.3. Another two sets of samples were prepared by SDS-graphene and GA-graphene, respectively, marked as SDS samples and GA samples.

For samples prepared with unmodified graphene, the graphene was first dispersed in liquid epoxy by bath sonication for thirty minutes at room temperature. Then the suspensions were mixed with hardener with a ratio of 2:1, epoxy:hardener, Following thorough hand mixing for ten minutes, vacuum degassing was carried out to remove the entrapped air bubbles. The mixtures were then mould casted and cured at room temperature for six hours, followed by post-curing at 80 ℃ for a further six hours.

For surfactants prepared nanocomposites, firstly, SDS and GA were dissolved in de-ionized water (2.25g/L) respectively in a beaker by bath sonication. Once a solution was achieved, graphene was added to the solution with care taken to avoid any graphene sticking to the sides of the beaker. After thirty minutes of sonication, the solutions were transferred into an oven and heated to 95℃ overnight to fully remove the water. The subsequent products were marked as SDS-graphene and GA-graphene respectively. Then the SDS-graphene and GA-graphene were used to prepare nanocomposites according to the same method of G-0.3 samples. The materials and characterization techniques were described in chapter 3.

8.3 Results and Discussion

8.3.1 FTIR Test

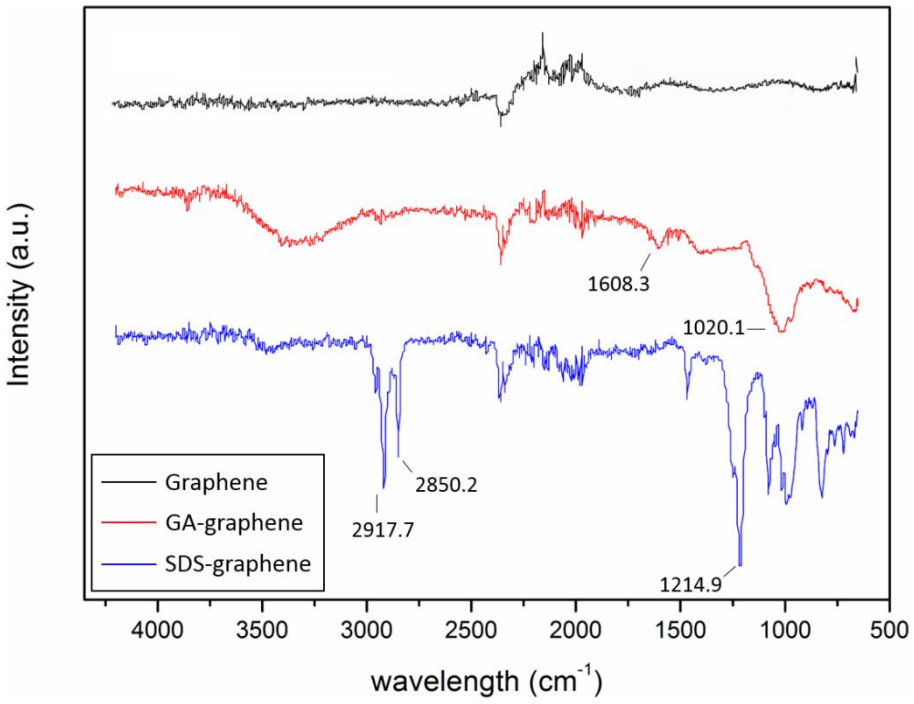

Figure 8. 1. FTIR spectrum of modified and unmodified graphene.

To evaluate if SDS and GA were successfully grafted to graphene surfaces, FTIR of the original and modified graphene were tested and the results are shown in Figure 8.1. For original graphene, because it constitutes of carbon only, no specific functional group can be seen on the spectrum. For GA-graphene samples, the peaks at 1608.3 cm^{-1} and 1020 cm^{-1} were attributed to the stretching vibrations of C=O and C–O–C structures of the GA. Another evidence of GA was present on the surface of graphene was the wide diffraction peak in the range of 3000-3700 cm^{-1}, this features the hydroxyl groups of the polysaccharide, which is the main composition of GA. For the spectrum of SDS-graphene samples, the two peaks at 2850.2cm^{-1} and 2917.7 cm^{-1} showed the C–H of the saturated alky groups, the peak at 1214.9 cm^{-1} showed the stretching of S=O. These peaks are characteristic of SDS, and implied the presence of SDS on the graphene surface.

8.3.2 Tensile Test

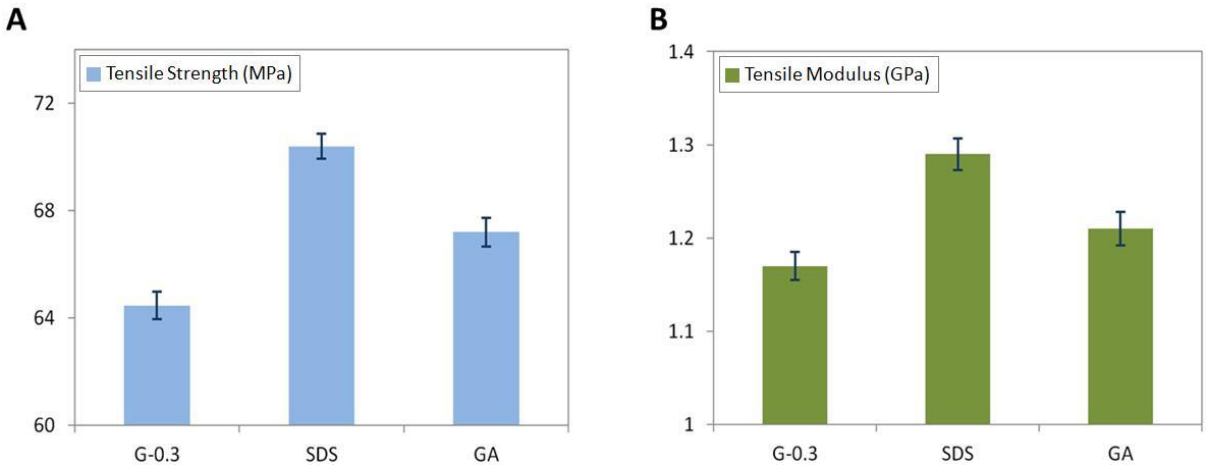

Figure 8. 2. Tensile properties of nanocomposites: (A) Tensile strength; (B) Tensile modulus.

The tensile properties of nanocomposites are shown in Figure 8.2. As can be seen from Figure 8.2(A), G-0.3 showed the lowest tensile strength of 64.46MPa. Both SDS and GA samples showed increased tensile strength. GA samples showed a medium increase, with a tensile strength of 67.2MPa. The highest tensile strength was shown in SDS samples, which was 70.40MPa.

The tensile modulus of the nanocomposites is shown in Figure 8.2(B). G-0.3 samples showed the tensile modulus of 1.17GPa. A medium increase in the tensile modulus was observed in GA samples with 1.21GPa, SDS samples showed the highest tensile modulus, which was 1.29GPa.

The results showed that after introduced surfactants, the tensile properties of nanocomposites increased. This increase was occurred because surfactants improved the dispersion of graphene. Uniformly dispersed graphene shortened the distance among cross-linking points, and thus increased the cross-linking density of the resulting network. Consequently, this also enhanced the mechanical properties of the nanomaterial. In general, SDS samples showed higher tensile properties than GA samples, indicating that SDS hada higher dispersion efficiency than GA.

8.3.3 Flexural Test

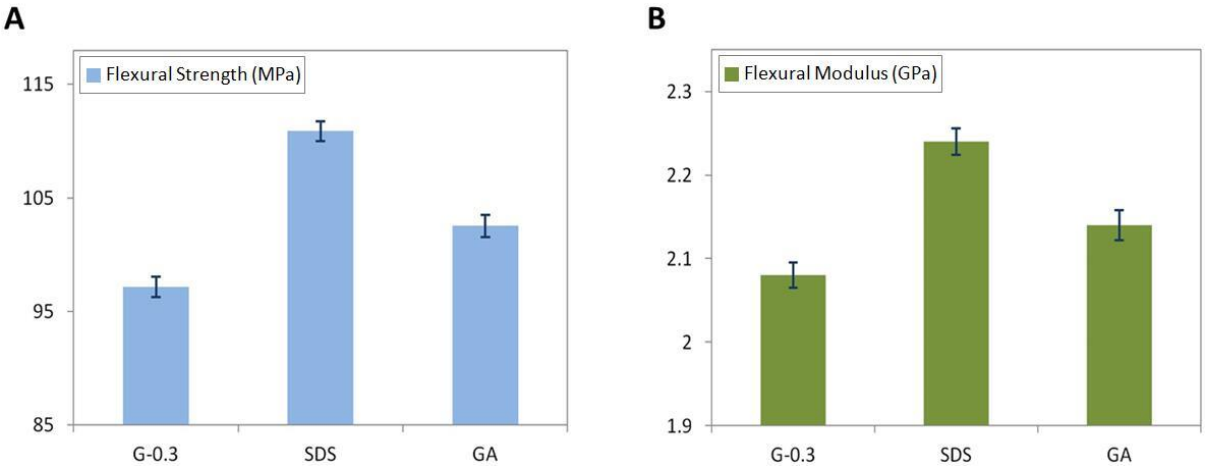

Figure 8. 3. Flexural properties of nanocomposites: (A) Flexural strength; (B) Flexural modulus.

Compared with tensile properties, similar trends were observed in flexural properties for the nanocomposites. G-0.3 samples showed lowest flexural properties. The flexural strength and flexural modulus increased with the usage of SDS and GA. As shown in Figure 8.3(A), G-0.3 showed the lowest flexural strength of 97.1MPa. The maximum increase in flexural strength was obtained in SDS samples with a value of 110.89MPa. The flexural strength for GA samples also showed improvements because of the improved dispersion of graphene in the epoxy matrix, with a flexural strength of 102.53MPa.

The flexural modulus of nanocomposites is shown in Figure 8.3(B). G-0.3 showed the flexural modulus of 2.08GPa. After introduced SDS, the maximum flexural modulus was obtained at 2.24GPa. GA samples also showed increased flexural modulus with the value of 2.14GPa.

In general, after introducing surfactants, flexural properties were improved. These improvements were the result of improved dispersion of graphene in epoxy. For these two surfactants, it is clear that SDS dispersed graphene more efficiently than GA

8.3.4 Fracture Test

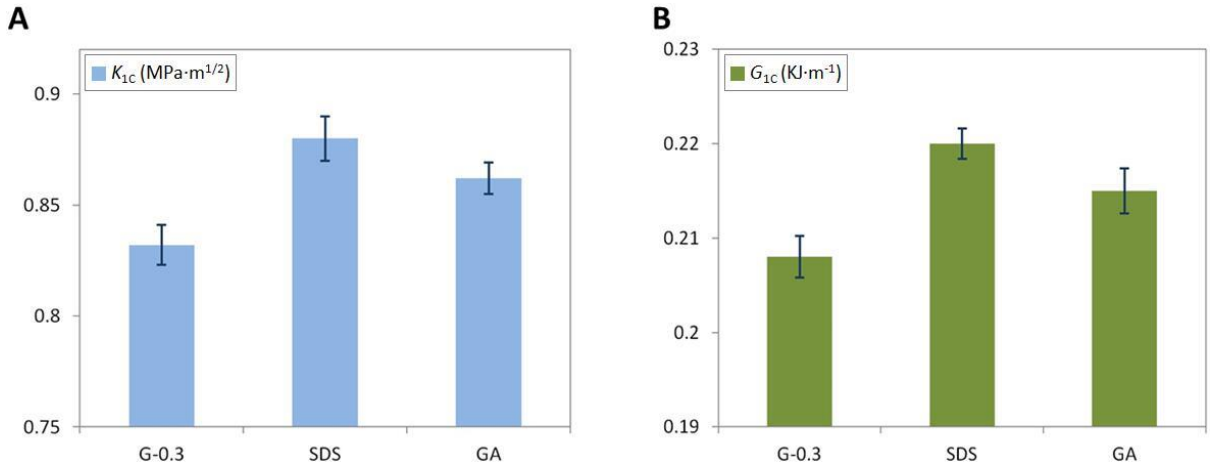

Figure 8. 4. Fracture properties of nanocomposites: (A) Fracture toughness (K_{1C}); (B) Critical strain energy release rate (G_{1C}).

The variation in K_{1C} is shown in Figure 8.4(A). G-0.3 samples showed the K_{1C} of 0.832MPa·m$^{1/2}$. The maximum K_{1C} increased to 0.88MPa·m$^{1/2}$, as observed in SDS samples. GA samples showed the K_{1C} of 0.862MPa·m$^{1/2}$. The variation of G_{1C} is shown in Figure 8.4(B), the lowest G_{1C} was observed in G-0.3 samples, which was 0.208KJ·m^{-1}. In SDS samples, it can be seen that the G_{1C} increased to 0.22KJ·m^{-1}GPa, showing the maximum improvement. GA samples showed a medium increase in G_{1C} with a value of 0.215GPa.

In general, when compared to nanocomposites prepared without surfactants, nanocomposites prepared by SDS and GA showed increased fracture resistance properties. This was due to the enhanced dispersion of graphene in the epoxy matrix. The uniformly dispersed graphene improved the energy absorbing capacity, as a result improving the fracture toughness of nanocomposites.

8.3.5 Hardness Test

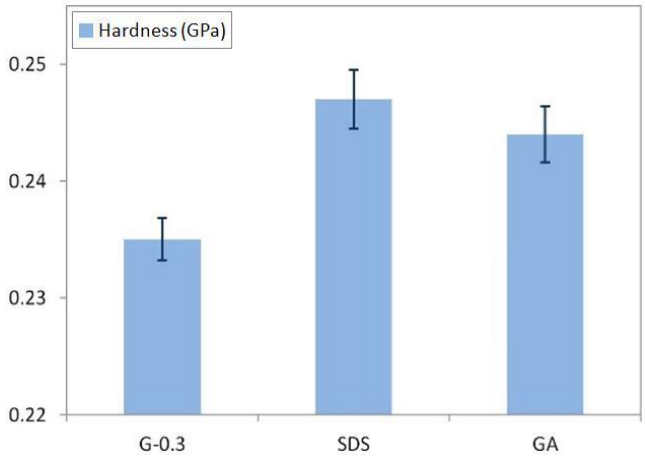

Figure 8. 5. Hardness of nanocomposites.

As seen in Figure 8.5, samples prepared with unmodified graphene showed a hardness of 0.235GPa. GA samples showed the surface hardness of 0.244GPa. A higher hardness can be observed in the SDS samples, at 0.247GPa. Such an improved hardness indicates better dispersion of graphene in epoxy.

Good dispersion of graphene in the epoxy matrix attributed to the improvements in hardness. As described above, homogeneously dispersed graphene shortened the distance among cross-linking points, thus increasing the cross-linking density of the matrix, and then plays a positive role to improve the mechanical properties.

8.3.6 DMA Test

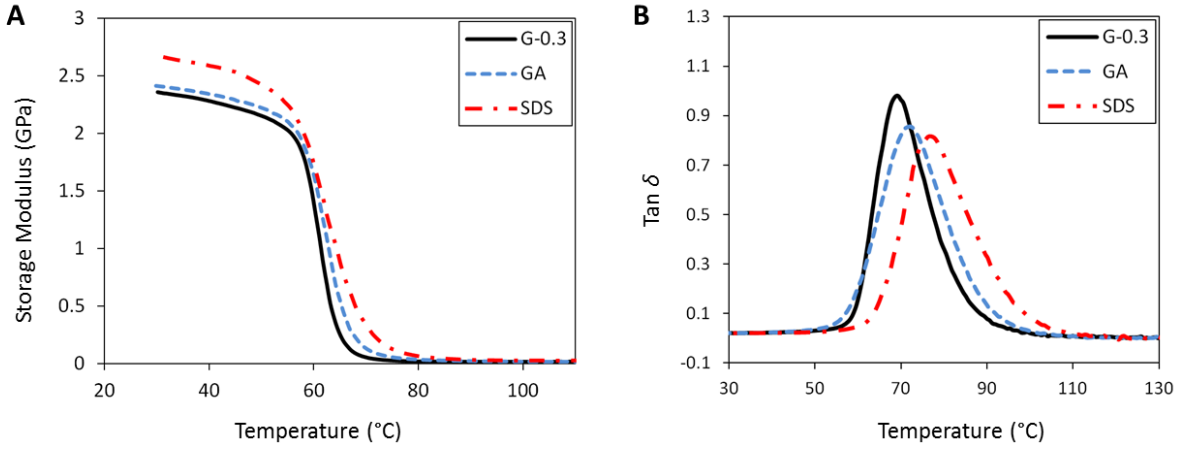

Figure 8. 6. DMA results of nanocomposites, (A). storage modulus and (B). tan δ.

Figure 8.6(A) shows the storage modulus (E') as a function of temperature for epoxy/graphene nanocomposites. As shown in the picture, the storage modulus of samples prepared with surfactants increased significantly over the samples prepared with simple graphene throughout the temperature range investigated. Specifically, SDS prepared samples showed 2.71GPa in the storage modulus, which was higher than the 2.44GPa of GA samples and 2.35GPa of G-0.3 samples.

Glass transition temperature (T_g) characterizes the segmental motion of polymers and was taken as the temperature value at the peak of tan δ curves as shown in Figure 8.6(B). The figure shows that tan δ peak was observed at 69.28 ℃ for nanocomposites prepared with simple graphene. For nanocomposites prepared with SDS and GA, T_g shifted to higher temperatures. This can be ascribed to the fact that the uniformly dispersed graphene restricted chain mobility of the epoxy matrix, thus leading to increased T_g. Among all of the samples, SDS prepared samples showed the highest T_g of 76.96 ℃, which was more than 7 ℃ higher than that of G-0.3 samples, while only slight increase (~3 ℃) in T_g was obtained for GA samples. As described above, the uniformly dispersed graphene can increase the cross-linking density of epoxy networks, and improvesthe thermal stability.

8.3.7 TGA Test

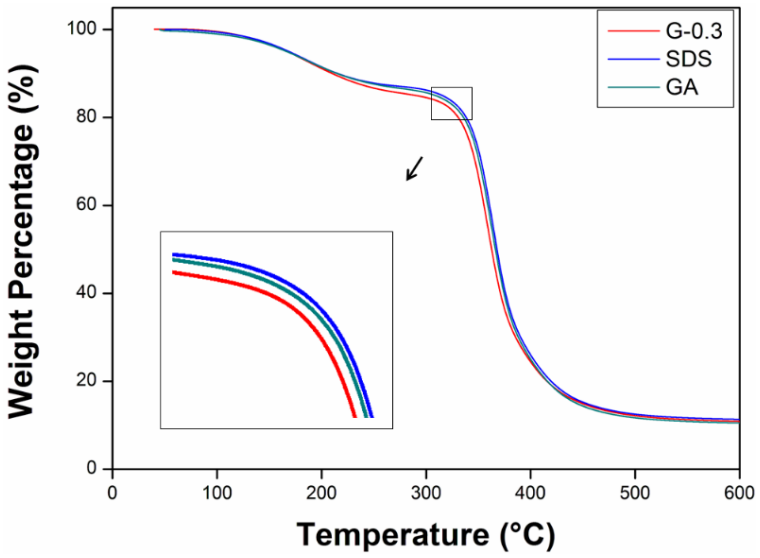

Figure 8. 7. TGA curves of epoxy/graphene nanocomposites.

Thermal decomposition is a fundamental thermal property and is critical for practical applications. Figure 8.7 shows the TGA curves of the nanocomposites in a nitrogen atmosphere. All samples had a similar two-stage weight loss, indicating that all samples had a similar thermal degradation mechanism. The first weight loss from 100 ℃ to 230 ℃ was attributed to the decomposition of small molecules on the side chain. The second weigh loss occurred from 250 ℃ to 500 ℃ showing the decomposition of the main polymer chain. As shown in the figure, G-0.3 showed the highest decomposition rate, indicating the lowest thermal stability. After introducing surfactants, the nanocomposites decomposed at a lower rate. SDS samples showed lower decomposition rates as compare to that of GA samples, indicating better thermal stability of the SDS samples.

This phenomenon can be ascribed to the fact that graphene increased the cross-linking density of the nanocomposites. Generally, the cross-linking density refers to the concentration of cross-linked bonds per volume. As for typical polymer nanocomposites, the higher the cross-linking density is, the stronger the polymer chains bond to each other,

therefore improving the nanocomposites' capacity to withstand heat. Compared to that of GA samples and G-0.3 samples, the uniformly dispersed graphene in SDS samples tends to shorten the distance among the cross-linking points, and thus increases the cross-linking density of the resulting network. On the other hand, the uniformly dispersed graphene can form a continuous network in the matrix, which reduces the volatilization rate of the decomposition products.

In general, the use of SDS resulted in a higher heat capacity of nanocomposites and a better barrier effect of the graphene network. The improvements in thermal stability were the result of enhanced dispersion of graphene.

8.3.8 SEM Test

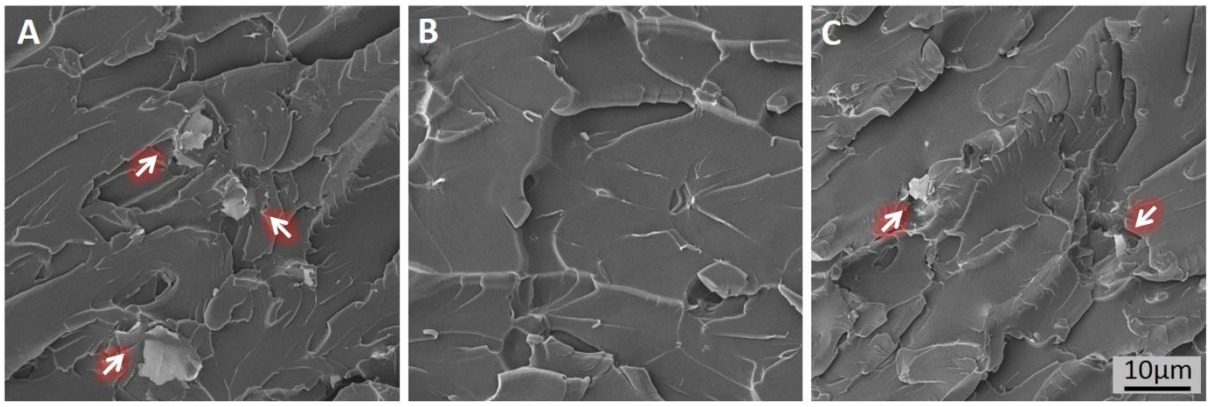

Figure 8. 8. SEM images of fracture surfaces of (A) G-0.3 samples; (B) SDS samples, and (C) GA samples.

The fracture surfaces were studied using SEM and are shown in Figure 8.8. For G-0.3 samples, as shown in Figure 8.8(A), poorly dispersed graphene can be seen on the fracture surface, this featured a poor interfacial interaction between the epoxy matrix and graphene, which showed the brittle nature of material and poor resistance to crack initiation. Compared with G-0.3 samples, the fracture surface of SDS samples showed a clear fracture pattern, as

shown in Figure 8.8(B). This clear fracture pattern featured the fracture mechanism of sheet-sheet delamination for the nanocomposite, and revealed that the usage of SDS produced better dispersion of graphene. The uniformly dispersed graphene bridged growing cracks, thus stabilizing and stopping them from developing into larger and more harmful cracks, thus enhancing the properties of the nanomaterials. However, for GA samples, as shown in Figure 8.8(C), some poorly dispersed graphene can still be seen on the surface. The poorly dispersed graphene formed defects in the nanocomposites, which acted to concentrate the stresses locally, eventually causing a localized weakness, thus decreasing the properties of the nanocomposites.

8.4 Summary

As a material with superior mechanical properties, graphene can significantly improve the properties of epoxy at extremely low loadings, and the key point to the successful preparation of epoxy/graphene nanocomposites is to obtain a good dispersion state of graphene in the matrix. However, due to the strong van der Waals forces between separately dispersed graphene nanosheets, graphene has a strong tendency to reagglomerate in the matrix. Therefore, the usage of chemicals to surface modify graphene becomes a very important way to resist this reagglomeration.

In this work, epoxy/graphene nanocomposites were prepared, SDS and GA were chosen to investigate their dispersion effectiveness of graphene in epoxy matrices. The electrostatic repulsions provided by SDS and the steric repulsion provided by GA were able to de-bundle graphene from their agglomerates and resulted in improved dispersion and homogenous mixing of graphene in epoxy. Mechanical properties, DMA, TGA, and SEM images of nanocomposites were tested to evaluate their dispersing effectiveness.

The results show that samples prepared with simple graphene showed the lowest mechanical properties, storage modulus, and T_g, and non-uniformly dispersed graphene can be observed clearly on the fracture surface of G-0.3 samples. After introducing surfactants, the properties of nanocomposites increased significantly, which meant that both SDS and GA produced fine and homogeneous graphene dispersions. However, it should be noted that some small agglomerates could still be seen on the fracture surface of GA samples, which signifies lower dispersion effectiveness. SDS samples showed higher mechanical properties and T_g, hence it is concluded that SDS is a better dispersing agent than GA for graphene in epoxy matrices.

This research gives guidelines in the usage of SDS and GA in the preparation of epoxy/graphene nanocomposites, and could also be utilised for other polymer composites where the use of surfactants as dispersant is required.

9. Conclusions and Future work

Conclusions

Epoxy/graphene nanocomposites have attracted extensive research interest because of the remarkable enhancements in mechanical, electrical, and thermal performance of the nanocomposites at small graphene loadings. This material combines the advantages of the high mechanical properties of graphene and the easy processability of epoxy. However, due to the large van der Waals force existing on graphene surfaces, graphene tends to reagglomerate in the matrix, these agglomerates act as defects in the matrix and decrease the properties of the material. Therefore, obtaining good distribution of graphene is currently a great challenge in the preparation of epoxy/graphene nanocomposites. This work researched different processing variates and aimed to make homogeneously dispersed epoxy/graphene nanocomposites. In this work, SEM, XRD and optical microscope had been used to characterize the interior structure of the material. Mechanical properties, thermal properties had been tested to characterize the macroscopic properties of the nanocomposites. From this research, the following conclusions can be drawn:

1. UV-Vis spectroscopy was used for the first time to in-situ observe the reagglomeration behaviour of graphene in liquid epoxy systems. Processing varieties like sonication time, storage time, graphene concentration, and sonication temperature on the dispersion of graphene have been analysed.
2. Graphene can be dispersed with greater uniformity with the extension of sonication time. By testing the light transmittance of graphene dispersion in UV-Vis spectroscopy, it can be concluded that the more uniformly graphene dispersed, the lower the light transmittance is, and vice versa.

3. In general, graphene dispersion is stable in the liquid epoxy and hardener. However, graphene tends to reagglomerate more in the hardener, which is due to the low viscosity of hardener.
4. Graphene is easier to disperse at low concentrations, while the reagglomeration behaviour is more pronounced at high concentrations.
5. Higher temperatures accelerate the mobility of molecules in a liquid system, therefore it can be concluded that higher temperatures accelerate the dispersion of graphene.
6. In samples with 0.1-1wt% graphene loading, the tensile modulus, flexural modulus, storage modulus and Vickers hardness of nanocomposites increase with the increasing of graphene contents. However, the tensile strength, flexural strength, fracture toughness and glass transition temperatures shows the maximum value at 0.3wt%. Therefore, in consideration of the overall effects, 0.3wt% graphene loading is recommended for this epoxy system.
7. Bath sonication shows the highest dispersing efficiency, with tip sonication second. However, hand mixing is not suitable to produce uniform graphene dispersion.
8. The relationship among solvent dosage, graphene dispersion state, and the properties of the nanocomposites had been researched for the first time. It is found that large dose of solvent impairs the final properties of the material, which is due to the long processing time required to remove the solvent. Therefore, a lower solvent dosage is recommended to process the nanocomposites, e.g., 100ml.
9. DCB was used for the first time in the preparation of epoxy/graphene nanocomposites and showed higher dispersing efficiencies than DMF and ethanol.
10. The dispersing efficiencies of SDS and GA had been compared for the first time in this work. The results show that both SDS and GA can de-bundle graphene from its agglomerates. SDS showed higher dispersing efficiencies than GA in making homogeneous epoxy/graphene nanocomposites.

By doing this research, epoxy/graphene nanocomposites were prepared with different preparation variables, Table 4 summed up the properties of all the nanocomposites.

Table 4. Properties of nanocomposites.

	Tensile Strength (MPa)	Tensile Modulus (GPa)	Flexural Strength (MPa)	Flexural Modulus (GPa)	K_{1C} (MPa·m$^{1/2}$)	G_{1C} (KJ·m^{-1})	Hardness (GPa)	T_g (℃)	Storage Modulus (GPa)
Epoxy	57.23	0.87	88.32	1.72	0.688	0.172	0.216	66.08	1.92
Bath Sonic	64.46	1.17	97.17	2.08	0.832	0.208	0.235	69.28	2.35
Hand Mix	57.42	0.92	89.76	1.84	0.714	0.179	0.224	66.41	2.04
Tip Sonic	59.24	0.96	92.48	1.92	0.776	0.194	0.227	67.05	2.17
G-0.1	60.47	1.03	93.46	1.90	0.762	0.191	0.225	68.11	2.13
G-0.3	64.46	1.17	97.17	2.08	0.832	0.208	0.235	69.28	2.35
G-0.5	63.84	1.22	95.63	2.27	0.806	0.201	0.246	70.76	2.45
G-1	58.51	1.36	90.24	2.42	0.734	0.184	0.255	72.43	2.51
DMF-100	66.34	1.18	102.08	2.13	0.852	0.213	0.239	73.78	2.45
DMF-300	66.66	1.21	101.73	2.15	0.856	0.214	0.241	74.22	2.52
DMF-500	66.16	1.23	101.44	2.16	0.872	0.218	0.244	75.57	2.60
DMF-1500	65.84	1.22	101.26	2.14	0.864	0.216	0.241	65.78	2.31
DCB	69.32	1.23	104.77	2.2	0.869	0.217	0.247	76.57	2.61
DMF	66.34	1.18	102.08	2.13	0.852	0.213	0.239	73.78	2.45
Ethanol	66.25	1.18	99.67	2.11	0.84	0.21	0.238	73.36	2.38
SDS	70.40	1.29	110.89	2.24	0.88	0.22	0.247	76.96	2.71
GA	67.20	1.21	102.53	2.14	0.862	0.215	0.244	72.19	2.44

Table 4 provides a direct view for the properties of the nanocomposites, in this table, *Epoxy, Bath sonic, Hand mix, Tip sonic* corresponds to the samples in Chapter 5. *G-0.1, G-0.3, G-0.5, G-1* corresponds to the samples in Chapter 6. *DMF-100, DMF-300, DMF-500,*

DMF-1500 corresponds to the samples in Chapter 7 Part I. *DCB, DMF, Ethanol* corresponds to the samples in Chapter 7 part II. *SDS, GA* corresponds to the samples in Chapter 8.

In all, appropriate amount of graphene can reinforce epoxy evidently, the usage of solvents and surfactants can disperse graphene effectively.

Future work

In this work, the reagglomeration behaviour of graphene in epoxy system has been studied, various methods have been applied to disperse graphene in epoxy system, nanocomposites have been made, the processing variates have been examined and the processing techniques have been optimised. However, for further exploration of property enhancements of graphene in epoxy system, some work still need to be done:

1. As demonstrated in Chapter 7, larger dosages of solvents induce reagglomeration of graphene, and smaller dosages of solvent show better results in the preparationof epoxy/graphene nanocomposites. However, although larger dosages of solvent induces reagglomeration in the process, this work only demonstratesthe general trend. More work still needs to be carried out to fully understand the best usage of solvents.
2. Covalent functionalisation of graphene has attracted lots of research interest in recent years. Covalent functionalisation can not only improve the dispersion of graphene, but also enhance the interfacial interactions between graphene and the matrix. Therefore, covalent functionalisation of graphene can be carried out to modify graphene and make nanocomposites.
3. Different fillers have different structures and different properties, and their effects on epoxy are different. Some fillers show very good reinforcement effects with epoxy, such as CNTs, carbon fibers, nanoclays, etc. The synergic effects of graphene and other fillers can be investigated.

4. Other work related to epoxy/graphene nanocomposites, such as the effects of graphene morphology on the properties of nanocomposites, degradation of materials under corrosive environments, etc.

References

1. Yazyev, O.V., et al., *Polycrystalline graphene and other two-dimensional materials.* Nature Nanotechnology, 2014. **9**(10): p. 755-767.
2. Huang, X., et al., *Graphene-based composites.* Chem Soc Rev, 2012. **41**(2): p. 666-86.
3. Inam, F., et al., *Transmission light microscopy of carbon nanotubes-epoxy nanocomposites involving different dispersion methods.* Advanced Composites Letters, 2006. **15**(1): p. 7-13.
4. Young, R.J., et al., *The mechanics of graphene nanocomposites: A review.* Composites Science and Technology, 2012. **72**(12): p. 1459-1476.
5. Deng, S., et al., *Thermoplastic–epoxy interactions and their potential applications in joining composite structures – A review.* Composites Part A: Applied Science and Manufacturing, 2015. **68**: p. 121-132.
6. Mittal, G., et al., *A review on carbon nanotubes and graphene as fillers in reinforced polymer nanocomposites.* Journal of Industrial and Engineering Chemistry, 2015. **21** (1): p. 11-25
7. Ye, S., et al., *Highly elastic graphene oxide–epoxy composite aerogels via simple freeze-drying and subsequent routine curing.* Journal of Materials Chemistry A, 2013. **1**(10): p. 3495.
8. Heo, Y., et al., *The influence of Al(OH)3-coated graphene oxide on improved thermal conductivity and maintained electrical resistivity of Al2O3/epoxy composites.* Journal of Nanoparticle Research, 2012. **14**(10).
9. Wang, X., et al., *The effect of metal oxide decorated graphene hybrids on the improved thermal stability and the reduced smoke toxicity in epoxy resins.* Chemical Engineering Journal, 2014. **250**: p. 214-221.
10. Wang, X., et al., *Self-assembly of Ni–Fe layered double hydroxide/graphene hybrids for reducing fire hazard in epoxy composites.* Journal of Materials Chemistry A, 2013. **1**(13): p. 4383.
11. Yang, Y., et al., *Hydrogen passivation induced dispersion of multi-walled carbon nanotubes.* Advanced Materials, 2012. **24**(7): p. 881-885.
12. Kango, S., et al., *Surface modification of inorganic nanoparticles for development of organic–inorganic nanocomposites-A review.* Progress in Polymer Science, 2013. **38**(8): p. 1232-1261.
13. Guadagno, L., et al., *Development of epoxy mixtures for application in aeronautics and aerospace.* RSC Advances, 2014. **4**(30): p. 15474.
14. Mohan, P., *A Critical Review: The Modification, Properties, and Applications of Epoxy Resins.* Polymer-Plastics Technology and Engineering, 2013. **52**(2): p. 107-125.
15. Inam, F., *Epoxy - the hub for the most versatile polymer with exceptional combination of superlative features.* epoxy, 2014. **1**: p. 1-2.
16. Li, P., et al., *A solvent-free graphene oxide nanoribbon colloid as filler phase for epoxy-matrix composites with enhanced mechanical, thermal and tribological performance.* Carbon, 2016. **96**: p. 40-48.
17. Mikhalchan, A., et al., *Aligned carbon nanotube–epoxy composites: the effect of nanotube organization on strength, stiffness, and toughness.* Journal of Materials Science, 2016. **51**(22): p. 10005-10025.
18. Gouda, P.S.S., et al., *Drawdown prepreg coating method using epoxy terminated butadiene nitrile rubber to improve fracture toughness of glass epoxy composites.* Journal of Composite Materials, 2015. **50**(7): p. 873-884.
19. Naresh, K., et al., *Effect of high strain rate on glass/carbon/hybrid fiber reinforced epoxy laminated composites.* Composites Part B: Engineering, 2016. **100**: p. 125-135.
20. Ratna, D., *Modification of epoxy resins for improvement of adhesion: a critical review.* Journal of Adhesion Science and Technology, 2003. **17**(12): p. 1655-1668.
21. Hodgkin, J.H., et al., *Thermoplastic toughening of epoxy resins- a critical review.* Polymers for Advanced Technologies, 1998. **9**: p. 3-10.

22. Jiang, L., et al., *Aliphatic Diamide as Novel Asphalt-Modified Epoxy Curing Agent for Enhanced Performance.* Advances in Polymer Technology, 2016.
23. Wan, J., et al., *Branched 1,6-Diaminohexane-Derived Aliphatic Polyamine as Curing Agent for Epoxy: Isothermal Cure, Network Structure, and Mechanical Properties.* Industrial & Engineering Chemistry Research, 2017. **56**(17): p. 4938-4948.
24. Tzounis, L., et al., *CNT-grafted glass fibers as a smart tool for epoxy cure monitoring, UV-sensing and thermal energy harvesting in model composites.* RSC Adv., 2016. **6**(60): p. 55514-55525.
25. Garden, L., et al., *Critique of dielectric cure monitoring in epoxy resins – Does the method work for commercial formulations?* International Journal of Adhesion and Adhesives, 2017. **74**: p. 6-14.
26. Raponi, O.D.A., et al., *Development of a Simple Dielectric Analysis Module for Online Cure Monitoring of a Commercial Epoxy Resin Formulation.* Materials Research, 2017(0).
27. Ma, C., et al., *Economical and environment-friendly synthesis of a novel hyperbranched poly(aminomethylphosphine oxide-amine) as co-curing agent for simultaneous improvement of fire safety, glass transition temperature and toughness of epoxy resins.* Chemical Engineering Journal, 2017. **322**: p. 618-631.
28. Rezazadeh, V., et al., *Effect of amine-functionalized dispersant on cure and electrical properties of carbon nanotube/epoxy nanocomposites.* Progress in Organic Coatings, 2017. **111**: p. 389-394.
29. Sharp, N., et al., *Effects of water on epoxy cure kinetics and glass transition temperature utilizing molecular dynamics simulations.* Journal of Polymer Science Part B: Polymer Physics, 2017. **55**(15): p. 1150-1159.
30. Li, C., et al., *Facile synthesis of imidazole microcapsules via thiol-click chemistry and their application as thermally latent curing agent for epoxy resins.* Composites Science and Technology, 2017. **142**: p. 198-206.
31. Li, C., et al., *Green Synthesis of a Bio-Based Epoxy Curing Agent from Isosorbide in Aqueous Condition and Shape Memory Properties Investigation of the Cured Resin.* Macromolecular Chemistry and Physics, 2016. **217**(13): p. 1439-1447.
32. Neisiany, R.E., et al., *Encapsulation of epoxy and amine curing agent in PAN nanofibers by coaxial electrospinning for self-healing purposes.* RSC Adv., 2016. **6**(74): p. 70056-70063.
33. Ganapathi, A.S., et al., *Influence of cure kinetic, rheological and thermo-mechanical behavior on micro-level curing strain of an epoxy prepreg.* Journal of Thermal Analysis and Calorimetry, 2015. **124**(1): p. 305-316.
34. Al-Sabagh, A.M., et al., *Investigations using potentiodynamic polarization measurements, cure durability, ultra violet immovability and abrasion resistance of polyamine cured ilmenite epoxy coating for oil and gas storage steel tanks in petroleum sector.* Egyptian Journal of Petroleum, 2017.
35. Ghodhbani, N., et al., *Ultrasound monitoring of the cure kinetics of an epoxy resin: Identification, frequency and temperature dependence.* Polymer Testing, 2016. **56**: p. 156-166.
36. Fiore, V., et al., *Effect of plasma treatment on mechanical and thermal properties of marble powder/epoxy composites.* Polymer Composites, 2016: p. 127-134.
37. Goh, C.K., et al., *Effects of different surface modification and contents on municipal solid waste incineration fly ash/epoxy composites.* Waste Management, 2016. **58**: p. 309-315.
38. Reshmi B. et al., *Effect of Temperature Variation on Surface Treatment of Short Jute Fiber-Reinforced Epoxy Composites.* Materials Today Proceedings, 2018. **5**(1): p. 1271-1277.
39. Phan, C.H., et al., *Electromagnetic interference shielding performance of epoxy composites filled with multiwalled carbon nanotubes/manganese zinc ferrite hybrid fillers.* Journal of Magnetism and Magnetic Materials, 2016. **401**: p. 472-478.

40. Guan, F. L., et al., *Enhanced thermal conductivity and satisfactory flame retardancy of epoxy/alumina composites by combination with graphene nanoplatelets and magnesium hydroxide.* Composites Part B: Engineering, 2016. **98**: p. 134-140.
41. Meier, R., et al., *Evaluating vibration assisted vacuum infusion processing of hexagonal boron nitride sheet modified carbon fabric/epoxy composites in terms of interlaminar shear strength and void content.* Composites Science and Technology, 2016. **128**: p. 94-103.
42. Qi, H., et al., *Exploring the influence of counterpart materials on tribological behaviors of epoxy composites.* Tribology International, 2016. **103**: p. 566-573.
43. Bensadoun, F., et al., *Fatigue behaviour assessment of flax–epoxy composites.* Composites Part A: Applied Science and Manufacturing, 2016. **82**: p. 253-266.
44. Pickering, K.L., et al., *High performance aligned short natural fiber – Epoxy composites.* Composites Part B: Engineering, 2016. **85**: p. 123-129.
45. Jin, X., et al., *Improvement of coating durability, interfacial adhesion and compressive strength of UHMWPE fiber/epoxy composites through plasma pre-treatment and polypyrrole coating.* Composites Science and Technology, 2016. **128**: p. 169-175.
46. Uppin, V.S., et al., *Interlaminar Fracture toughness in Glass-Cellulose Reinforced Epoxy hybrid composites.* IOP Conference Series: Materials Science and Engineering, 2016. **149**: p. 012113.
47. Barari, B., et al., *Mechanical, physical and tribological characterization of nano-cellulose fibers reinforced bio-epoxy composites: An attempt to fabricate and scale the 'Green' composite.* Carbohydr Polym, 2016. **147**: p. 282-93.
48. Bindu Sharmila, T.K., et al., *Mechanical, thermal and dielectric properties of hybrid composites of epoxy and reduced graphene oxide/iron oxide.* Materials & Design, 2016. **90**: p. 66-75.
49. Meeuw, H., et al., *Morphological influence of carbon nanofillers on the piezoresistive response of carbon nanoparticle/epoxy composites under mechanical load.* European Polymer Journal, 2016. **85**: p. 198-210.
50. Wan, M., et al., *Temperature dependent ultrasonic and thermo-physical properties of polyaniline nanofibers reinforced epoxy composites.* Composites Part B: Engineering, 2016. **87**: p. 40-46.
51. Şahin, Y., et al., *Tribological behaviour of unidirectional carbon fiber-reinforced epoxy composites.* IOP Conference Series: Materials Science and Engineering, 2017. **174**: p. 012009.
52. Lian, G., et al., *Vertically Aligned and Interconnected Graphene Networks for High Thermal Conductivity of Epoxy Composites with Ultralow Loading.* Chemistry of Materials, 2016. **28**(17): p. 6096-6104.
53. Kim, J., et al., *Strength dependence of epoxy composites on the average filler size of non-oxidized graphene flake.* Carbon, 2017. **113**: p. 379-386.
54. Li, X.H., et al., *Thermally Annealed Anisotropic Graphene Aerogels and Their Electrically Conductive Epoxy Composites with Excellent Electromagnetic Interference Shielding Efficiencies.* ACS Appl Mater Interfaces, 2016. **8**(48): p. 33230-33239.
55. Shukla, M.J., et al., *An assessment of flexural performance of liquid nitrogen conditioned glass/epoxy composites with multiwalled carbon nanotube.* Journal of Composite Materials, 2016. **50**(22): p. 3077-3088.
56. Terenzi, A., et al., *Analysis and simulation of the electrical properties of CNTs/epoxy nanocomposites for high performance composite matrices.* Polymer Composites, 2017. **38**(1): p. 105-115.
57. Lamberti, P., et al., *Analysis of the Effects of Hydrotalcite Inclusion on the Temperature-Sensing Properties of CNT-Epoxy Nanocomposites.* IEEE Sensors Journal, 2016. **16**(22): p. 7977-7985.

58. Anwar, Z., et al., *Advances in Epoxy/Graphene Nanoplatelet Composite with Enhanced Physical Properties: A Review.* Polymer-Plastics Technology and Engineering, 2015. **55**(6): p. 643-662.
59. Micheli, D., et al., *Ballistic and electromagnetic shielding behaviour of multifunctional Kevlar fiber reinforced epoxy composites modified by carbon nanotubes.* Carbon, 2016. **104**: p. 141-156.
60. Liu, X., et al., *Characterization of enhanced interfacial bonding between epoxy and plasma functionalized carbon nanotube films.* Composites Science and Technology, 2017. **145**: p. 114-121.
61. Suri, A., et al., *A simple chemical treatment for easy dispersion of carbon nanotubes in epoxy matrix for improving mechanical properties.* Journal of Materials Science, 2016. **51**(24): p. 10775-10781.
62. Starost, K., et al., *Assessment of nanoparticles release into the environment during drilling of carbon nanotubes/epoxy and carbon nanofibers/epoxy nanocomposites.* J Hazard Mater, 2017. **340**: p. 57-66.
63. Saha, S., et al., *Degradation in Mechanical and Thermal Properties of Partially Aligned CNT/Epoxy Composites due to Seawater Absorption.* IOP Conference Series: Materials Science and Engineering, 2017. **178**: p. 012027.
64. Jojibabu, P., et al., *Effect of different carbon nano-fillers on rheological properties and lap shear strength of epoxy adhesive joints.* Composites Part A: Applied Science and Manufacturing, 2016. **82**: p. 53-64.
65. Soares, B.G., et al., *Dual-role of phosphonium – Based ionic liquid in epoxy/MWCNT systems: Electric, rheological behavior and electromagnetic interference shielding effectiveness.* European Polymer Journal, 2016. **84**: p. 77-88.
66. Shabestari, M.E., et al., *Effect of nitrogen and oxygen doped carbon nanotubes on flammability of epoxy nanocomposites.* Carbon, 2017. **121**: p. 193-200.
67. Wang, B., et al., *Enhanced epoxy adhesion between steel plates by surface treatment and CNT/short-fiber reinforcement.* Composites Science and Technology, 2016. **127**: p. 149-157.
68. Üstün, T., et al., *Enhanced fatigue performances of hybrid nanoreinforced filament wound carbon/epoxy composite pipes.* Composite Structures, 2016. **150**: p. 124-131.
69. Ayatollahi, M.R., et al., *Effects of multi-walled carbon nanotube and nanosilica on tensile properties of woven carbon fabric-reinforced epoxy composites fabricated using VARIM.* Journal of Composite Materials, 2017: p. 002199831769998.
70. Abdelal, N., et al., *Enhancement of pyramid solar still productivity using absorber plates made of carbon fiber/CNT-modified epoxy composites.* Desalination, 2017. **419**: p. 117-124.
71. Saber, A.T., et al., *Epoxy composite dusts with and without carbon nanotubes cause similar pulmonary responses, but differences in liver histology in mice following pulmonary deposition.* Part Fiber Toxicol, 2016. **13**(1): p. 37.
72. Kwon, D.J., et al., *Evaluation of optimal dispersion conditions for CNT reinforced epoxy composites using cyclic voltammetry measurements.* Advanced Composite Materials, 2016. **26**(3): p. 219-227.
73. Prusty, R.K., et al., *Evaluation of the role of functionalized CNT in glass fiber/epoxy composite at above- and sub-zero temperatures: Emphasizing interfacial microstructures.* Composites Part A: Applied Science and Manufacturing, 2017. **101**: p. 215-226.
74. Saboori, B., et al., *Experimental fracture study of MWCNT/epoxy nanocomposites under the combined out-of-plane shear and tensile loading.* Polymer Testing, 2017. **59**: p. 193-202.
75. Rafique, I., et al., *Exploration of Epoxy Resins, Hardening Systems, and Epoxy/Carbon Nanotube Composite Designed for High Performance Materials: A Review.* Polymer-Plastics Technology and Engineering, 2015. **55**(3): p. 312-333.
76. Gómez-del Río, T., et al., *Fracture behaviour of epoxy nanocomposites modified with triblock copolymers and carbon nanotubes.* Composites Part B: Engineering, 2016. **87**: p. 343-349.

77. Cha, J., et al., *Functionalization of carbon nanotubes for fabrication of CNT/epoxy nanocomposites.* Materials & Design, 2016. **95**: p. 1-8.
78. Chen, Y., et al., *High-Performance Epoxy Nanocomposites Reinforced with Three-Dimensional Carbon Nanotube Sponge for Electromagnetic Interference Shielding.* Advanced Functional Materials, 2016. **26**(3): p. 447-455.
79. Cha, J., et al., *Improvement of modulus, strength and fracture toughness of CNT/Epoxy nanocomposites through the functionalization of carbon nanotubes.* Composites Part B: Engineering, 2017. **129**: p. 169-179.
80. Vaganov, G., et al., *Influence of multiwalled carbon nanotubes on the processing behavior of epoxy powder compositions and on the mechanical properties of their fiber reinforced composites.* Polymer Composites, 2016. **37**(8): p. 2377-2383.
81. Fujigaya, T., et al., *Interfacial engineering of epoxy/carbon nanotubes using reactive glue for effective reinforcement of the composite.* Polymer Journal, 2015. **48**(2): p. 183-188.
82. Shin, P.-S., et al., *Interfacial properties and water resistance of epoxy and CNT-epoxy adhesives on GFRP composites.* Composites Science and Technology, 2017. **142**: p. 98-106.
83. Liu, W., et al., *Investigation on the mechanical and electrical properties of carbon nanotube/epoxy composites produced by resin transfer molding.* Journal of Composite Materials, 2016. **51**(14): p. 2035-2043.
84. Shiravand, F., et al., *A novel comparative study of different layered silicate clay types on exfoliation process and final nanostructure of trifunctional epoxy nanocomposites.* Polymer Testing, 2016. **56**: p. 148-155.
85. Tomić, M.D., et al., *Anticorrosive epoxy/clay nanocomposite coatings: rheological and protective properties.* Journal of Coatings Technology and Research, 2016. **13**(3): p. 439-456.
86. Singh, K., et al., *Compatibilization of polypropylene fibers in epoxy based GFRP/clay nanocomposites for improved impact strength.* Composites Part A: Applied Science and Manufacturing, 2017. **98**: p. 207-217.
87. Tcherbi-Narteh, A., et al., *Effects of Different Montmorillonite Nanoclay Loading on Cure Behavior and Properties of Diglycidyl Ether of Bisphenol A Epoxy.* Journal of Nanomaterials, 2016. **2016**: p. 1-12.
88. Gurusideswar, S., et al., *High strain rate sensitivity of epoxy/clay nanocomposites using non-contact strain measurement.* Polymer, 2016. **86**: p. 197-207.
89. Ghadami, F., et al., *Hot-cured epoxy-nanoparticulate-filled nanocomposites: Fracture toughness behavior.* Engineering Fracture Mechanics, 2016. **162**: p. 193-200.
90. Rafiq, A., et al., *Impact resistance of hybrid glass fiber reinforced epoxy/nanoclay composite.* Polymer Testing, 2017. **57**: p. 1-11.
91. Liang, M., et al., *Improving the Long-term Performance of Composite Insulators Use Nanocomposite: A Review.* Energy Procedia, 2017. **110**: p. 168-173.
92. Gajjela, S., et al., *Influence of interphase material and clay particle shape on the effective properties of epoxy-clay nanocomposites.* Composites Part B: Engineering, 2016. **88**: p. 11-18.
93. Madhup, M.K., et al., *Investigation and improvement of abrasion resistance, water vapor barrier and anticorrosion properties of mixed clay epoxy nanocomposite coating.* Progress in Organic Coatings, 2017. **102**: p. 186-193.
94. Maleki Moghadam, R., et al., *On the tensile behavior of clay–epoxy nanocomposite considering interphase debonding damage via mixed-mode cohesive zone material.* Composites Part B: Engineering, 2016. **89**: p. 303-315.
95. Silva, A.A., et al., *Organoclay-epoxy nanocomposites modified with polyacrylates: The effect of the clay mineral dispersion method.* Applied Clay Science, 2016. **124-125**: p. 46-53.
96. Kiani, M.A., et al., *Preparation and characteristics of epoxy/clay/B4C nanocomposite at high concentration of boron carbide for neutron shielding application.* Radiation Physics and Chemistry, 2017. **141**: p. 223-228.

97. Gul, S., et al., *Technical Relevance of Epoxy/Clay Nanocomposite with Organically Modified Montmorillonite: A Review.* Polymer-Plastics Technology and Engineering, 2016. **55**(13): p. 1393-1415.

98. Sharifi, M., et al., *Preparation and characterization of a high performance powder coating based on epoxy/clay nanocomposite.* Progress in Organic Coatings, 2017. **106**: p. 69-76.

99. Quan, D., et al., *Carbon nanotubes and core–shell rubber nanoparticles modified structural epoxy adhesives.* Journal of Materials Science, 2016. **52**(8): p. 4493-4508.

100. Irez, A.B., et al., *Design and Mechanical-Physical Properties of Epoxy-Rubber Based Composites Reinforced with Nanoparticles.* Procedia Engineering, 2017. **184**: p. 486-496.

101. Vertuccio, L., et al., *Effect of carbon nanotube and functionalized liquid rubber on mechanical and electrical properties of epoxy adhesives for aircraft structures.* Composites Part B: Engineering, 2017. **129**: p. 1-10.

102. Vijayan P, P., et al., *Elastomer/thermoplastic modified epoxy nanocomposites: The hybrid effect of 'micro' and 'nano' scale.* Materials Science and Engineering: R: Reports, 2017. **116**: p. 1-29.

103. Sharova, I.A., et al., *Effect of modification with rubber on properties and process of curing of epoxy–rubber adhesive compositions.* Polymer Science Series D, 2016. **9**(4): p. 437-440.

104. Konnola, R., et al., *Mechanical, thermal, and viscoelastic response of novel in situ CTBN/POSS/epoxy hybrid composite system.* Polymer Composites, 2016. **37**(7): p. 2109-2120.

105. Bain, E.D., et al., *Failure processes governing high-rate impact resistance of epoxy resins filled with core–shell rubber nanoparticles.* Journal of Materials Science, 2015. **51**(5): p. 2347-2370.

106. Qiao, H., et al., *Enhanced interfacial interaction and excellent performance of silica/epoxy group-functionalized styrene-butadiene rubber (SBR) nanocomposites without any coupling agent.* Composites Part B: Engineering, 2017. **114**: p. 356-364.

107. Wang, F., et al., *Enhancement of fracture toughness, mechanical and thermal properties of rubber/epoxy composites by incorporation of graphene nanoplatelets.* Composites Part A: Applied Science and Manufacturing, 2016. **87**: p. 10-22.

108. Quan, D., et al., Ivankovic, *Fracture behaviour of epoxy adhesive joints modified with core-shell rubber nanoparticles.* Engineering Fracture Mechanics, 2017.

109. Mansour, G., et al., *Investigation of the dynamic mechanical properties of epoxy resins modified with elastomers.* Composites Part B: Engineering, 2016. **94**: p. 152-159.

110. Quan, D., et al.,, *Fracture behaviour of a rubber nano-modified structural epoxy adhesive: Bond gap effects and fracture damage zone.* International Journal of Adhesion and Adhesives, 2017. **77**: p. 138-150.

111. Xu, F., et al., *Temperature effect on nano-rubber toughening in epoxy and epoxy/carbon fiber laminated composites.* Composites Part B: Engineering, 2016. **95**: p. 423-432.

112. Halawani, N., et al., *Electrical, thermal and mechanical properties of poly-etherimide epoxy-diamine blend.* Composites Part B: Engineering, 2017. **110**: p. 530-541.

113. Katti, P., et al., *Improved mechanical properties through engineering the interface by poly (ether ether ketone) grafted graphene oxide in epoxy based nanocomposites.* Polymer, 2017. **122**: p. 184-193.

114. Gu, H., et al., *A low loading of grafted thermoplastic polystyrene strengthens and toughens transparent epoxy composites.* J. Mater. Chem. C, 2017. **5**(17): p. 4275-4285.

115. Vyas, A., et al., *Clay induced thermoplastic crystals in thermoset matrix: Thermal, Dynamic mechanical, and morphological analysis of clay/nylon-6-epoxy nanocomposites.* Polymer Composites, 2016. **37**(7): p. 2206-2217.

116. Wei, X., et al., *Conductive herringbone structure carbon nanotube/thermoplastic polyurethane porous foam tuned by epoxy for high performance flexible piezoresistive sensor.* Composites Science and Technology, 2017. **149**: p. 166-177.
117. Cicala, G., et al., *Effects of mixing di- and tri-functional epoxy monomers on epoxy/thermoplastic blends.* Advances in Polymer Technology, 2017.
118. Phua, J.L., et al., *Influence of thermoplastic spacer on the mechanical, electrical, and thermal properties of carbon black filled epoxy adhesives.* Polymers for Advanced Technologies, 2017. **28**(3): p. 345-352.
119. Frey, M., et al., *Assessing glass-fiber modification developments by comparison of glass-fiber epoxy composites with reference materials: Some thoughts on relevance.* Proceedings of the Institution of Mechanical Engineers, Part L: Journal of Materials: Design and Applications, 2016. **231**(1-2): p. 49-54.
120. De Parscau du Plessix, B., et al., *Characterization and modeling of the polymerization-dependent moisture absorption behavior of an epoxy-carbon fiber-reinforced composite material.* Journal of Composite Materials, 2015. **50**(18): p. 2495-2505.
121. Khashaba, U.A., et al., *Drilling analysis of thin woven glass-fiber reinforced epoxy composites.* Journal of Materials Processing Technology, 2017. **249**: p. 415-425.
122. Kim, K.W., et al., *Cure behaviors and mechanical properties of carbon fiber-reinforced nylon6/epoxy blended matrix composites.* Composites Part B: Engineering, 2017. **112**: p. 15-21.
123. Vacche, S.D., et al., *Curing kinetics and thermomechanical properties of latent epoxy/carbon fiber composites.* IOP Conference Series: Materials Science and Engineering, 2016. **139**: p. 012049.
124. Carrillo-Escalante, H.J., et al., *Effect of fiber-matrix adhesion on the fracture behavior of a carbon fiber reinforced thermoplastic-modified epoxy matrix.* Carbon letters, 2016. **19**: p. 47-56.
125. Grugel, R.N., et al., *Evaluation of carbon fiber composites fabricated using ionic liquid based epoxies for cryogenic fluid applications.* Results in Physics, 2016. **6**: p. 1188-1189.
126. Yuan, X., et al., *Optimization of interfacial properties of carbon fiber/epoxy composites via a modified polyacrylate emulsion sizing.* Applied Surface Science, 2017. **401**: p. 414-423.
127. Sharma, B., et al., *Effect of surface treatment of nanoclay on the mechanical properties of epoxy/glass fiber/clay nanocomposites.* Composite Interfaces, 2016. **23**(7): p. 623-640.
128. Choudhury, P., et al., *Enhanced crack suppression ability of hybrid glass fiber reinforced laminated composites fabricated using GNP/epoxy system by optimized UDM parameters.* Ultrason Sonochem, 2017. **39**: p. 174-187.
129. Patel, J.S., et al., *Effect of fabric structure and polymer matrix on flexural strength, interlaminar shear stress, and energy dissipation of glass fiber-reinforced polymer composites.* Textile Research Journal, 2015. **86**(2): p. 127-137.
130. Mahmood, H., et al., *Enhancement of interfacial adhesion in glass fiber/epoxy composites by electrophoretic deposition of graphene oxide on glass fibers.* Composites Science and Technology, 2016. **126**: p. 149-157.
131. Vu, C.M., et al., *Environmentally benign green composites based on epoxy resin/bacterial cellulose reinforced glass fiber: Fabrication and mechanical characteristics.* Polymer Testing, 2017. **61**: p. 150-161.
132. San Juan, V., et al., *Evaluation of the fill yarns effect on the out-of-plane compressive fatigue behavior for an unidirectional glass fiber reinforced epoxy composite.* Composite Structures, 2016. **138**: p. 237-242.
133. He, D., et al., *Impact of the spatial distribution of high content of carbon nanotubes on the electrical conductivity of glass fiber fabrics/epoxy composites fabricated by RTM technique.* Composites Science and Technology, 2017. **147**: p. 107-115.
134. Ma, H.l., et al., *Impact properties of glass fiber/epoxy composites at cryogenic environment.* Composites Part B: Engineering, 2016. **92**: p. 210-217.

135. Zhang, D., et al., *Improved sand erosion resistance and mechanical properties of multifunctional carbon nanofiber nanopaper-enhanced fiber reinforced epoxy composites.* Advances in Polymer Technology, 2017.

136. Zheng, N., et al., *Improvement of atomic oxygen erosion resistance of carbon fiber and carbon fiber/epoxy composite interface with a silane coupling agent.* Materials & Design, 2016. **109**: p. 171-178.

137. Sui, X., et al., *Interfacial and fatigue-resistant synergetic enhancement of carbon fiber/epoxy hierarchical composites via an electrophoresis deposited carbon nanotube-toughened transition layer.* Composites Part A: Applied Science and Manufacturing, 2017. **92**: p. 134-144.

138. Zhao, X., et al., *Influence of phenylphosphonate based flame retardant on epoxy/glass fiber reinforced composites (GRE): Flammability, mechanical and thermal stability properties.* Composites Part B: Engineering, 2017. **110**: p. 511-519.

139. Pathak, A.K., et al., *Improved mechanical properties of carbon fiber/graphene oxide-epoxy hybrid composites.* Composites Science and Technology, 2016. **135**: p. 28-38.

140. Kang, K., et al., *Development of ultralight and thin bipolar plates using epoxy-carbon fiber prepregs and graphite composites.* International Journal of Hydrogen Energy, 2017. **42**(3): p. 1691-1697.

141. Lei, C., et al,. *A design of gradient interphase reinforced by silanized graphene oxide and its effect on carbon fiber/epoxy interface*. Materials Chemistry and Physics, 2014. **145**(58): p. 186-196.

142. Kong, Q.Q., et al., *Hierarchical Graphene–Carbon Fiber Composite Paper as a Flexible Lateral Heat Spreader.* Advanced Functioanl Materials. 2014, **74**(24): p. 4222–4228.

143 Zhuo, D.X., et al., *Flame Retardancy Effects of Graphene Nanoplatelet/Carbon Nanotube Hybrid Membranes on Carbon Fiber Reinforced Epoxy Composites*. Journal of Nanomaterials. 2013. **(2013)**: p. 820901.

144. Llobet, J., et al., *A fatigue damage and residual strength model for unidirectional carbon/epoxy composites under on-axis tension-tension loadings.* International Journal of Fatigue, 2017. **103**: p. 508-515.

145. Hu, Y., et al., *A novel approach for Al2O3/epoxy composites with high strength and thermal conductivity.* Composites Science and Technology, 2016. **124**: p. 36-43.

146. Kumar, R., *A Review on Epoxy and Polyester Based Polymer Concrete and Exploration of Polyfurfuryl Alcohol as Polymer Concrete.* Journal of Polymers, 2016. **2016**: p. 1-13.

147. Saba, N., et al., *A review on flammability of epoxy polymer, cellulosic and non-cellulosic fiber reinforced epoxy composites.* Polymers for Advanced Technologies, 2016. **27**(5): p. 577-590.

148. Jin, F.L., et al., *Synthesis and application of epoxy resins: A review.* Journal of Industrial and Engineering Chemistry, 2015. **29**: p. 1-11.

149. Pontes, J.F.R., et al., *Effect of Corrosion Inhibitor Used in Surface Treatment on the Anticorrosive Performance of an Epoxy Paint System.* Materials Sciences and Applications, 2016. **07**(10): p. 593-609.

150. Rajan, R., et al., *Studies on the anticorrosive & antifouling properties of the Gracilaria edulis extract incorporated epoxy paint in the Gulf of Mannar Coast, Mandapam, India.* Progress in Organic Coatings, 2016. **90**: p. 448-454.

151. Savvilotidou, M., et al., *Effects of aging in dry environment on physical and mechanical properties of a cold-curing structural epoxy adhesive for bridge construction.* Construction and Building Materials, 2017. **140**: p. 552-561.

152. Jia, Z., et al., *Mechanical properties of an epoxy-based adhesive under high strain rate loadings at low temperature environment.* Composites Part B: Engineering, 2016. **105**: p. 132-137.

153. Altaf, K., et al., *Determining the effects of thermal conductivity on epoxy molds using profiled cooling channels with metal inserts.* Journal of Mechanical Science and Technology, 2016. **30**(11): p. 4901-4907.

154. Fernandes, A.d.C., et al., *Mechanical and dimensional characterization of polypropylene injection moulded parts in epoxy resin aluminium inserts for rapid tooling.* International Journal of Materials and Product Technology, 2016. **52**: p. 37-52.
155. McKinnon, M.B., et al., *Pyrolysis model for a carbon fiber/epoxy structural aerospace composite.* Journal of Fire Sciences, 2016. **35**(1): p. 36-61.
156. Lee, S., et al., *Polyimide–Epoxy Composites with Superior Bendable Properties for Application in Flexible Electronics.* Journal of Electronic Materials, 2017. **46**(8): p. 4740-4749.
157. Reit, R., et al., *Thiol–epoxy/maleimide ternary networks as softening substrates for flexible electronics.* Journal of Materials Chemistry B, 2016. **4**(32): p. 5367-5374.
158. Zhou, Q., et al., *Piezoelectric single crystals for ultrasonic transducers in biomedical applications.* Progress in Materials Science, 2014. **66**: p. 87-111.
159. Monmaturapoj, N., et al., *Properties of poly(lactic acid)/hydroxyapatite composite through the use of epoxy functional compatibilizers for biomedical application.* J Biomater Appl, 2017. **32**(2): p. 175-190.
160. Yan, L., et al., *Crashworthiness characteristics of flax fiber reinforced epoxy tubes for energy absorption application.* Materials & Design, 2013. **51**: p. 629-640.
161. Hoge, J., et al., *Epoxy resin infused boat hulls.* Reinforced Plastics, 2016. **60**(4): p. 221-223.
162. Zhang, G., et al., *Epoxy metabolites of docosahexaenoic acid (DHA) inhibit angiogenesis, tumor growth, and metastasis.* Proceedings of the National Academy of Sciences of the United States of America, 2013. **110**: p. 6530-6535.
163. Rodriguez-Mella, Y., et al., *Durability of an industrial epoxy vinyl ester resin used for the fabrication of a contemporary art sculpture.* Polymer Degradation and Stability, 2014. **107**: p. 277-284.
164. Yongqiang, T., et al., *Water shut off in a horizontal well: Lab experiments with starch graft copolymer agent.* Journal of Petroleum Science and Engineering, 2013. **108**: p. 230-238.
165. Zhao, F., et al., *The dispersion of graphene in conductive epoxy composites investigated by Raman spectroscopy.* Journal of Raman Spectroscopy, 2017. **48**(3): p. 432-436.
166. Sanes, J., et al., *Synergy between single-walled carbon nanotubes and ionic liquid in epoxy resin nanocomposites.* Composites Part B: Engineering, 2016. **105**: p. 149-159.
167. Shen, X., et al., *Multilayer Graphene Enables Higher Efficiency in Improving Thermal Conductivities of Graphene/Epoxy Composites.* Nano Lett, 2016. **16**(6): p. 3585-93.
168. Kausar, A., et al., *Recent Developments in Epoxy/Graphite, Epoxy/Graphene, and Epoxy/Graphene Nanoplatelet Composites: A Comparative Review.* Polymer-Plastics Technology and Engineering, 2016. **55**(11): p. 1192-1210.
169. Nam, T.H., et al., *Improving mechanical properties of high volume fraction aligned multi-walled carbon nanotube/epoxy composites by stretching and pressing.* Composites Part B: Engineering, 2016. **85**: p. 15-23.
170. Shrivastava, R., et al., *Mechanical Properties of Coir/ G Lass Fiber Epoxy Resin Hybrid Composite.* Materials Today: Proceedings, 2017. **4**(2): p. 3477-3483.
171. Gálvez, V.S., et al., *High-speed Impact Performance of Carbon/Epoxy Composites at Very Low Temperatures.* Procedia Engineering, 2016. **167**: p. 116-119.
172. Novoselov, K.S., et al., *Electric Field Effect in Atomically Thin Carbon Films.* Science, 2004. **306**: p. 666-669.
173. Sham, A.Y.W., et al., *A review of fundamental properties and applications of polymer–graphene hybrid materials.* Soft Matter, 2013. **9**(29): p. 6645.
174. https://graphene-flagship.eu/

175. Zhu, Y., et al., *Graphene and graphene oxide: synthesis, properties, and applications.* Adv Mater, 2010. **22**(35): p. 3906-3924.
176. Park, S., et al., *Chemical methods for the production of graphenes.* Nature Nanotechnology, 2009. **4**: p. 217-224.
177. Whitby, R.L.D., *Chemical Control of Graphene Architecture: Tailoring Shape and Properties.* ACS nano, 2014. **8**(10): p. 9733-9754
178. Chen, J.H., et al., *Intrinsic and extrinsic performance limits of graphene devices on SiO2.* Nature Nanotechnology, 2008. **3**: p. 206-209.
179. Mayorov, A.S., et al., *Micrometer-scale ballistic transport in encapsulated graphene at room temperature.* NANo letters, 2011. **11**: p. 2396-2399.
180. Kamyshny, A., et al., *Conductive Nanomaterials for Printed Electronics.* Small, 2014. **10**: p. 3515-3535.
181. Yang, X., et al., *Liquid-Mediated Dense Integration of Graphene Materials for Compact Capacitive Energy Storage.* Science, 2013. **341**: p. 534-537.
182. Kim, K., et al., *Ultrathin organic solar cells with graphene doped by ferroelectric polarization.* ACS Applied Materials Interfaces, 2014. **6**: p. 3299-3304.
183. Prasai, D., et al., *Graphene: Corrosion-Inhibiting Coating.* ACS nano, 2012. **6**: p. 1102–1108.
184. Sambasivudu, K., et al., *Challenges and opportunities for the mass production of high quality graphene: an analysis of worldwide patents.* Nanotech Insights, 2012. **3**: p. 6-19.
185. H., F., *Single crystals of graphite and mica as specimen support for electron microscopy.* Journal of Applied Physics, 1960. **31**: p. 1844.
186. Soldano, C., et al., *Production, properties and potential of graphene.* Carbon, 2010. **48**(8): p. 2127-2150.
187. Ren, W., et al., *The global growth of graphene.* Nat Nanotechnol, 2014. **9**(10): p. 726-30.
188. Paton, K.R., et al., *Scalable production of large quantities of defect-free few-layer graphene by shear exfoliation in liquids.* nature materials, 2014. **13**: p. 624-630.
189. Jeona, I.Y., et al., *Edge-carboxylated graphene nanosheets via ball milling.* Proceedings of the National Academy of Sciences of the United States of America, 2012. **109**: p. 5588–5593.
190. Pei, S.F., *Method for preparing high-quality graphene.* Chinese patent ZL.201110282370.5 2011.
191. Noorden, R.V., *Beyond sticky tape.* Nature, 2012. **483**: p. S32-S33.
192. Na, S.R., et al., *Selective Mechanical Transfer of Graphene from Seed Copper Foil Using Rate Effects.* ACS Nano, 2015. **9**(2): p. 1325-1335.
193. Li, X., et al., *Large-area synthesis of high-quality and uniform graphene films on copper foils.* Science, 2009. **324**: p. 1312-1314
194. Kim, K.S., et al., *Large-scale pattern growth of graphene films for stretchable transparent electrodes.* Nature materials, 2009. **457**: p. 706-710.
195. Mittal, G., et al., *A review on carbon nanotubes and graphene as fillers in reinforced polymer nanocomposites.* Journal of Industrial and Engineering Chemistry, 2015. **21**(25): p. 11-25.
196. Pei, S., et al., *The reduction of graphene oxide.* Carbon, 2012. **50**: p. 3210-3228.
197. Yao, J., et al., *Chemistry, physics and biology of graphene-based nanomaterials: new horizons for sensing, imaging and medicine.* Journal of Materials Chemistry, 2012. **22**: p. 14313-14329.
198. Wu, Z., et al., *Synthesis of Graphene Sheets with High Electrical Conductivity and Good Thermal Stability by Hydrogen Arc Discharge Exfoliation.* ACS Nano, 2009. **2**: p. 411–417.
199. Zhang, W., et al., *A Strategy for Producing Pure Single-Layer Graphene Sheets Based on a Confined Self-Assembly Approach.* Angewandte Chemie International Edition, 2009. **121**(32): p. 5978–5982.

200. Shao, Y., et al., *Facile and controllable electrochemical reduction of graphene oxide and its applications.* Journal of Materials Chemistry, 2010. **20**: p. 743-748.
201. Sakamoto, J., et al., *Two-Dimensional Polymers: Just a Dream of Synthetic Chemists.* Angewandte Chemie International Edition, 2009. **48**(6): p. 1030-1069.
202. Soldano, C., et al., *Production, properties and potential of graphene.* Carbon, 2010. **48**: p. 2127-2150.
203. Guo, S., et al., *Graphene nanosheet: synthesis, molecular engineering, thin film, hybrids, and energy and analytical applications.* Chemical Society Reviews, 2011. **40**: p. 2644-2672.
204. Coclite, A.M., et al., *CVD polymers: a new paradigm for surface modification and device fabrication.* Adv Mater, 2013. **25**(38): p. 5392-423.
205. Hummers, W., et al., *Preparation of Graphitic Oxide.* Journal of American Chemical Society, 1958. **80**: p. 1339.
206. Staudenmaier, L., *Verfahren zur Darstellung der Graphitsaure.* Ber. Deut. Chem. Ges, 1898. **31**: p. 1481-1487.
207. Brodie, B.C., *Sur le poids atomique du graphite.* Ann. Chim. Phys, 1860. **59**: p. 466.
208. Hu, X., et al., *Preparation and properties of dopamine reduced graphene oxide and its composites of epoxy.* Journal of Applied Polymer Science, 2014. **131**(2).
209. He, H., et al., *A new structural model for graphite oxide.* Chemical Physics Letters, 1998. **287**: p. 53-56.
210. Paredes, J.I., et al., *Graphene Oxide Dispersions in Organic Solvents.* Langmuir, 2008. **24**: p. 10560–10564.
211. Zurutuza, A., et al., *Challenges and opportunities in graphene commercialization.* Nat Nanotechnol, 2014. **9**(10): p. 730-734.
212. Inam, F., et al., *Effects of dispersion surfactants on the properties of ceramic–carbon nanotube (CNT) nanocomposites.* Ceramics International, 2014. **40**(1): p. 511-516.
213. Wajid, A.S., et al., *Polymer-stabilized graphene dispersions at high concentrations in organic solvents for composite production.* Carbon, 2012. **50**(2): p. 526-534.
214. Liew, K.M., et al., *Mechanical analysis of functionally graded carbon nanotube reinforced composites: A review.* Composite Structures, 2015. **120**: p. 90-97.
215. Kim, J., et al., *The effects of functionalized graphene nanosheets on the thermal and mechanical properties of epoxy composites for anisotropic conductive adhesives (ACAs).* Microelectronics Reliability, 2012. **52**(3): p. 595-602.
216. Lee, J.K., et al., *Functionalized graphene sheets-epoxy based nanocomposite for cryotank composite application.* Polymer Composites, 2012. **33**(8): p. 1263-1273.
217. Qiu, S.L., *Effects of graphene oxides on the cure behaviors of a tetrafunctional epoxy resin.* Express Polymer Letters, 2011. **5**(9): p. 809-818.
218. Kim, J., et al., *Thermal and electrical conductivity of Al(OH)3 covered graphene oxide nanosheet/epoxy composites.* Journal of Materials Science, 2011. **47**(3): p. 1418-1426.
219. Jiang, T., et al., *Enhanced mechanical properties of silanized silica nanoparticle attached graphene oxide/epoxy composites.* Composites Science and Technology, 2013. **79**: p. 115-125.
220. Layek, R.K., et al., *A review on synthesis and properties of polymer functionalized graphene.* Polymer, 2013. **54**(19): p. 5087-5103.
221. Hu, K., et al., *Graphene-polymer nanocomposites for structural and functional applications.* Progress in Polymer Science, 2014. **39**(11): p. 1934-1972.
222. Liao, S.H., et al., *One-Step Reduction and Functionalization of Graphene Oxide with Phosphorus-Based Compound to Produce Flame-Retardant Epoxy Nanocomposite.* Industrial & Engineering Chemistry Research, 2012. **51**(12): p. 4573-4581.

223. Georgakilas, V., *Functionalization of Graphene[M].* Wiley, 2014.
224. Park, M.J., et al., *Covalent Modification of Multiwalled Carbon Nanotubes with Imidazolium-Based Ionic Liquids: Effect of Anions on Solubility.* Chemistry of Materials, 2006. **18**: p. 1546–1551.
225. Kuila, T., et al., *Chemical functionalization of graphene and its applications.* Progress in Materials Science, 2012. **57**(7): p. 1061-1105.
226. Yang, H., et al., *Covalent functionalization of polydisperse chemically-converted graphene sheets with amine-terminated ionic liquid.* Chem Commun (Camb), 2009(26): p. 3880-2.
227. Bao, C., et al., *In situ preparation of functionalized graphene oxide/epoxy nanocomposites with effective reinforcements.* Journal of Materials Chemistry, 2011. **21**(35): p. 13290.
228. Cai, D., et al., *Recent advance in functionalized graphene/polymer nanocomposites.* Journal of Materials Chemistry, 2010. **20**(37): p. 7906.
229. Fan, J., et al., *Glycidyl methacrylate-modified gum arabic mediated graphene exfoliation and its use for enhancing mechanical performance of hydrogel.* Polymer, 2013. **54**(15): p. 3921-3930.
230. Muradyan, V.E., et al., *The effect of addition of functionalized graphene oxide on the dielectric properties of epoxy composite.* Technical Physics Letters, 2013. **39**(9): p. 798-800.
231. Wang, X., et al., *Functionalization of graphene with grafted polyphosphamide for flame retardant epoxy composites: synthesis, flammability and mechanism.* Polymer Chemistry, 2014. **5**(4): p. 1145.
232. Song, S.H., et al., *Enhanced thermal conductivity of epoxy-graphene composites by using non-oxidized graphene flakes with non-covalent functionalization.* Adv Mater, 2013. **25**(5): p. 732-7.
233. Zhang, Y., et al., *Tuning the interface of graphene platelets/epoxy composites by the covalent grafting of polybenzimidazole.* Polymer, 2014. **55**(19): p. 4990-5000.
234. Pokharel, P., et al., *Multi-step microwave reduction of graphite oxide and its use in the formation of electrically conductive graphene/epoxy composites.* Composites Part B: Engineering, 2014. **64**: p. 187-193.
235. Lu, S., et al., *Epoxy nanocomposites filled with thermotropic liquid crystalline epoxy grafted graphene oxide.* RSC Advances, 2013. **3**(23): p. 8915.
236. Prolongo, S.G., et al., *Graphene nanoplatelets thickness and lateral size influence on the morphology and behavior of epoxy composites.* European Polymer Journal, 2014. **53**: p. 292-301.
237. Martin-Gallego, M., et al., *Comparison of filler percolation and mechanical properties in graphene and carbon nanotubes filled epoxy nanocomposites.* European Polymer Journal, 2013. **49**(6): p. 1347-1353.
238. Sydlik, S.A., *Effects of graphene and carbon nanotube fillers on the shear properties of epoxy.* Journal of Polymer Science Part B, 2013. **51**(13): p. 997-1006.
239. Kim, S.C., et al., *Effect of pyrene treatment on the properties of graphene/epoxy nanocomposites.* Macromolecular Research, 2010. **18**(11): p. 1125-1128.
240. Hsiao, M.C., et al., *Thermally conductive and electrically insulating epoxy nanocomposites with thermally reduced graphene oxide-silica hybrid nanosheets.* Nanoscale, 2013. **5**(13): p. 5863-5871.
241. Mittal, V., *Functional Polymer Nanocomposites with Graphene: A Review.* Macromolecular Materials and Engineering, 2014. **299**(8): p. 906-931.
242. Chatterjee, S., et al., *Mechanical reinforcement and thermal conductivity in expanded graphene nanoplatelets reinforced epoxy composites.* Chemical Physics Letters, 2012. **531**: p. 6-10.
243. Guo, Y., et al., *In Situ Polymerization of Graphene, Graphite Oxide, and Functionalized Graphite Oxide into Epoxy Resin and Comparison Study of On-the-Flame Behavior.* Industrial & Engineering Chemistry Research, 2011. **50**(13): p. 7772-7783.

244. Ganguli, S., et al., Anderson, *Improved thermal conductivity for chemically functionalized exfoliated graphite/epoxy composites.* Carbon, 2008. **46**(5): p. 806-817.

245. Chen, Z., et al., *Improving the mechanical properties of multiwalled carbon nanotube/epoxy nanocomposites using polymerization in a stirring plasma system.* Composites Part A: Applied Science and Manufacturing, 2014. **56**: p. 172-180.

246. Li, W., et al., *Carbon nanotube–graphene nanoplatelet hybrids as high-performance multifunctional reinforcements in epoxy composites.* Composites Science and Technology, 2013. **74**: p. 221-227.

247. Kuilla, T., et al., *Recent advances in graphene based polymer composites.* Progress in Polymer Science, 2010. **35**(11): p. 1350-1375.

248. Rafiee, M.A., et al., *Enhanced Mechanical Properties of Nanocomposites at Low Graphene Content.* ACS nano, 2009. **3**: p. 3884-3890.

249. Fang, M., et al., *Constructing hierarchically structured interphases for strong and tough epoxy nanocomposites by amine-rich graphene surfaces.* Journal of Materials Chemistry, 2010. **20**(43): p. 9635.

250. Tang, L.C., et al., *The effect of graphene dispersion on the mechanical properties of graphene/epoxy composites.* Carbon, 2013. **60**: p. 16-27.

251. Jiang, T., et al., *Effects of surface-modified silica nanoparticles attached graphene oxide using isocyanate-terminated flexible polymer chains on the mechanical properties of epoxy composites.* Journal of Materials Chemistry A, 2014. **2**(27): p. 10557.

252. Guan, L.Z., et al., *Toward effective and tunable interphases in graphene oxide/epoxy composites by grafting different chain lengths of polyetheramine onto graphene oxide.* Journal of Materials Chemistry A, 2014. **2**(36): p. 15058.

253. Zaman, I., et al., *Interface modification of clay and graphene platelets reinforced epoxy nanocomposites: a comparative study.* Journal of Materials Science, 2014. **49**(17): p. 5856-5865.

254. Meng, Q., et al., *Processable 3-nm thick graphene platelets of high electrical conductivity and their epoxy composites.* Nanotechnology, 2014. **25**(12): p. 125707.

255. Wan, Y.J., et al., *Mechanical properties of epoxy composites filled with silane-functionalized graphene oxide.* Composites Part A: Applied Science and Manufacturing, 2014. **64**: p. 79-89.

256. T.K, B.S., et al., *Microwave exfoliated reduced graphene oxide epoxy nanocomposites for high performance applications.* Polymer, 2014. **55**(16): p. 3614-3627.

257. Wan, Y.J., et al., *Grafting of epoxy chains onto graphene oxide for epoxy composites with improved mechanical and thermal properties.* Carbon, 2014. **69**: p. 467-480.

258. Liu, T., et al., *Preparation and characterization of epoxy nanocomposites containing surface-modified graphene oxide.* Journal of Applied Polymer Science, 2014. **131**(9).

259. Yu, G., et al., *Effect of chemically modified graphene oxide on the phase separation behaviour and properties of an epoxy/polyetherimide binary system.* Polymer Chemistry, 2014. **5**(1): p. 96.

260. Corcione, C.E., et al., *The aspect ratio of epoxy matrix nanocomposites reinforced with graphene stacks.* Polymer Engineering & Science, 2013. **53**(3): p. 531-539.

261. Li, Z., et al., *The role of functional groups on graphene oxide in epoxy nanocomposites.* Polymer, 2013. **54**(21): p. 5821-5829.

262. Wajid, A.S., et al., *High-Performance Pristine Graphene/Epoxy Composites With Enhanced Mechanical and Electrical Properties.* Macromolecular Materials and Engineering, 2013. **298**(3): p. 339-347.

263. Feng, H., et al., *Fabrication of Spirocyclic Phosphazene Epoxy-Based Nanocomposites with Graphene via Exfoliation of Graphite Platelets and Thermal Curing for Enhancement of Mechanical and Conductive Properties.* Industrial & Engineering Chemistry Research, 2013. **52**(30): p. 10160-10171.
264. Wang, X., et al., *An investigation of the mechanism of graphene toughening epoxy.* Carbon, 2013. **65**: p. 324-333.
265. Cao, L., et al., *How a bio-based epoxy monomer enhanced the properties of diglycidyl ether of bisphenol A (DGEBA)/graphene composites.* Journal of Materials Chemistry A, 2013. **1**(16): p. 5081.
266. Yousefi, N., et al., *Simultaneous in situ reduction, self-alignment and covalent bonding in graphene oxide/epoxy composites.* Carbon, 2013. **59**: p. 406-417.
267. Li, Z., et al., *Control of the functionality of graphene oxide for its application in epoxy nanocomposites.* Polymer, 2013. **54**(23): p. 6437-6446.
268. Yang, Y., et al., *Enhancing graphene reinforcing potential in composites by hydrogen passivation induced dispersion.* Sci Rep, 2013. **3**: p. 2086.
269. Wan, Y.J., et al., *Improved dispersion and interface in the graphene/epoxy composites via a facile surfactant-assisted process.* Composites Science and Technology, 2013. **82**: p. 60-68.
270. Zaman, I., et al., *A Facile Approach to Chemically Modified Graphene and its Polymer Nanocomposites.* Advanced Functional Materials, 2012. **22**(13): p. 2735-2743.
271. Bortz, D.R., et al., *Impressive Fatigue Life and Fracture Toughness Improvements in Graphene Oxide/Epoxy Composites.* Macromolecules, 2012. **45**(1): p. 238-245.
272. Liu, W., et al., *Simultaneous catalyzing and reinforcing effects of imidazole-functionalized graphene in anhydride-cured epoxies.* Journal of Materials Chemistry, 2012. **22**(35): p. 18395.
273. Huang, X., et al., *Toward Effective Synergetic Effects from Graphene Nanoplatelets and Carbon Nanotubes on Thermal Conductivity of Ultrahigh Volume Fraction Nanocarbon Epoxy Composites.* The Journal of Physical Chemistry C, 2012. **116**(44): p. 23812-23820.
274. Zaman, I., et al., *Epoxy/graphene platelets nanocomposites with two levels of interface strength.* Polymer, 2011. **52**(7): p. 1603-1611.
275. Kim, K.S., et al., *Edge-functionalized graphene-like platelets as a co-curing agent and a nanoscale additive to epoxy resin.* Journal of Materials Chemistry, 2011. **21**(20): p. 7337.
276. Liang, J., et al., *Electromagnetic interference shielding of graphene/epoxy composites.* Carbon, 2009. **47**(3): p. 922-925.
277. Wei, J., et al., *N, N-Dimethylformamide (DMF) usage in epoxy/graphene nanocomposites: problems associated with reagglomeration*. Polymers, 2017. **9**(6): p. 193-202.
278. Wei, J., et al., *Dichlorobenzene: an Effective solvent for Epoxy/Graphene Nanocomposites Preparation*. Royal Society Open Science, 2017. **4**: p. 170778.
279. Wei, J., et al., *Effects of Surfactants on the Properties of Epoxy/Graphene Nanocomposites*. Journal of Reinforced Plastics and Composites, 2018. DOI: 10.1177/0731684418765369.
280. Im, H., et al., *Thermal conductivity of a graphene oxide–carbon nanotube hybrid/epoxy composite.* Carbon, 2012. **50**(15): p. 5429-5440.
281. Li, Q., et al., *Ultrahigh Thermal Conductivity of Assembled Aligned Multilayer Graphene/Epoxy Composite.* Chemistry of Materials, 2014. **26**(15): p. 4459-4465.
282. Jia, J., et al., *Exceptional Electrical Conductivity and Fracture Resistance of 3D Interconnected Graphene Foam-Epoxy Composites.* ACS nano, 2014. **8**: p. 5774-5783.
283. Martin-Gallego, M., et al., *Epoxy-Graphene UV-cured nanocomposites.* Polymer, 2011. **52**(21): p. 4664-4669.

284. Sangermano, M., et al., *Graphene oxide–epoxy hybrid material as innovative photocatalyst.* Journal of Materials Science, 2013. **48**(15): p. 5204-5208.

285. Yu, L., et al., *Carbon hybrid fillers composed of carbon nanotubes directly grown on graphene nanoplatelets for effective thermal conductivity in epoxy composites.* Nanotechnology, 2013. **24**(15): p. 155604.

286. Hsu, C.H., et al., *Physical study of room-temperature-cured epoxy/thermally reduced graphene oxides with various contents of oxygen-containing groups.* Polymer International, 2014. **63**(10): p. 1765-1770.

287. Sarkar, S., et al., *Processing and properties of carbon nanotube-alumina nanocomposites - a review.* REVIEWS ON ADVANCED MATERIALS SCIENCE, 2014. **37**: p. 53-82.

288. Kim, H., et al., *Graphene/Polyurethane Nanocomposites for Improved Gas Barrier and Electrical Conductivity.* Chemistry of Materials, 2010. **22**: p. 3441-3450.

289. Potts, J.R., et al., *Graphene-based polymer nanocomposites.* Polymer, 2011. **52**(1): p. 5-25.

290. Teng, C.C., et al., *Thermal conductivity and structure of non-covalent functionalized graphene/epoxy composites.* Carbon, 2011. **49**(15): p. 5107-5116.

291. Naebe, M., et al., *Mechanical property and structure of covalent functionalised graphene/epoxy nanocomposites.* Sci Rep, 2014. **4**: p. 4375.

292. Cao, Y., et al., *AFM study on amyloid peptide - graphene oxide assembly and its interaction with liposome.* Journal of Self-Assembly and Molecular Electronics, 2015. **3**.

293. Savage, N., *super carbon.* Nature, 2012. **483**: p. 30-31.

294. Ramos-Galicia, L., et al., *Improved Performance of an Epoxy Matrix as a Result of Combining Graphene Oxide and Reduced Graphene.* International Journal of Polymer Science, 2013. **2013**: p. 1-7.

295. Wang, D., et al., *Surface Modification of Graphene with Layered Molybdenum Disulfide and Their Synergistic Reinforcement on Reducing Fire Hazards of Epoxy Resins.* Industrial & Engineering Chemistry Research, 2013. **52**(50): p. 17882-17890.

296. Qi, B., *Enhanced thermal and mechanical properties of epoxy composites by mixing thermotropic liquid crystalline epoxy grafted graphene oxide.* Express Polymer Letters, 2014. **8**(7): p. 467-479.

297. Shen, X.J., et al., *The reinforcing effect of graphene nanosheets on the cryogenic mechanical properties of epoxy resins.* Composites Science and Technology, 2012. **72**(13): p. 1581-1587.

298. Bai, S., et al., *Graphene–inorganic nanocomposites.* RSC Advances, 2012. **2**(1): p. 64.

299. Chandrasekaran, S., et al., *Fracture toughness and failure mechanism of graphene based epoxy composites.* Composites Science and Technology, 2014. **97**: p. 90-99.

300. Yu, W., et al., *A graphene hybrid material functionalized with POSS: Synthesis and applications in low-dielectric epoxy composites.* Composites Science and Technology, 2014. **92**: p. 112-119.

301. Bai, H., et al., *Functional composite materials based on chemically converted graphene.* Adv Mater, 2011. **23**(9): p. 1089-115.

302. Cooper, D.R., et al., *Experimental Review of Graphene.* ISRN Condensed Matter Physics, 2012. **2012**: p. 1-56.

303. Sandler, J.K.W., et al., *Ultra-low electrical percolation threshold in carbon-nanotube-epoxy composites.* Polymer, 2003. **44**(19): p. 5893-5899.

304. Monti, M., et al., *Morphology and electrical properties of graphene–epoxy nanocomposites obtained by different solvent assisted processing methods.* Composites Part A: Applied Science and Manufacturing, 2013. **46**: p. 166-172.

305. Huxtable, S.T., et al., *Interfacial heat flow in carbon nanotube suspensions.* Nature Materials, 2003. **2**: p. 731-734.

306. Veca, L.M., et al., *Carbon Nanosheets for Polymeric Nanocomposites with High Thermal Conductivity.* Advanced Materials, 2009. **21**(20): p. 2088-2092.
307. Pollack, G., *Kapitza Resistance.* Reviews of Modern Physics 1969. **41**: p. 48-81.
308. Martin-Gallego, M., et al., *Thermal conductivity of carbon nanotubes and graphene in epoxy nanofluids and nanocomposites.* Nanoscale Research Letters, 2011. **6**: p. 610-616.
309. Wang, S., et al., *Thermal Expansion of Graphene Composites.* Macromolecules, 2009. **42**(14): p. 5251-5255.
310. Yu, A., et al., *Graphite nanoplatelet-epoxy composite thermal interface materials.* The Journal of Physical Chemistry C, 2007. **111**: p. 7565-7569.
311. Ren, F., et al., *In situ polymerization of graphene oxide and cyanate ester–epoxy with enhanced mechanical and thermal properties.* Applied Surface Science, 2014. **316**: p. 549-557.
312. Liu, S., et al., *Effect of graphene nanosheets on morphology, thermal stability and flame retardancy of epoxy resin.* Composites Science and Technology, 2014. **90**: p. 40-47.
313. Shen, M.Y., et al., *Preparation, Characterization, Thermal, and Flame-Retardant Properties of Green Silicon-Containing Epoxy/Functionalized Graphene Nanosheets Composites.* Journal of Nanomaterials, 2013. **2013**: p. 1-10.
314. Yang, S.Y., et al., *Synergetic effects of graphene platelets and carbon nanotubes on the mechanical and thermal properties of epoxy composites.* Carbon, 2011. **49**(3): p. 793-803.
315. Kim, H., et al., *Graphene/Polymer Nanocomposites.* Macromolecules, 2010. **43**(16): p. 6515-6530.
316. Kotsilkova, R., et al., *Thermoset Nanocomposites for Engineering Applications*. Journal of Nanomaterials, 2009. **2009:** p. 1762
317. Chen, L., et al., *Enhanced epoxy/silica composites mechanical properties by introducing graphene oxide to the interface.* ACS Appl Mater Interfaces, 2012. **4**(8): p. 4398-4404.
318. Park, J.K., et al., *Effects of an aminosilane and a tetra-functional epoxy on the physical properties of di-functional epoxy/graphene nanoplatelets nanocomposites.* Polymer Engineering & Science, 2014. **54**(4): p. 969-976.
319. Galpaya, D., et al., *Preparation of graphene oxide/epoxy nanocomposites with significantly improved mechanical properties.* Journal of Applied Physics, 2014. **116**(5): p. 053518.
320. Saurín, N., et al., *Effect of Graphene and Ionic Liquid Additives on the Tribological Performance of Epoxy Resin.* Tribology Letters, 2014. **56**(1): p. 133-142.
321. Liu, F., et al., *Reinforcing epoxy resin through covalent integration of functionalized graphene nanosheets.* Polymers for Advanced Technologies, 2014. **25**(4): p. 418-423.
322. Liu, K., et al., *Edge-functionalized graphene as reinforcement of epoxy-based conductive composite for electrical interconnects.* Composites Science and Technology, 2013. **88**: p. 84-91.
323. Zhang, X., et al., *Strengthened magnetic epoxy nanocomposites with protruding nanoparticles on the graphene nanosheets.* Polymer, 2013. **54**(14): p. 3594-3604.
324. Prolongo, S.G., et al., *In situ processing of epoxy composites reinforced with graphene nanoplatelets.* Composites Science and Technology, 2013. **86**: p. 185-191.
325. Chen, L., et al., *A design of gradient interphase reinforced by silanized graphene oxide and its effect on carbon fiber/epoxy interface.* Materials Chemistry and Physics, 2014. **145**(1-2): p. 186-196.
326. Wang, X., et al., *The effect of graphene presence in flame retarded epoxy resin matrix on the mechanical and flammability properties of glass fiber-reinforced composites.* Composites Part A: Applied Science and Manufacturing, 2013. **53**: p. 88-96.

327. Huang, G., et al., *A novel intumescent flame retardant-functionalized graphene: Nanocomposite synthesis, characterization, and flammability properties.* Materials Chemistry and Physics, 2012. **135**(2-3): p. 938-947.

328. Sarkos, C.P., *The Effect of Cabin Materials on Aircraft Postcrash Fire Survivability.* Technical Papers of the Annual Technical Conference, 1996. **54**(3): p. 3068-3071.

329. Pack, S., *A Review of Non-halogen Flame Retardants in Epoxy-Based Composites and Nanocomposites: Flame Retardancy and Rheological Properties.* Flame Retardants, 2015: p. 115-130.

330. Wang, X., et al., *Simultaneous reduction and surface functionalization of graphene oxide with POSS for reducing fire hazards in epoxy composites.* Journal of Materials Chemistry, 2012. **22**(41): p. 22037.

331. Wang, Z., et al., *Dispersion of graphene oxide and its flame retardancy effect on epoxy nanocomposites.* Chinese Journal of Polymer Science, 2011. **29**(3): p. 368-376.

332. Qian, X., et al., *Novel organic–inorganic flame retardants containing exfoliated graphene: preparation and their performance on the flame retardancy of epoxy resins.* Journal of Materials Chemistry A, 2013. **1**: p. 6822-6830.

333. Huang, G., et al., *How can graphene reduce the flammability of polymer nanocomposites.* Materials Letters, 2013. **66**(1): p. 187-189.

334. Li, K.Y., et al., *Preparation and properties of novel epoxy/graphene oxide nanosheets (GON) composites functionalized with flame retardant containing phosphorus and silicon.* Materials Chemistry and Physics, 2014. **146**(3): p. 354-362.

335. Jiang, S.D., et al., *Synthesis of ZnS Decorated Graphene Sheets for Reducing Fire Hazards of Epoxy Composites.* Industrial & Engineering Chemistry Research, 2014. **53**(16): p. 6708-6717.

336. Zhuo, D., et al., *Flame Retardancy Effects of Graphene Nanoplatelet/Carbon Nanotube Hybrid Membranes on Carbon Fiber Reinforced Epoxy Composites.* Journal of Nanomaterials, 2013. **2013**: p. 1-7.

337. Inam, F., et al., *Multiscale HybridMicro-Nanocomposites Based on Carbon Nanotubes and Carbon Fibers.* Journal of Nanomaterials, 2010. **2010**: p. 453420.

338. Chatterjee, S., et al., *Size and synergy effects of nanofiller hybrids including graphene nanoplatelets and carbon nanotubes in mechanical properties of epoxy composites.* Carbon, 2012. **50**(15): p. 5380-5386.

339. Kumar, S., et al., *Dynamic synergy of graphitic nanoplatelets and multi-walled carbon nanotubes in polyetherimide nanocomposites.* Nanotechnology, 2010. **21**(10): p. 1-9.

340. Yu, A., et al., *Enhanced Thermal Conductivity in a Hybrid Graphite Nanoplatelet – Carbon Nanotube Filler for Epoxy Composites.* Advanced Materials, 2008. **20**(24): p. 4740-4744.

341. Prasad, K.E., et al., *Extraordinary synergy in the mechanical properties of polymer matrix composites reinforced with 2 nanocarbons.* Proceedings of the National Academy of Sciences of the United States of America, 2009. **106**: p. 13186-13189.

342. Yue, L., et al., *Epoxy composites with carbon nanotubes and graphene nanoplatelets – Dispersion and synergy effects.* Carbon, 2014. **78**: p. 268-278.

343. Sethuraman, K., et al., *Flexible-capron toughened epoxy/graphene nanocomposites for high k dielectric and ultraviolet radiation-resistant applications.* RSC Advances, 2014. **4**(58): p. 30485.

344. Ghaleb, Z.A., et al., *Properties of graphene nanopowder and multi-walled carbon nanotube-filled epoxy thin-film nanocomposites for electronic applications: The effect of sonication time and filler loading.* Composites Part A: Applied Science and Manufacturing, 2014. **58**: p. 77-83.

345. Starkova, O., et al., *Hydrothermally resistant thermally reduced graphene oxide and multi-wall carbon nanotube based epoxy nanocomposites.* Polymer Degradation and Stability, 2013. **98**(2): p. 519-526.

346. Li, Y., et al., *Synergistic toughening of epoxy with carbon nanotubes and graphene oxide for improved long-term performance.* RSC Advances, 2013. **3**(23): p. 8849.

347. Pathangi, H., et al., *Quantifying the Agglomeration Factor in Carbon Nanotube Dispersions by Absorption Spectroscopy.* Journal of Nanoscience, 2014. **2014**: p. 328627.

348. Inam, F., et al., *Re-agglomeration of carbon nanotubes in two-component epoxy system.* Journal of Nanostructured Polymers and Nanocomposites, 2006. **2**: p. 87-95.

349. Ni, Y., et al., *Superior Mechanical Properties of Epoxy Composites Reinforced by 3D Interconnected Graphene Skeleton.* ACS Appl Mater Interfaces, 2015. **7**(21): p. 11583-91.

350. Shen, X.J., et al., *Significantly modified tribological performance of epoxy nanocomposites at very low graphene oxide content.* Polymer, 2013. **54**(3): p. 1234-1242.

351. An, J.E., et al., *Structure and electric heating performance of graphene/epoxy composite films.* European Polymer Journal, 2013. **49**(6): p. 1322-1330.

352. Pu, N.W., et al., *Dispersion of graphene in aqueous solutions with different types of surfactants and the production of graphene films by spray or drop coating.* Journal of the Taiwan Institute of Chemical Engineers, 2012. **43**(1): p. 140-146.

353. Inam, F., et al., *Structural stability studies of graphene in sintered ceramic nanocomposites.* Ceramics International, 2014. **40**(10): p. 16227-16233.

354. Moriche, R., et al., *Reversible phenomena and failure localization in self-monitoring GNP/epoxy nanocomposites.* Composite Structures, 2016. **136**: p. 101-105.

355. Atif, R., et al., *Use of morphological features of carbonaceous materials for improved mechanical properties of epoxy nanocomposites.* RSC Adv., 2016. **6**(2): p. 1351-1359.

356. Shokrieh, M.M., et al., *Effects of graphene nanoplatelets and graphene nanosheets on fracture toughness of epoxy nanocomposites.* Fatigue & Fracture of Engineering Materials & Structures, 2014. **37**(10): p. 1116-1123.

357. Ribeiro, H., et al., *Glass transition improvement in epoxy/graphene composites.* Journal of Materials Science, 2013. **48**(22): p. 7883-7892.

358. Meschi Amoli, B., et al., *SDS-stabilized graphene nanosheets for highly electrically conductive adhesives.* Carbon, 2015. **91**: p. 188-199.

359. Mahanta, N.K., et al., *Graphite–graphene hybrid filler system for high thermal conductivity of epoxy composites.* Journal of Materials Research, 2015. **30**(07): p. 959-966.

360. Kausar, A., et al., *Perspectives of Epoxy/Graphene Oxide Composite: Significant Features and Technical Applications.* Polymer-Plastics Technology and Engineering, 2015. **55**(7): p. 704-722.

361. Guadagno, L., et al., *Optimization of graphene-based materials outperforming host epoxy matrices.* RSC Adv., 2015. **5**(46): p. 36969-36978.

362. Liu, T., et al., *Synergistic Effect of Carbon Nanotubes and Graphene on Diopside Scaffolds.* Biomed Res Int, 2016. **2016**: p. 7090635.

363. Li, Z., et al., *Effect of the orientation of graphene-based nanoplatelets upon the Young's modulus of nanocomposites.* Composites Science and Technology, 2016. **123**: p. 125-133.

364. Ling, Y., et al., *Epoxy resin reinforced with nanothin polydopamine-coated carbon nanotubes: a study of the interfacial polymer layer thickness.* RSC Adv., 2016. **6**(37): p. 31037-31045.

365. Liu, Q., et al., *Mechanical and thermal properties of epoxy resin nanocomposites reinforced with graphene oxide.* Polymer-Plastics Technology and Engineering, 2012. **51**: p. 251-256.

366. Rafiee, M.A., et al., *Fracture and fatigue in graphene nanocomposites.* Small, 2010. **6**(2): p. 179-83.

367. Wang, X., et al., *Covalent functionalization of graphene with organosilane and its use as a reinforcement in epoxy composites.* Composites Science and Technology, 2012. **72**(6): p. 737-743.

368. Gogoi, P., et al., *Jatropha curcas oil based alkyd/epoxy/graphene oxide (GO) bionanocomposites: Effect of GO on curing, mechanical and thermal properties.* Progress in Organic Coatings, 2015. **84**: p. 128-135.

369. Pu, X., et al., *Thermally conductive and electrically insulating epoxy nanocomposites with silica-coated graphene.* RSC Advances, 2014. **4**(29): p. 15297.

370. Ming, P., et al., *Bioinspired highly electrically conductive graphene–epoxy layered composites.* RSC Adv., 2015. **5**(28): p. 22283-22288.

371. Wang, J., et al., *Enhanced microwave absorption performance of lightweight absorber based on reduced graphene oxide and Ag-coated hollow glass spheres/epoxy composite.* Journal of Applied Physics, 2015. **117**(15): p. 154903.

372. Wang, J., et al., *Enhanced microwave absorption properties of epoxy composites reinforced with Fe50Ni50-functionalized graphene.* Journal of Alloys and Compounds, 2015. **653**: p. 14-21.

373. Wang, C., et al., *Microstructure and properties of carbon fiber sized with pickering emulsion based on graphene oxide sheets and its composite with epoxy resin.* Journal of Applied Polymer Science, 2015. **132**(29).

374. Umer, R., et al., *The effect of graphene oxide (GO) nanoparticles on the processing of epoxy/glass fiber composites using resin infusion.* The International Journal of Advanced Manufacturing Technology, 2015. **81**(9-12): p. 2183-2192.

375. Yang, H., et al., *Convenient preparation of tunably loaded chemically converted graphene oxide/epoxy resin nanocomposites from graphene oxide sheets through two-phase extraction.* Journal of Materials Chemistry, 2009. **19**(46): p. 8856.

376. Wang, R., et al., *Attapulgite–graphene oxide hybrids as thermal and mechanical reinforcements for epoxy composites.* Composites Science and Technology, 2013. **87**: p. 29-35.

377. Liu, F., et al., *Effect of molecular chain length on the properties of amine-functionalized graphene oxide nanosheets/epoxy resins nanocomposites.* RSC Adv., 2015. **5**(57): p. 45987-45995.

378. Galpaya, D.G.D., et al., *The effect of graphene oxide and its oxidized debris on the cure chemistry and interphase structure of epoxy nanocomposites.* Polymer, 2015. **71**: p. 122-134.

379. Monfared Zanjani, J.S., et al., *Nano-engineered design and manufacturing of high-performance epoxy matrix composites with carbon fiber/selectively integrated graphene as multi-scale reinforcements.* RSC Adv., 2016. **6**(12): p. 9495-9506.

380. Wang, R., et al., *A novel nanosilica/graphene oxide hybrid and its flame retarding epoxy resin with simultaneously improved mechanical, thermal conductivity, and dielectric properties.* J. Mater. Chem. A, 2015. **3**(18): p. 9826-9836.

381. Tan, Y., et al., *Lightweight graphene nanoplatelet/boron carbide composite with high EMI shielding effectiveness.* AIP Advances, 2016. **6**(3): p. 035208.

382. Qiao, S.J., et al., *Simultaneous Reduction and Functionalization of Graphene Oxide by 4-Hydrazinobenzenesulfonic Acid for Polymer Nanocomposites.* Nanomaterials, 2016. **6**(2): p. 29.

383. Barletta, M., et al., *High performance composite coatings on plastics: UV-curable cycloaliphatic epoxy resins reinforced by graphene or graphene derivatives.* Surface and Coatings Technology, 2015. **272**: p. 322-336.

384. Zong, P., et al., *Effect of aminopropylisobutyl polyhedral oligomeric silsesquioxane functionalized graphene on the thermal conductivity and electrical insulation properties of epoxy composites.* RSC Adv., 2016. **6**(13): p. 10498-10506.

385. Arooj, Y., et al., *Combined effect of graphene oxide and MWCNTs on microwave absorbing performance of epoxy composites.* Polymers for Advanced Technologies, 2015. **26**(6): p. 620-625.

386. Wang, P.N., et al., *Synergetic Effects of Mechanical Properties on Graphene Nanoplatelet and Multiwalled Carbon Nanotube Hybrids Reinforced Epoxy/Carbon Fiber Composites.* Journal of Nanomaterials, 2015. **2015**: p. 1-9.

387. Chang, H.P., et al., *Using supercritical CO2-assisted mixing to prepare graphene/carbon nanotube/epoxy nanocomposites.* Polymer, 2015. **75**: p. 125-133.

388. Hou, G., et al., *Preparation and properties characterization of gallic acid epoxy resin/succinic anhydride bionanocomposites modified by green reduced graphene oxide.* Soft Materials, 2015. **14**(1): p. 27-37.

389. Zeng, C., et al., *Enhanced thermal and mechanical properties of epoxy composites by mixing noncovalently functionalized graphene sheets.* Polymer Bulletin, 2014. **72**(3): p. 453-472.

390. Gong, L.X., et al., *Balanced electrical, thermal and mechanical properties of epoxy composites filled with chemically reduced graphene oxide and rubber nanoparticles.* Composites Science and Technology, 2015. **121**: p. 104-114.

391. Li, W., et al., *Enhanced mechanical and thermal properties of bismaleimide composites with covalent functionalized graphene oxide.* RSC Adv., 2016. **6**(59): p. 54410-54417.

392. Wang, J., et al., *Combined use of lightweight magnetic Fe3O4-coated hollow glass spheres and electrically conductive reduced graphene oxide in an epoxy matrix for microwave absorption.* Journal of Magnetism and Magnetic Materials, 2016. **401**: p. 209-216.

393. Singh, A.K., et al., *Recent Developments on Epoxy Based Thermally Conductive Adhesives (TCA): A Review.* Polymer-Plastics Technology and Engineering, 2017.

394. Hamilton, C.E., et al., *High-Yield Organic Dispersions of Unfunctionalized Graphene.* Nano Letters, 2009. **9**(10): p. 3460-3462.

395. Ham, H.T., et al., *An explanation of dispersion states of single-walled carbon nanotubes in solvents and aqueous surfactant solutions using solubility parameters.* J Colloid Interface Sci, 2005. **286**(1): p. 216-23.

396. Inam, F., et al., *Dimethylformamide: an effective dispersant for making ceramic-carbon nanotube composites.* Nanotechnology, 2008. **19**(19): p. 195710.

397. Jiang, L., et al., *Production of aqueous colloidal dispersions of carbon nanotubes.* Journal of Colloid and Interface Science, 2003. **260**(1): p. 89-94.

398. Rajdip, B., et al., *Stabilizationof individual carbon nanotubes in aqueous solutions.* Nano letters, 2002. **2**(1): p. 25-28.

399. Hajian, M., et al., *Preparation and characterization of Polyvinylbutyral/Graphene Nanocomposite.* Journal of Polymer Research, 2012. **19**(10).

400. Moradi, M., et al., *Mechanical properties of the poly(vinyl alcohol) based nanocomposites at low content of surfactant wrapped graphene sheets.* Polymer, 2015. **60**: p. 207-214.

401. Choi, S.H., et al., *Properties of Graphene/Waterborne Polyurethane Nanocomposites Cast from Colloidal Dispersion Mixtures.* Journal of Macromolecular Science, Part B, 2012. **51**(1): p. 197-207.

402. Hu, H., et al., *Preparation and properties of graphene nanosheets–polystyrene nanocomposites via in situ emulsion polymerization.* Chemical Physics Letters, 2010. **484**(4-6): p. 247-253.

403. Fan, J., et al., *Gum arabic assisted exfoliation and fabrication of Ag–graphene-based hybrids.* Journal of Materials Chemistry, 2012. **22**(27): p. 13764.

404. Chabot, V., et al., *High yield production and purification of few layer graphene by gum arabic assisted physical sonication.* Sci Rep, 2013. **3**: p. 1378.

405. Uysal Unalan, I., et al., *Polysaccharide-assisted rapid exfoliation of graphite platelets into high quality water-dispersible graphene sheets.* RSC Adv., 2015. **5**(34): p. 26482-26490.

406. Lee, H.B., et al., *Preparation and Characterization of Poly(ethylene oxide)/Graphene Nanocomposites from an Aqueous Medium.* Journal of Macromolecular Science, Part B, 2010. **49**(4): p. 802-809.

List of Publications

Journal Papers

1. Wei, J., Saharudin, M.S., Vo, T. and Inam, F., *Effects of Surfactants on the Properties of Epoxy/Graphene Nanocomposites*. Journal of Reinforced Plastics and Composites. 2018. DOI: 10.1177/0731684418765369

2. Wei, J., Saharudin, M.S., Vo, T. and Inam, F., *Dichlorobenzene: an Effective solvent for Epoxy/Graphene Nanocomposites Preparation*. Royal Society Open Science, 2017. 4: 170778.

3. Wei, J., Saharudin, M.S., Vo, T. and Inam, F., *N, N-Dimethylformamide (DMF) usage in epoxy/graphene nanocomposites: problems associated with reagglomeration*. Polymers, 2017. 9(6): 193.

4. Wei, J. and Inam, F., *Processing of epoxy/graphene nanocomposites: effects of surfactants*. Journal of Polymer Science & Applications, 2017: 1(1).

5. Wei, J., Atif, R., Vo, T. and Inam, F., *Graphene nanoplatelets in epoxy system: Dispersion, reagglomeration, and mechanical properties of nanocomposites*. Journal of Nanomaterials, 2015. 16(1): 374.

6. Wei, J., Vo, T. and Inam, F., *Epoxy/graphene nanocomposites–processing and properties: a review*. RSC Advances, 2015. 5(90): 73510-73524.

7. Saharudin, M.S., Wei, J., Shyha, I. and Inam, F., *Biodegradation of halloysite nanotubes-polyester nanocomposites exposed to short term seawater immersion*. Polymers, 2017. 9(8): 314.

8. Saharudin, M.S., Wei, J., Shyha, I. and Inam, F., *Flexural Properties of Halloysite Nanotubes-Polyester Nanocomposites Exposed to Aggressive Environment*. World Academy of Science, Engineering and Technology, International Journal of Chemical, Molecular, Nuclear, Materials and Metallurgical Engineering, 2017. 11(4): 278-282.

9. Saharudin, M.S., Wei, J., Shyha, I. and Inam, F., *Environmental stress cracking resistance of halloysite nanoclay-polyester nanocomposites*. World Journal of Engineering and Technology, 2017. 5(3): 389-403.

10. Saharudin, M.S., Wei, J., Shyha, I. and Inam, F., *The degradation of mechanical properties in halloysite nanoclay-polyester nanocomposites exposed in seawater environment*. Journal of Nanomaterials, 2016 (2016).

11. Atif, R., Wei, J., Shyha, I. and Inam, F., *Use of morphological features of carbonaceous materials for improved mechanical properties of epoxy nanocomposites*. RSC Advances, 2016. 6(2): 1351-1359.

Conference Abstract

1. Wei, J., Vo, T. and Inam, F., *Reinforcement effect of graphene on the mechanical properties of epoxy*. In: BIT's 5th Annual World Congress of Advanced Materials-2016 (WCAM-2016), 6th - 8th June 2016, Chongqing.

Conference Posters

1. Wei, J., Vo, T. and Inam, F., *Processing of epoxy/graphene nanocomposites.* In: 6th Chemical Nanoscience Symposium (CNSN-6), 17th March 2016, Newcastle upon Tyne.

2. Aravinda, L. S., Bhat, K. U., Wei, J., Inam, F. and Bhat, B. R., *Flexible Binder free electrode for ultracapacitor*. In: 5th Chemical Nanoscience Symposium (CNSN-5), 26th March 2015, Newcastle upon Tyne.